FABRICATION OF WET PHASE INVERSION CAPILLARY MEMBRANE, DIMENSION AND DIFFUSION EFFECTS

By

U. Jack

A thesis submitted in fulfilment of the requirements for the degree in Master of Technology in Chemical Engineering

Supervisors: Mr. B.A. Hendry

Prof. E.P. Jacobs

Cape Peninsula University of Technology

February 2006

DECLARATION

I, the undersigned, hereby declare that the work contained in this thesis is my own original work, except where specifically acknowledged in the text. I have not previously in its entirety or in part submitted to any other University or Technikon.

U. Jack

February 2006

ACKNOWLEDGEMENTS

I wish to express my sincere appreciation to the following people for their contribution in making this study possible:

Mr. B.A. Hendry, my supervisor, for his guidance, support and technical input during the time this research was undertaken.

Prof. E.P. Jacobs for providing me with the experimental materials and equipment and the motivation during the diploma years.

Deon Koen for his assistance with membrane spinning and guidance.

WRC and Pentech for their financial support.

My family and friends for their support and encouragement.

Thank you Lord.

ABSTRACT

A protocol already exists for fabrication of a capillary membrane having an internal ultra-filtration skin supported by a finger-like pore structure in the external capillary wall (Jacobs and Leukes, 1996; Jacobs and Sanderson, 1997). These membranes have been produced at the Institute of Polymer Science, University of Stellenbosch, South Africa.

Two major applications emerged from the development of these internally skinned membranes. One application was in the production of potable water by Ultra-filtration (UF) from sources containing coloured water. A second application was in the immobilization of a white rot fungus in a "gradostat" membrane bioreactor. Here a nutrient gradient through the membrane wall and fungal mat can be established and manipulated in order to stimulate continuous production of secondary metabolites (extra-cellular enzymes). These enzymes are useful in the degradation of polycyclic aromatic compounds, notably PCB species in contaminated water and soils (Jacobs and Sanderson, 1997).

Two objectives emerged from experiences with the above applications. The first objective was to improve membrane performance in UF applications. In this case a reduction was sought in trans-membrane pressure differential required to attain a desired flux without sacrificing rejection. The pressure required for a given desired flux across a membrane depends on the resistance of the membrane skin layer and of its supporting sub-layer which together comprises the capillary wall and defines its overall structure. If any of these resistances could be reduced, the overall resistance to transport of water would be reduced. Then it would be possible to operate the membrane at lower trans-membrane pressure differences. On the other hand, operation with higher pressure would also increase flux but require a thicker capillary wall to resist this pressure. In the attempt to optimise these properties of the capillary membrane, capillary membranes produced in the study reported here were tested to find the relationship of flux performance with the structures that resulted from varying key parameters affecting structure and integrity.

The objective in the case of immobilizing fungi in membrane bioreactor applications was to attain thicker walls thus providing better support for the fungal mass. The internally skinned capillary membrane has finger-like microvoids that start next to the UF skin layer and extend across the capillary membrane wall and open at the external membrane periphery, giving an

ideal structure for retaining the fungal biomass. The idea of a membrane with this type of morphology to immobilize white rot fungi was to anchor the growing fungus within these microvoids which imitate the natural environment in which these organisms live, that is, in the fibrous structure of decaying wood. The requirement to inoculate the microvoids with fungal spores (reproductive cells), implies that they need to be accessible from the outside, requiring a membrane wall that is externally unskinned.

In the formation of the capillary membrane the processes of formation of the porous UF skin and the finger-like microvoids are mainly governed by diffusion of solvent out of a polymer dope (gel phase) and of non-solvent into the dope phase. Such exchanges are of primary importance between the bore fluid (containing non-solvent) and dope (containing solvent) or between the external spinning bath (high in solvent content) and dope. Diffusion effects also occur between the nascent pore voids and the precipitating polymer matrix. There are also expected to be some convection effects due to shear between the bore fluid and the moving dope gel phase and due to shrinkage of the gel phase.

The variables selected for experimentation in the study reported here were: the dope extrusion rate (DER); dope composition (viscosity effects); bore fluid flow rate (BFF); bore fluid composition and wall thickness and diameter effects (determined largely by spinneret dimensions). Each of these has an expected effect on membrane structure and its resulting performance. Most were varied over narrow ranges indicated in the literature and by experience to be effective and critical. In addition, the effects of altering the wall thickness were investigated by using two different spinneret sizes.

The external spinning bath composition (solvent content) was reported in the literature to be a particularly important parameter in the formation of externally unskinned membranes. Maintaining a high content of solvent in the external spinning bath could prevent skin formation. Too high a solvent content could, however, prevent phase transition and lead to later precipitation of a dense skin on contact with the non-solvent in the later (humidification and rinsing) steps in the finishing of the capillary membrane product. The external bath composition was therefore varied so as to find the bath composition that would match the cloud point for the polymer dope employed.

As expected, the thickness of the membranes increased with DER increase. However, it was found that there is a critical wall thickness where an external skin layer is formed as a result of increasing the DER. A certain volumetric ratio of DER to BFF (1,5:1 for this study) was therefore maintained in order to produce externally unskinned membranes. This shows that although the final membrane structure is determined by the casting dope formulation, the fabrication protocol plays an equally important role in controlling structural properties and performance. There was no significant change with the membrane thickness as a result of changing BFF but the voids became longer and more in number as the BFF was increased.

Too high solvent content (99% NMP in this study) resulted in an external skin layer being formed. According to Smolders et.al. (1992), when the solvent content in the external spinning bath is too high, the polymer at the surface of the newly formed membrane slowly dissolves in the external spinning bath re-forming a dope-like solution. When the newly formed membrane passes through the humidifier, the dope-like solution solidifies to form an external skin. At the same instance, too low solvent (93% for this study) resulted in external skin being formed. Externally unskinned membranes were formed at 94 and 96% NMP bath composition. The use of a small spinneret resulted in very thin walled externally unskinned membranes.

LIST OF FIGURES

LIST OF TABLES

LIST OF ABBREVIATIONS

NMP	N, Methyl 2- pyrrolidone
Psf	Polysulfone
PEG	Poly Ethylene glycol
PVP	Polyvinyl-pyrrolidone
MC	Methyl Cellosolve acetate also known as 2-Methoxyethanol acetate
PES	Poly Ethersulfone
OD	Outside Diameter
ID	Inside Diameter
BFF	Bore fluid flow-rate
DER	Dope extrusion rate
UF	Ultra-filtration
SEM	Scanning Electron Microscope
PWP	Pure Water Permeability
DMAc	N,N-dimethyl acetamide
DMF	Dimethylformamide
IPS	Institute of Polymer Science

CHAPTER 1

1.1 Introduction and Background

Membranes and their uses

A membrane is a selective barrier that permits the separation of dissolved and suspended matter from a fluid by a combination of sieving and sorption mechanisms. A membrane should be always associated with its application according to this definition. These applications can range across water desalination, filtration, and gas separation. Depending on the application, different membrane structures are used. The use of membranes over other conventional mass transfer equipments, such as distillation columns may be preferred for the following reasons:

i. Membrane modules have a much larger ratio of membrane surface area per unit of module volume, (with a reported value of $8000m^2/m^3$) (Van de Walt, 1999). They hence have higher productivity per unit volume of membrane module compared to bubble columns, sieve trays and packed towers that have a maximum specific contact area between gas and liquid of about $800m^2/m^3$).

ii. In terms of energy, membrane separation has an important advantage in that, unlike evaporation and distillation, no change of phase is involved in the process, thus avoiding latent heat requirements.

Membrane structures and their separation mechanisms

Loeb and Sourirajan developed the first synthetic membranes in the 1960's using a phase-separation process (Young and Chen, 1993). They were flat sheet cellulose acetate having an asymmetric structure. An asymmetric membrane consists of a very thin layer, approximately 0.1 - 1μm, of selective skin on a highly porous and thick, approximately 100 – 200 μm substructure. The very thin skin represents the actual membrane. The porous sub-layer serves only as a support for the thin and fragile skin and has an insignificant effect on separation characteristics or the rate of solution transfer through a membrane. Nowadays membranes having asymmetric structure are the favourite choice for separation processes, because:

- they are mostly known to be fouling resistant because separation is by sieving, separated particles are not sorbed within the membrane structure.
- they are self-supporting and can be back-flushed.

- the flux across an asymmetric membrane is higher than that of the symmetric membrane because of the thin top skin.

Membranes can also have a symmetric structure in which case it is referred to as a dense homogeneous membrane (Porter, 1990). The active layer of this membrane is dense. It does not separate on the basis of sieving mechanism. Separation involves the entrapment of particles within the filter structure.

Important properties of membranes

From the technological point of view, the most important properties of membranes are their functional properties such as permeability and rejection, which are closely related to their structural properties. For example, much attention has been paid to the design of synthetic polymer membranes with controlled permeability of water and selectivity. Many techniques have been used to combine membrane technology with living biological cells in order to treat specific diseases e.g. the artificial pancreas. The membrane has to be permeable to small molecules such as antibodies and lymphocytes. Therefore, it is necessary to prepare membranes with a proper pore size and distribution to meet the requirements for application.

Goals in membrane fabrication

An important goal in membrane fabrication is to control membrane structure and thus its performance. This objective is not easy to achieve because the membrane structure and performance depend on many factors such as the polymer concentration, precipitation medium and precipitation temperature among others. By changing one or more of these factors, which are dependent on each other, membranes can be made with a very large range of pore sizes. This shows that although the final membrane structure is determined by the casting dope formulation, the fabrication protocol plays an equally important role in controlling structural properties and performance. This is due to the rates of mass transfer that result from the nature of the dope, bore fluid, external spinning bath and their temperatures.

Membrane technology development

In the 1970's the first polysulfone (Psf) hollow fibre membranes, (the category under which capillary membranes fall), were generated by Henis and Tripod (Porter, 1990). Capillary membranes are narrow bore, tubular type membranes, typically with outside diameters that range from 0,7mm to 3mm, and inside diameters that range from 0,4mm to 2,4mm. They can

be produced as internally skinned, externally skinned or double skinned depending on how the bore fluid and the external spinning bath are introduced. These capillary membranes are applied for ultra-filtration that separates particles that range from 0,01 to 0,1 microns in size. The type of membrane to be discussed in this thesis is a capillary membrane having a thin dense skin on the inside (externally unskinned or internally skinned) and microvoids on the underlying layer, originating from just below the skin to the periphery of the membrane.

1.2 Historical development of externally unskinned or internally skinned capillary membranes

1.2.1 Introduction

Externally unskinned capillary membranes were produced from polysulfone and poly-ethersulfone, by means of wet phase separation method, at the Institute of Polymer Science (Jacobs and Leukes, 1996; Jacobs and Sanderson, 1997). According to these authors, two applications emerged for the development of these externally unskinned membranes. The first application was for the production of potable water by UF from sources containing coloured water. The objective of this study for this application was to improve membrane performance in UF applications.

In this case a reduction was sought in trans-membrane pressure differential required to attain a desired flux without sacrificing rejection. The pressure required for a given desired flux across a membrane depends on the resistance of the membrane skin layer and of its supporting sub-layer which together comprises the capillary wall and defines its overall structure. If any of these resistances could be reduced, the overall resistance to transport of water would be reduced. Then it would be possible to operate the membrane at lower trans-membrane pressure differences. On the other hand, operation with higher pressure would also increase flux but require a thicker capillary wall to resist this pressure. In the attempt to optimise these properties of the capillary membrane, capillary membranes produced in the study reported here were tested to find the relationship of flux performance with the structures that resulted from varying key parameters affecting structure and integrity.

The second application was for the immobilization of a fungus in a membrane bioreactor. The objective in the case of immobilizing fungi in membrane bioreactor applications was to

attain thicker walls thus providing better support for the fungal mass. The internally skinned capillary membrane has finger-like microvoids that start next to the UF skin layer and extend across the capillary membrane wall and open at the external membrane periphery, giving an ideal structure for retaining the fungal biomass. The idea of a membrane with this type of morphology to immobilize white rot fungi was to anchor the growing fungus within these microvoids which imitate the natural environment in which these organisms live, that is, in the fibrous structure of decaying wood. The requirement to inoculate the microvoids with fungal spores (reproductive cells), implies that they need to be accessible from the outside, requiring a membrane wall that is externally unskinned (Jacobs and Sanderson, 1997).

1.2.2 Polymer dope preparation

Polymer dope is a uniform molecular dispersion of a macromolecular polymer in a solvent. In some instances, additives such as high molecular weight polymers and non-solvents can be added to adjust the viscosity of the dope (Jacobs and Sanderson, 1997). When dissolving a polymer in a solvent, the solvent first permeates the polymer granules. The polymer near the surface swells to accommodate the incoming molecules of a solvent whilst the individual long chain molecules of a polymer are freed and dissolved into the solvent. If a hydrophobic polymer is used, it has to be dried before usage and solvents used have to be distilled to remove water. These polymers do not dissolve in water and tend to repel the water molecules; therefore, water sorbed by a solvent may cause unevenness of the membrane structure. The unevenness of the membrane structure may be seen as a bubble on the surface or a very thin film surrounded by a thick rough layer.

At the start of membrane fabrication (1980's) at IPS, the polymer and solvent were put in a tightly closed bottle, which was placed on a roller to get mixing. It was found that the polymer particles tend to aggregate and form one or more lumps in the forming dope, which took a long time to dissolve completely. Another way of mixing, using an electric stirrer was later (1990's) introduced. This electric stirrer is inserted into a flask containing the polymer and solvent to be mixed. This method keeps the polymer particles apart, and therefore takes less time to dissolve an individual polymer particle. The dope then has to be degassed, to remove air bubbles entrained during stirring. Air bubbles can also cause unevenness of the membrane structure.

1.2.3 Spinning equipment and process

A gear pump is used to force the dope through a tube-within-tube type spinneret, which consists of a central bore and an annulus side. Dope is introduced at the annulus side of the spinneret. Pure water as bore fluid is metered, by means of a pump or flow by gravity from the reservoir, into the bore side of the spinneret. To produce an externally unskinned membrane, precipitation on the outside must be avoided therefore an external spinning bath, containing a high concentration of solvent should be introduced very close to the spinneret. The spinneret can be positioned at the bottom of the spinning bath, and the membrane drawn vertically from the spinneret by rollers. Alternatively, the spinneret can be positioned very close to the liquid surface of the external spinning bath and with the membrane being allowed to fall freely from the spinneret into the bath. The forming membrane then moves via a roller into the bath whilst being drawn vertically upwards, guided by rollers. The forming membrane becomes swollen and gel-like on the outside due to the high solvent content in the spinning bath, which prevents precipitation. Once the membrane has been drawn from the spinning bath, it is exposed to non-solvent vapour to fix the structure. Excess solvent is removed in the non-solvent rinse bath and a take-up drum collects the membrane.

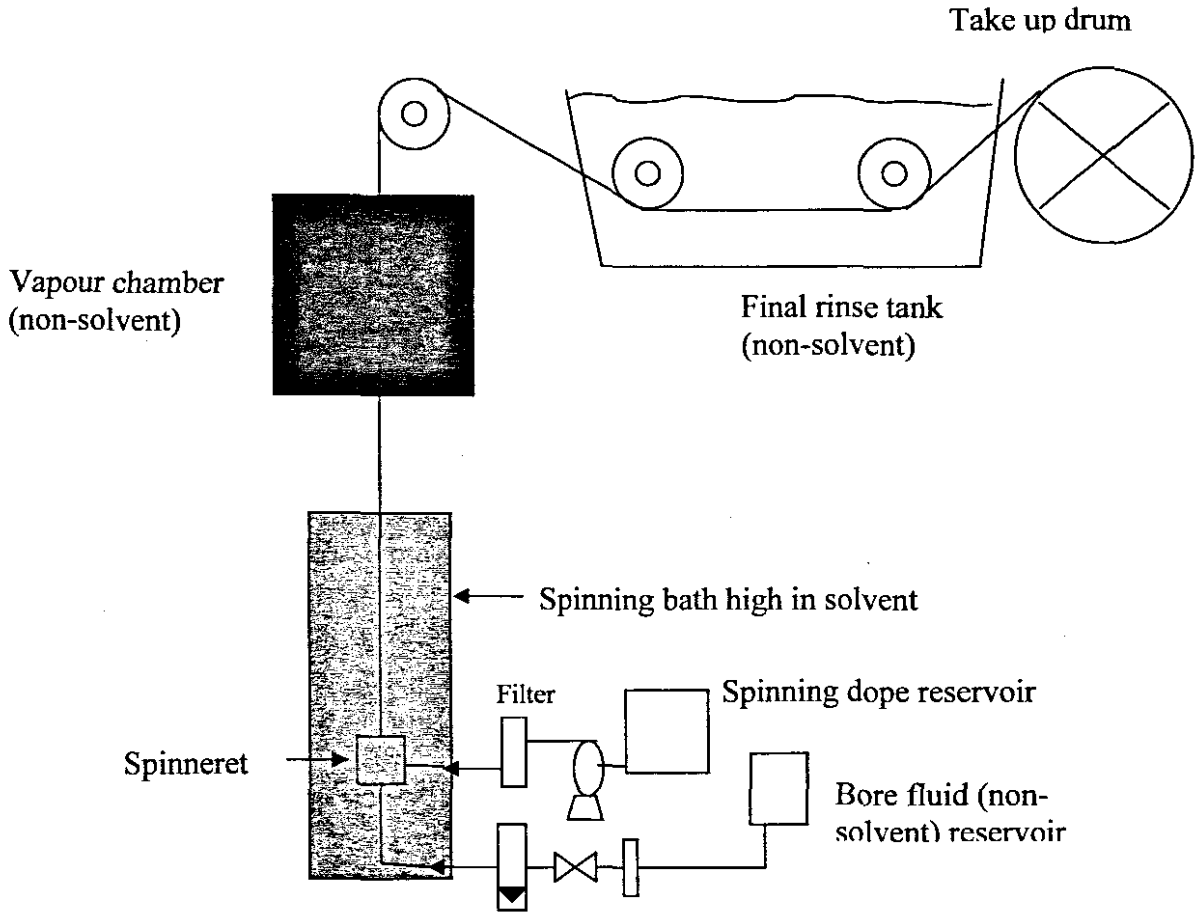

Figure 1.2.3 (a): Schematic representation of the externally unskinned membrane spinning line

The external spinning bath contains N, Methyl 2-pyrrolidone (NMP), a solvent that has the hazardous effects listed in appendix B. Protective gloves, a gas mask, safety spectacles and protective clothing are worn when fabricating the membranes. The spinning bath has to be covered at all times to prevent NMP vapour emission into air. With the membrane having to be spun directly in the bath, covering the spinning bath is difficult to achieve. Extraction fans are used therefore to avoid accumulation of NMP vapour in the air.

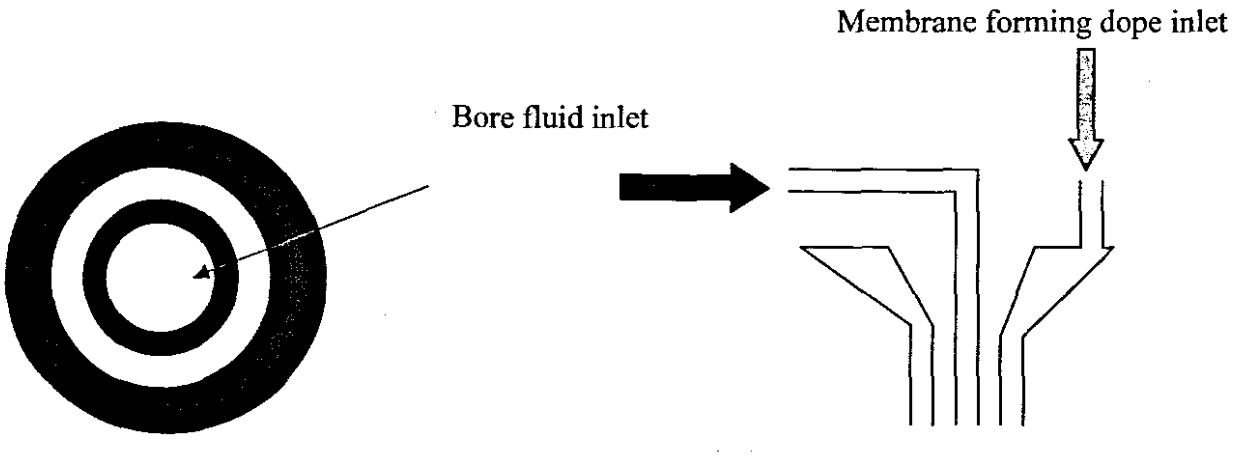

Figure 1.2.3(b): Schematic presentation of a spinneret body

1.3 Research objectives

As pointed out earlier in section 1.2.1, the idea of a membrane with microvoids and no external skin layer morphology to immobilize fungi was to imitate the natural habitat of these organisms, which is, the fibrous nature of decaying wood. The problem encountered was that as the fungi grew within the confines of the microvoids, it also formed a layer on the outer surface of the membrane. This fungal layer thickened with time, causing the membrane to sag. Hence the aim of this study was to rationalize a fabrication protocol to produce a thick-walled, externally unskinned membrane for use as a matrix in a fungal bioreactor.

The membrane was also used for ultra-filtration purposes; therefore the produced membranes were tested for performance, that is, flux and rejection. These membranes require a very skilful handling to fabricate and very stringent process control is required to obtain the requisite structure. Therefore it was necessary to revisit and study the different factors that affect the membrane structure. The fabrication protocol includes the following parameters, which were found to play a significant role in the resultant membrane structure including wall thickness, skin and microvoid formation. Diffusion of solvent and non-solvent takes place between the dope, bore fluid and external spinning bath. Hence the specific objectives are as follows:

- To investigate the effect of Dope Extrusion Rate (DER) and viscosity on membrane structure and performance

- To investigate the effect of Bore Fluid Flow rate (BFF) and composition on membrane structure and performance
- To investigate the effect of external spinning bath composition on the structure and UF performance of the membrane
- To investigate the effect of the size and position of the spinneret on membrane structure and performance

CHAPTER 2

THEORY OF PHASE SEPARATION AND MECHANISMS OF MEMBRANE FORMATION

2.1 Introduction

In the process of phase separation, a homogeneous polymer dope is transformed into a two-phase system in which a solidified polymer rich phase forms the continuous membrane matrix and a polymer poor phase fills the pores. The concept "phase separation process" covers a range of different techniques, each leading to a specific membrane structure, for example:

i. ***Precipitation from the vapour phase*** - which yields symmetric membranes.
During this process, phase separation of the polymer dope is induced by diffusion of non-solvent vapour into the dope.

ii. ***Immersion precipitation*** –The polymer dope is spread as a thin film on a glass plate, which is typically 500μm thick, and precipitated in a non-solvent. Solvent in the dope diffuses out of the dope to the casting bath, whilst non-solvent from the bath diffuses into the dope. The direction of the solvent and non-solvent diffusion is shown in figure 2.1 below. As a result of precipitation, the homogeneous dope separates into two phases, that is:

- a solid membrane structure that is rich in polymer and
- the liquid filled membrane pores rich in solvent

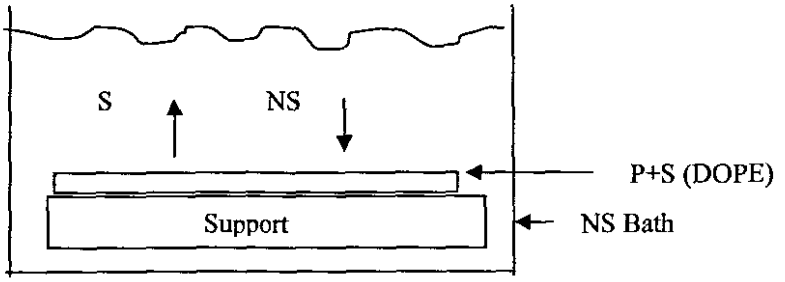

P – is the polymer
S – is the solvent
NS – is the non-solvent

Figure 2.1: Phase separation process by immersion precipitation

iii. ***Thermally induced phase separation*** – is based on the phenomenon that the rate of solvent evaporation decreases when the temperature is decreased.

iv. Air casting of a polymer dope – where the polymer is dissolved in a mixture of a volatile solvent and a less volatile non-solvent. During the evaporation of the volatile solvent, the solubility of the polymer decreases and then phase separation takes place.

2.2 Phase separation steps

2.2.1 Liquid-liquid (polymer poor and polymer rich) phase separation

This can be caused by variation in temperature and/or composition of the mixture. When a polymer dope becomes thermodynamically unstable, it decreases its free energy of mixing by dividing into two liquid phases of different compositions. This decrease in free energy of mixing can be expressed as follows:

i) a stable state where all components are miscible in a single phase.

In this state, the free energy of mixing is positive.

$$\Delta G > 0$$

ii) an unstable state where the homogeneous dope separates spontaneously into two phases, which are in equilibrium.

This is located within the miscibility gap; the free energy of mixing is negative.

$$\Delta G < 0$$

iii) an equilibrium state given by the phase boundary composition.

In this state, the free energy of mixing is zero.

$$\Delta G = 0$$

The two liquid phases are a nucleus of the polymer-poor phase that forms the nascent pore and a polymer-rich phase that surrounds the pore.

2.2.2 Solidification of polymer rich phase

Referring to figure 2.2; the polymer rich phase solidifies when the polymer dope crosses the binodal boundary (where all three are miscible) from 1 to 111 or from 11 to 111. As a result

of an increase in polymer dope viscosity, the motion of polymer chains is limited and the system can be regarded as a solid to specify the membrane structure.

2.2.3 Leaching of polymer poor phase

Putting the membrane into a treated water bath leaches the liquid filling the pores out.
This can be shown by means of the Ternary phase diagram

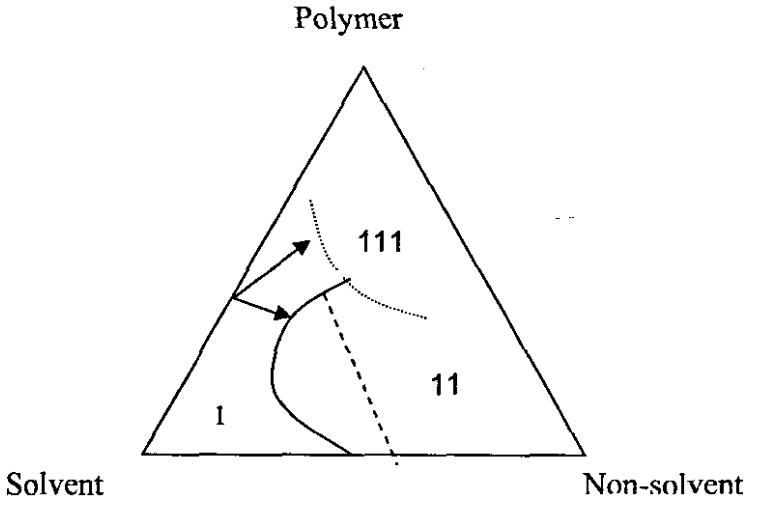

Figure 2.2.3: Ternary phase diagram for phase separation forming paths

2.2.4 Phase separation explanation in terms of the ternary diagram

1. The mutual affinity between the solvent and the non-solvent has an effect on the position of the binodal boundary. Young and Chen (1995) explained that the high mutual affinity favours the de-mixing of the ternary system, that is, the tendency of the location of the miscibility gap is to move towards the polymer-solvent axis in the ternary diagram. Less non-solvent is needed for liquid-liquid phase separation.
2. The low end point of the tie line shifts towards the solvent corner of the ternary diagram when the mutual affinity between the solvent and the non-solvent increases. This means that the volume fraction of non-solvent in the polymer-poor phase required is only in small amounts. Therefore an increase in mutual affinity lowers the amount of non-solvent necessary for pore formation.

3. The polymer concentration in the polymer-poor phase rapidly approaches a very small value in many circumstances. However, the polymer concentration in the polymer-rich phase is much higher at low mutual affinity between the solvent and the non-solvent. Therefore the polymer-rich phase will slow down the solidification rate, and the pore wall will have more time to grow at high affinity between the solvent and the non-solvent.

2.3 Mass transport during the phase separation process

According to Stropnik et.al. (2000) the following are the ways by which mass is transported in a non-solvent, solvent and polymer system:

1. Primary non-solvent, solvent and polymer mass transport consists of:

a) Direct accumulation of polymer (direct solidification)

b) Diffusion of non-solvent and /or solvent

c) Convection of non-solvent, solvent and polymer

d) Hydrodynamic flow of non-solvent, solvent and polymer

All modes of mass transport of this first group are somehow represented in the ternary phase diagram. They present the transportation of the components only in the direction perpendicular to the contact boundary between the polymer dope and the coagulation bath. 1a) always takes place immediately, after the cast dope immersion, or is absent.

The remaining three modes, that is, 1(b, c and d) lead to:

2. Secondary mass transport (phase separation) which consists of three modes:

a) nucleation and growth of the polymer poor phase

b) spinodal phase separation. Spinodal phase is the point at which any disturbance in the system can cause phase separation.

c) nucleation and growth of the polymer rich phase

In these three modes of transport the transportation of the components takes place in all directions in space. All these three phase separation elementary processes in 2, above, are suppressed by some form of solidification, in the polymer rich phase (3):

3. solidification of accumulated polymer, which consists of:

a) gelation (thermo reversible)

b) glass transition (vitrification)

c) crystallisation

4. Following the ternary mass transport processes is:

a) leaching of the polymer poor phase from the nascent membrane usually by a non-solvent or water.

b) leaching of the non-solvent and solvent from a firm gel.

2.4 Skin formation theory

A polymer dope cast on a support when immersed in a bath containing non-solvent results in a skin being formed. In the case of capillary membranes, the dope comes into contact with bore fluid and/or external spinning bath containing non-solvent to form a skin. Immediately, after immersion or contact there is a rapid depletion of solvent from the polymer dope to the spinning bath or bore fluid. At the same time, there is relatively small penetration of non-solvent from the bore fluid and or spinning bath to the dope (Paul, 1968; Young and Chen, 1995). The result of these effects is an increase in polymer concentration at the dope/bath or dope/bore interface. The thin skin layer formed then acts as a resistance to solvent out-diffusion.

The study conducted by this author explained the reasons for the rate of solvent diffusing out of the dope being high compared to the rate of non-solvent diffusing in at the initial stage are the following: The polymers used, Psf and PES, are hydrophobic, so they repel water which is used as non-solvent. The solvent concentration difference between the spinning bath or bore fluid and dope is very large initially. Solvent diffuses into the spinning bath or bore fluid leaving the dope low in solvent content at the dope/bath or dope/bore fluid interface. Dope normally contains less than 50 % of solvent. The rate of solvent diffusion into the spinning bath or bore fluid decreases and eventually stops. At the same time, the spinning bath or bore fluid is still high in non-solvent content. Since the polymer dope does not contain any non-solvent, there is a large driving force for non-solvent to diffuse into the dope. The thickness of the skin layer will increase gradually until the diffusion of solvent

from the sub-layer dope through the dense skin layer into the spinning bath or bore fluid is restrained.

At positions beneath the top layer, phase separation will occur at a lower polymer and higher non-solvent concentration. Therefore the type of phase separation will be liquid-liquid phase separation (see section 2.2.1 for detailed explanation on this type of phase separation). The factor determining the type of phase separation at any point in the cast film is the local polymer concentration at the moment of precipitation (Smolders and Reuvers, 1992).

2.5 Alternative explanations for voids formation mechanisms

2.5.1 Voids formation involving diffusion and buoyancy

An extensive study as to what causes microvoids on membranes has been conducted by many researchers such as Young and Chen (1995); Pekny et. al (2002, 2003); Reuvers and Smolders (1995); Cabasso (1977). Most of them proposed the driving force to be the diffusion of solvent and non-solvent. A surface tension gradient, which accounts for the initiation of convection cells at the interfacial boundary of the forming membrane, was reported by Pekny et.al (2002, 2003) to be another possibility.

From the skin formation theory in section 2.4, it was learnt that the skin is formed as a result of rapid solvent diffusion out of the dope. As a result of the dense top layer that acts as a resistance to further solvent out diffusion, the composition of the sub-layer does not change as rapidly as it does when the dope is within the initial homogeneous region.

At the same time, the non-solvent diffuses through the dense top layer to underlying layer of the nascent membrane. When the amount of non-solvent has caused significant composition variation in the underlying layer, the dope becomes unstable. The first nucleus of the polymer poor phase occurs to form the nascent pore in the first layer of the sub-layer. When more non-solvent enters different sites of the first layer, more pores occur. A nascent pore will grow if non-solvent from the spinning bath or bore fluid can continually diffuse into it. That will induce the solvent surrounding the nascent pore to diffuse into the pore containing non-solvent. That is as a result of solvent concentration difference between the liquid in the pore

(non-solvent) and the solvent in the dope surrounding the pore. The diffusion of solvent into the growing pore will cause an increase in the polymer concentration of the polymer-rich phase surrounding the pore. When the surrounding polymer-rich phase solidifies, the pores stop their growth. Therefore the main driving force for the growth of the pores is the decrease in free energy on mixing solvent and non-solvent in the pores (Young and Chen, 1995). Finger-like structure formation requires that both solvent and non-solvent can rapidly and consecutively diffuse into a younger pore before the solidification of the pore wall.

Reuvers and Smolders (1995) argued that after microvoid initiation, growth occurs by diffusion of solvent to the microvoid nuclei that are the pores. Microvoid growth occurs when the diffusion of solvent from the polymer dope into the nuclei is larger than the flow of non-solvent from the nuclei into the polymer dope. As a result of this, the microvoid volume increases, resulting in larger buoyancy forces. Microvoids are less dense than the surrounding polymer; therefore a gravitationally induced buoyancy force opposes their growth.

2.5.2 Voids formation involving surface tension

Shojaie et. al. (1994) cited by (Pekny et. al, 2002, 2003) contended that microvoid growth cannot be a purely diffusive process, so they proposed a description based on an analysis of body forces at the microvoid/skin interface.

Pekny et. al, (2002) reported that the studies of Shojaie (1994) indicated that the surface tension increases with increasing water concentration and decreasing solvent concentration within the pore. Therefore, the surface tension of a growing microvoid is reduced near its leading edge relative to its trailing edge. At the leading edge, solvent is diffusing to the pore whilst at the trailing edge more non-solvent is diffusing to the pore. Due to this surface tension gradient, material along the microvoid/dope interface moves from the leading edge (low surface tension) to the trailing edge (high surface tension) of the microvoid. This process, known as soluto-capillary convection, exerts a force on the growing microvoid that propels it away from the skin/dope interface and into the underlying bulk dope. The bulk dope has a lower polymer concentration and thus a higher diffusivity than dope near the skin/dope interface.

Furthermore, Shojaie et. al. (1994) cited by Pekny et. al, (2002) claimed that the continuity of velocity at the microvoid/dope interface establishes convection cells in the bulk dope that serve to transfer solvent and non-solvent to the growing microvoid more rapidly than could diffusion alone. These two effects greatly increase the rate of mass transfer to a growing microvoid, thereby increasing its growth rate. It was emphasized that in order for a soluto capillary convection to have an effect, a microvoid must already be present. The soluto-capillary hypothesis predicts that microvoid growth is favoured in membranes cast under normal gravity.

2.6 Shrinkage phenomena during membrane formation

Jacobs and Sanderson (1997) postulated that, the capillary membrane is under slight tension when it leaves the spinneret, although it was found difficult to prove. The induced strain generates the formation of solvent-rich nuclei (growth centre for polymer-poor phase). Also, the membrane has a high shrinkage rate of > 14 %. At the point of extrusion, where the bore side comes into contact with the polymer dope, further stress is induced by two-dimensional shrinkage of the membrane, which may also lead to nucleation of solvent-rich sites that could subsequently grow into microvoids.

Stropnik et.al. (2000) explained the shrinkage phenomena during phase separation in the following way. When only the out diffusion of the solvent from the casting dope takes place, the polymer casting dope can be converted into a pure polymer. The solvent and /or non-solvent within the polymer is no longer present and a dense polymer membrane is formed which is evidently much thinner than the original cast dope. It is the thinnest possible membrane formed.

When the polymer, the solvent and non-solvent somehow maintain their position in space to form a porous structure, the formed porous nascent membrane is as thick as the original casting dope. In the polymeric membrane formation by wet phase separation, the thickness of the membrane lies somewhere between these two extremes where a more porous or dense nascent membrane is formed.

CHAPTER 3

LITERATURE REVIEW OF EFFECTS OF SPINNING CONDITIONS ON MEMBRANE STRUCTURE AND PERFORMANCE

Following is the literature review of the effects of spinning conditions on membrane structure and performance. The spinning conditions discussed in the chapter are the main study objective questions for this dissertation, that is, the effects of BFF and composition, DER and composition, external spinning bath composition and the spinneret position. Some additional variables which were investigated during the study are presented in Appendix C.

3.1 The effects of external spinning or casting bath composition (solvent content)

Most of the researchers, who conducted this study, fabricated flat sheet membranes and used the immersion method of precipitation (Smolders et. al., 1992; Wijmans et.al, 1983; Termonia, 1995;Broadhead and Tresco, 1998; Jacobs and Leukes, 1996). Their observations were as follows:

At too high casting bath solvent concentrations, precipitation did not take place and the polymer slowly dissolved in the casting bath (Smolders et.al., 1992). On studying the structure of membranes, these authors discovered that, when the solvent content was increased in the bath, the pore radii also gradually increased. It also came into notice that the membranes had a gradient in pore radius; the pores in the top layer were smaller than those in the bottom layer. This actually showed that changing the solvent concentration in the bath had a greater influence on the pore size in the top layer compared to the bottom layer.

Furthermore, Wijmans et.al. (1983) concentrated on how the addition of solvent to the casting bath prevents the formation of a skin. From the theoretical point of view, it had been stated that the ratio of solvent outflow to non-solvent inflow is important for skin formation. The structure of membranes changed from a finger-like into a uniform structure with increasing solvent in the casting bath (Wijmans, 1983, Termonia, 1995). A decrease in solvent and non-solvent miscibility leads to a less dense membrane structure. In such cases, the rate of precipitation decreases because the chemical potential between the solvent and

non-solvent is smaller. Therefore the driving force for diffusion of solvent and or non-solvent is less. For a skin layer to be formed, precipitation rate has to be very rapid. That is possible if the chemical potential difference between solvent and non-solvent is high.

A strong non-solvent is said to increase the miscibility gap in the ternary phase diagram (Jacobs and Leukes, 1996). Miscibility gap is the region in the ternary diagram where the solvent, non-solvent and polymer are miscible. That means, only a small amount of non-solvent is needed to induce phase separation. In order to suppress precipitation and favour liquid-liquid phase separation, the casting bath has to contain low concentrations of non-solvent. In this case, the rate of solvent outflow will be reduced because the driving force for diffusion is smaller. It was stated that if the composition of the casting bath equals that of the advancing polymer poor phase as it neared the membrane exterior, there should be no driving force for diffusion and the phase inversion process should stop. It is preferred to use a casting bath with a solvent/non-solvent ratio near the cloud point of the casting dope (Jacobs and Leukes, 1996). The lower limit of the solvent content in the casting bath should be the point at which the polymer dope in the bath actually starts to re-dissolve the nascent membrane. The solvent and the non-solvent used in membrane preparation determine both the activity co-efficient of the polymer at the point of precipitation and solidification.

3.2 The effects of dope extrusion rate and viscosity

3.2.1 DER

Researchers who reported on this all agreed that polymer dope extruding through a spinneret is subjected to various stresses which may affect the molecular orientation and relaxation and that certainly has an effect on the membrane structure. They also agreed that increasing dope extrusion rate would increase the shear stress and selectivity or rejection but reduce the permeability. (Feng et. al., 2001; Qin and Chung, 1999; Idris et. al., 2002; Porter, 1990).

Idris et. al. (2002) pointed out that both PWP and rejection increased with increasing dope extrusion rate. Qin and Chung (1999) learnt from their results that there was a critical dope extrusion rate over which the PWP and the rejection were not influenced dramatically. Qin (1999) spun the externally skinned membranes, and he observed that the membranes seemed to be thicker and denser with increasing dope extrusion rate. The outer edge of the cross

section was micro-porous for the lowest shear membrane and dense for higher shear membranes.

Qin (2001) continued with his study and he reported that the effect of shear rate on the performance of the final membrane capillaries also depends on the polymer concentration in the spinning dope. The most probable reason may be that the dope with high concentration has displayed different rheological behaviour from that with low concentration at high shear rates. He suggested that there may be two opposite factors within the spinneret during dope extrusion to influence the formation of the final membrane when the shear rate is increased:

1) The molecular chains tend to align themselves better and pack more closely to each other, leading to a denser skin formation.
2) A decrease in viscosity may occur at high shear rates because the reduction of chain entanglement results from the characteristic of a non-Newtonian power law fluid, resulting in a looser skin.

For the spinning dope with high polymer concentration, there was no critical shear rate to induce molecular orientation, which resulted in significant impact on the permeability and rejection performance of the final UF membrane. However, there was a critical shear rate for the spinning dope with low polymer concentration (Qin, 2001).

Graphically: - Qin and Idris showed the relationship between dope extrusion rate, flux and rejection as follows:

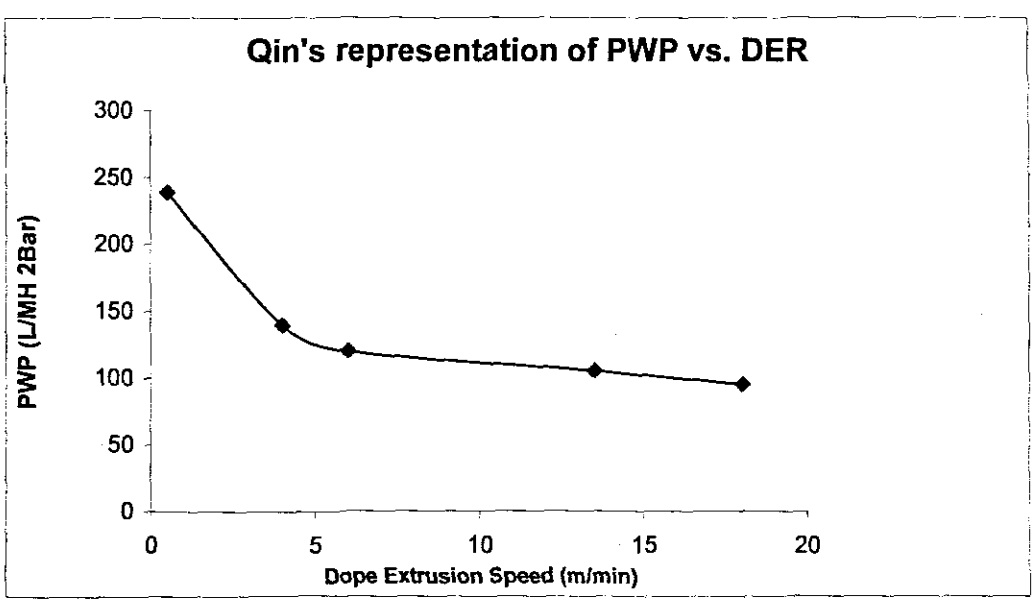

Figure 3.2.1: Qin's graphical representation of PWP vs. dope extrusion rate

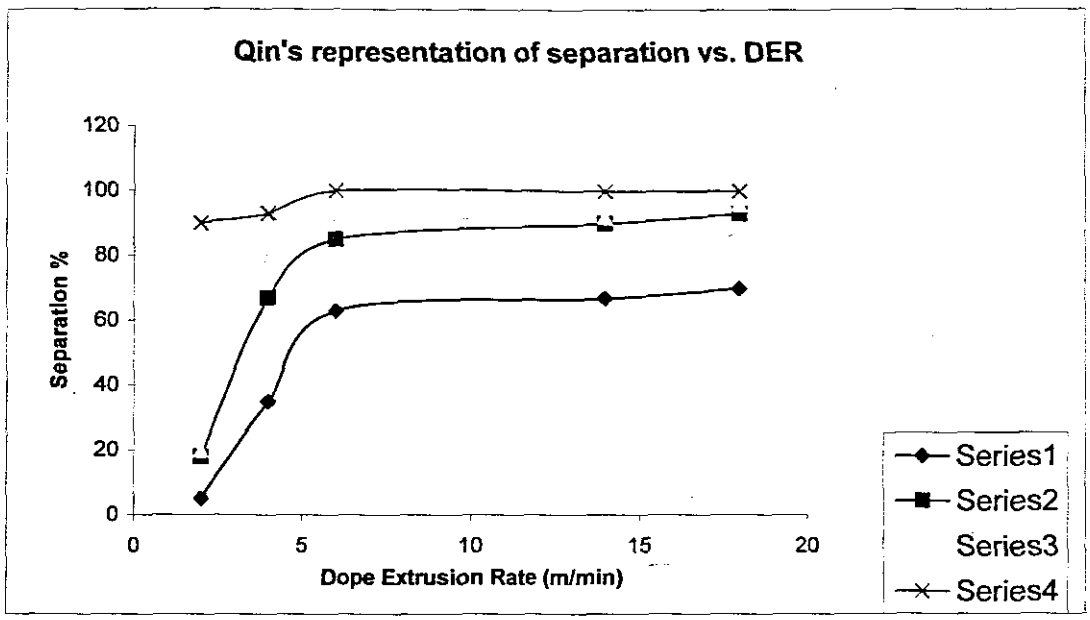

Figure 3.2.2: Qin's graphical representation of Separation% vs. dope extrusion rate

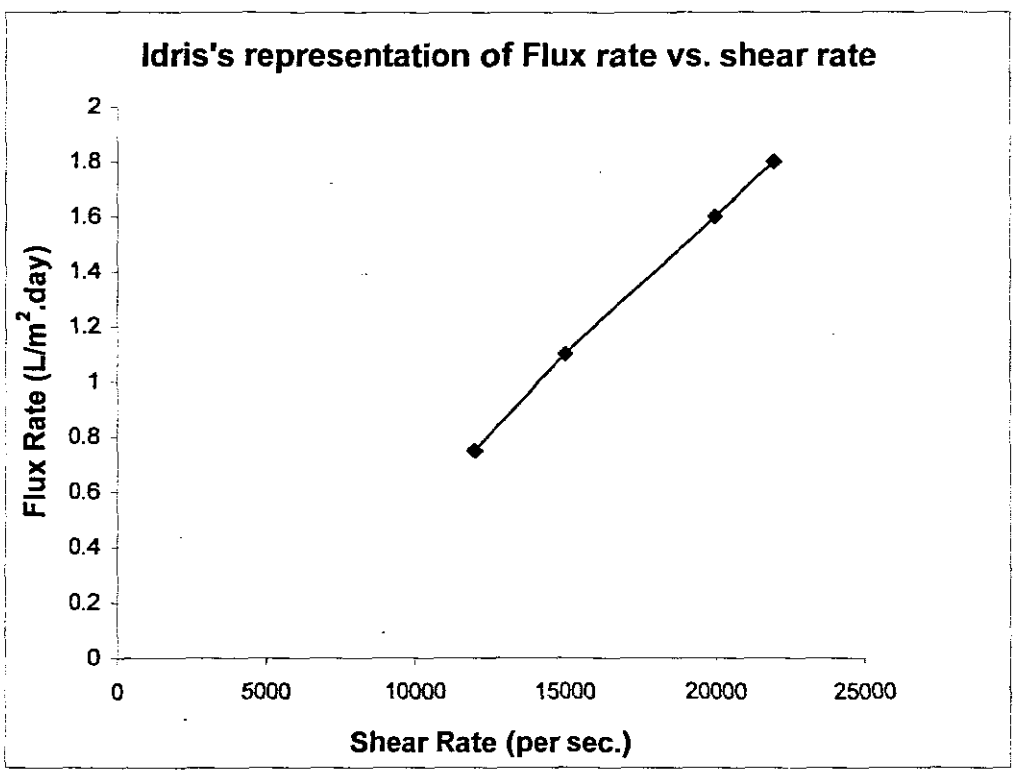

Figure 3.2.3: Idris et.al. graphical representation of flux vs. shear rate

3.2.2 Dope viscosity

The polymer concentration in the dope is one of the factors that determine the dope viscosity. At the same time, the dope viscosity can be adjusted by adding high molecular weight polymers. They are referred to as high molecular weight polymers (in some literature called non-solvents, polymer additives or surfactants) but the exact values of the limits of low or high molecular weights are not stated. More viscous or concentrated dope is said to be near its clouding point, which prevents the formation of †intrusion cells (Jacobs, 1997; Cabasso et. al. 1977).

Torrestiana et.al. (2002) conducted a study to gain an insight into the role of polymer additives on membrane formation and performance. Their standard polymer dopes contained 20% Polyethersulfone (PES) as the main polymer and 80% NMP as a solvent. The polymer additives used were Polyvinylpyrrolidone (PVP), polyethylene glycol (PEG) having the same molecular weight being 10 000 Dalton (that is considered to be a high molecular weight) and water. Addition of any of these polymer additives showed an increase in dope viscosity. Solutes used in the experiments for UF were, bovine serum albumin (BSA), with a molecular weight of 64 000 and lysozyme with a molecular weight of 13 000. The results showed that, as the viscosity of spinning dopes increased, the membrane thickness increased.

Han and Nam (2002) also used PVP as a polymer additive because of good miscibility with Psf and high solubility in water or non-solvent. PVP is known as an agent for suppressing microvoid formation in the phase separation membranes (Smolders and Reuvers, 1992; Wienk et. al, 1995). The higher the PVP content in the dope, the more the dope becomes thermodynamically unstable. At a low PVP level, the added PVP enhances liquid-liquid phase separation, therefore resulting in voids or pore formation. On the contrary, at a high level of PVP, the phase separation shows the reverse relationship, that is, an increase in phase separation time or the delay of de-mixing. In delayed de-mixing, solvent outward diffusion from the cast dope is favoured over inward diffusion of non-solvent into the dope.

---

†*Cavity, convection or intrusion cells- refer to those microvoids that extend to the fibre's internal or external surface*

Tsai et. al (2000) pointed out that for a hydrophilic non-solvent, hydrophilic polymer additives can enhance the formation of microvoids while lipophilic polymer additives cannot. For a lipophilic non-solvent, lipophilic polymer additives are more effective in changing membrane structure than hydrophobic polymer additives. Rejection increased with increasing the polymer additive content, while the permeation rate decreased gradually when the polymer additive content was increased. The low affinity between the polymer additive and the non-solvent plays an important role in the formation process of microvoids. Adding the hydrophobic polymer additive having low affinity with the non-solvent might be suppressing the formation of microvoids. Cabasso (1977) proposed that the location of intrusion cells[‡] and cavities depends upon the precipitating power of the non-solvent facing these surfaces. Smolders and Reuvers (1992) suggested that choosing a solvent-non-solvent pair with a low tendency of mixing with each other could suppress or even eliminate the formation of microvoids.

3.3 The effects of bore fluid flow rate and composition

Feng et. al. (2001) externally unskinned membranes and he noticed that an increase in bore fluid flow rate decreased the pore size on the outer surface of the hollow fibres, while it increased the pore size on the inner surface. He gave the results relating the BFF with PWP at 100 kPa and they showed an increasing PWP with increase in BFF. The inner diameter, outside diameter and the membrane thickness decreased with an increase in BFF.

Table 3.3: Feng's results showing the effect of bore fluid flow-rate on membrane dimensions and pure water permeability

BFF (ml/min)	OD (mm)	ID (mm)	Membrane thickness (mm)	PWP (L/m^2h)
0.1	1.5	0.92	0.29	41
0.2	1.4	0.92	0.24	127
0.3	1.3	0.86	0.22	176
0.4	1	0.8	0.1	198

Idris (2002) agreed that the membrane thickness decreases with increasing BFF because the polymer dope velocity relative to the bore fluid on the inner surface increases with an increase in BFF. The higher the BFF, the faster is the mass transfer at the inner surface, which means a higher rate of bore fluid/solvent exchange. That requires a shorter time for non-solvent/solvent exchange before polymer starts to solidify. Nucleation and growth of polymer-poor phase will proceed to a lesser extent. According to Porter (1990) very high precipitation rates (means short precipitation time) lead to a finger like microvoid structure. The use of a larger volume of bore fluid causes complete precipitation of the polymer as the non-solvent penetrates from the bore towards the outer periphery of the membrane wall. Slow precipitation rates, lead to asymmetric membranes with a sponge structure and very slow precipitation rates, lead to symmetric membranes with no definite skin at the surface. For a sponge type structure, the pore diameters are inversely proportional to the rate of precipitation. Higher precipitation rates, lead to finer pores whilst lower precipitation rates lead to coarser structures.

Termonia (1995) carried out the experiments by adding salt in the casting bath instead of a solvent. That showed a transition from a finger-like to a dense polymer structure at high salt concentrations. In this case, the transition was said not to be associated with any decrease in the rate of precipitation. It was advised to use a salt that is poorly miscible with the polymer solvent (Kools, 1998).

Kools (1998) suggested that the concentration of salt added should be low enough so that the diffusion of non-solvent in the polymer film can cause phase separation and the phase separated structure must be solidified to form a mechanical rigid structure.

3.4 An attempt at modelling the rate of skin growth in capillary membrane fabrication

3.4.1 Introduction

Flat sheet membranes are produced by casting a polymer dope as a thin film on a glass plate and immerse it into a casting bath containing non-solvent. For capillary membrane fabrication, dope is extruded as a hollow tube. It goes through a spinning bath, high in solvent content, to avoid precipitation on the external surface. Although four components,

namely, (polymer, polymer additive, co-solvent and solvent), are present in the polymer dope, only solvent and non-solvent will diffuse to a significant extent. Therefore this becomes a pseudo-binary diffusion case. The hydrophobic polymer does retreat from the interface and the forming pores that contain non-solvent but to a much less extent. The mobility of the polymer is much slower compared to the low molecular weight components (MW_{Psf} = 30 000 g/mol; MW_{NMP} = 99,13 g/mol and MW_{water} = 18,015 g/mol). The polymer can be regarded as a matrix phase in the dope in which the two components diffuse. Diffusion of the polymer additive and co-solvent are also insignificant.

The driving forces for mass transfer during membrane formation are the chemical potential gradients of solvent and non-solvent. Observations by Paul, 1968 have shown that a very distinct moving boundary is associated with nascent capillary membrane precipitation. One side of the boundary is dense, precipitated polymer, while the other side is the soft original dope. The boundary begins at the bore fluid/dope interface and moves outwards with time. Precipitation may be considered essentially complete when the boundary reaches the external surface.

Depending on the polymer-solvent-non-solvent system and the process parameters, there are three possible outcomes as the solvent diffuses into the bath and non-solvent diffuses into the dope:

1) a uniform and completely dense film having a density close to that of original polymer dope or
2) a homogeneous porous membrane or
3) an asymmetric membrane having a dense skin with a porous sub-layer.

The formation of such structures, that is, the uniform dense skin and porous structure have been discussed in detail in Chapter 2. The structure of membranes produced in this manner is determined by two distinct factors according to Young and Chen (1991):

1) the equilibrium properties of the ternary system and
2) the rate of phase separation.

Thus it is important to appreciate how the rates of transfer of the individual mobile components affect the structure of a formed membrane.

Kools (1998) stated that: "Today's membrane production by phase separation relies to a large extent on empiricism. Experimentally, phase separation processes are remarkably simple;

modelling of the process is as complicated. The high complexity of phase separation process makes a quantitative numerical simulation of diffusion process occurring during the de-mixing (voids formation) stage almost impossible."

Due to this complex interplay between various phenomena the present investigation has been strictly empirical. Nevertheless, a tentative discussion of modelling the skin formation is informative. The discussion is restricted to describing mass transfer on skin formation. The approach resembles the method used by Young and Chen (1991).

3.4.2 Theory

Many models have been proposed describing membrane formation by phase separation using flat sheet membrane formation. Reuvers et. al. (1987) and Kools (1998) simplified the moving boundary problem by describing the diffusion equations using polymer fixed co-ordinates. Cellulose acetate systems with different solvents and non-solvents were studied. These authors assumed the composition at the interface to be constant. This proposed model does not give an indication of the basis of the polymer fixed co-ordinates. Therefore, it was not adopted in this study.

Young and Chen (1991) proposed a model for developing equations of solvent and non-solvent diffusion by dividing the system into N hypothetic layers parallel to the surface of the casting dope and carry out the mass balance of solvent and non-solvent in each layer. With the casting dope immersed into the casting bath, the top layer, N, is formed. This happens rapidly at the casting dope /non-solvent interface. It also directly influences the second layer, N_2, by controlling the diffusion rate of solvent and non-solvent through the top layer. The composition variation of the second layer is thus governed mainly by the structure of the top layer. If there is a rough packing of polymer molecules in the top layer, then the permeation rate through the top layer of the casting dope is greater than the permeation rate through a dense packing of polymer molecules. In this way, the top and the second layer would influence the third layer, N_3.

Young and Chen (1991) proposed a model for developing equations of solvent and non-solvent diffusion on the following assumptions:

1. The membrane is divided into N hypothetical layers and there is a variation of composition from the surface (in case of flat sheet) or bore fluid/dope interface (in case of capillaries) in the casting dope to the inside part (flat sheet) or external surface (capillaries).
2. Each layer is assumed to be formed by the rapid aggregation of polymer molecules; that is to say, each layer undergoes phase separation immediately upon non-solvent diffusing into this layer. It therefore solidifies very rapidly to form a new film of solid polymer phase so that the rate of formation of the next layer is influenced. The above assumption can be justified by the fact that the overall process for the phase inversion needs only 1-2 seconds.
3. The perpendicular (flat sheet case) or radial (capillary case) movement of the polymer molecules is assumed to be negligible during the formation of each layer, so this model is a pseudo-binary one (only solvent and non-solvent are diffusing).
4. If the thickness of each layer is small enough, then the ratio of fluxes of solvent and non-solvent can be considered to be constant.

The flux ratio can be written as:

$$k = n_A / n_B \qquad (1)$$

Figure (a) represents the flat sheet case whilst (b) represents the capillary case (a portion)

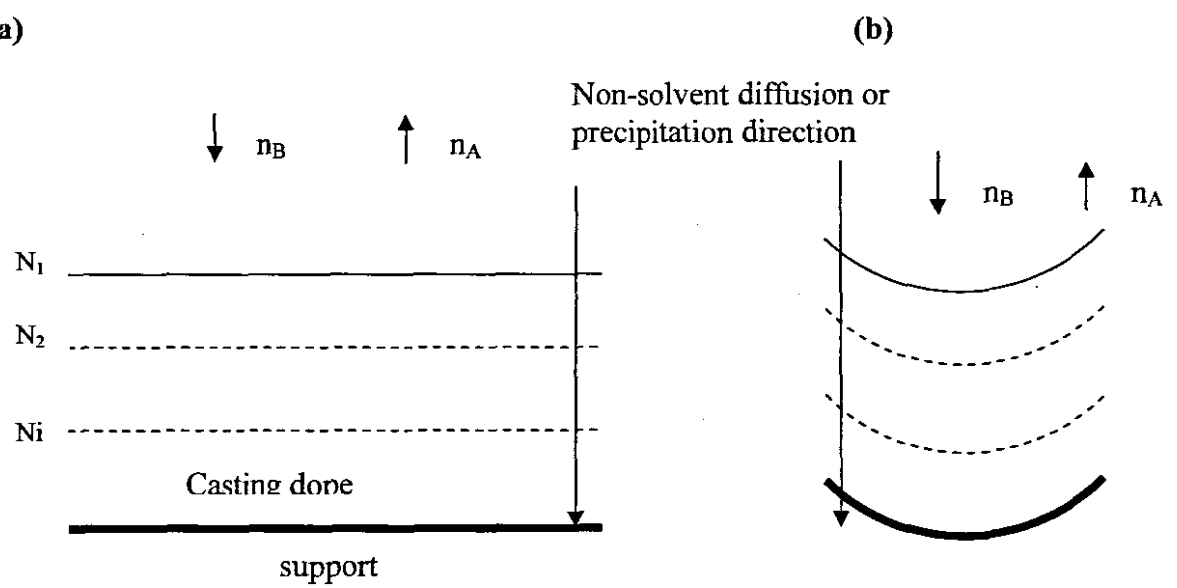

Figure 3.4.2 (a and b): Schematic presentation of diffusion during membrane formation

where n, is the flux in (L/m^2h) and N_1, N_2, ...is the series of hypothetic layers

The components are indexed as follows:

Solvent (A), non-solvent (B) and polymer (3).In general, each layer has a k_i value and $k_1 \neq k_2$ ..... $k_{N-1} \neq k_N$

They proposed the following diffusion equations describing the formation of each layer by using a constant flux ratio model:

$$\partial \bar{\rho}/\partial t = -\vec{\nabla}(\vec{n_B} + \vec{n_A}) \qquad \text{.....(2)}$$

$$\partial \bar{\rho}_A/\partial t = -\vec{\nabla}\vec{n_A} \qquad \text{.....(3)}$$

In these equations,ρ is the dope density and overbars are to signify mass fraction and $\vec{n}$ signifies flux in a given direction. Since the net perpendicular movement of the polymer molecules is neglected during the formation of each layer by assumption 3 above. Therefore the non-solvent flux based on pseudo-binary diffusion equation formalism becomes:

$$\vec{n_A} = -\bar{\rho} D \vec{\nabla} \bar{W}_A + \bar{W}_A(\vec{n_A} + \vec{n_B}) \qquad \text{.....(4)}$$

The following figure gives a general idea of various composition paths that would compare to different k values on the ternary equilibrium diagram.

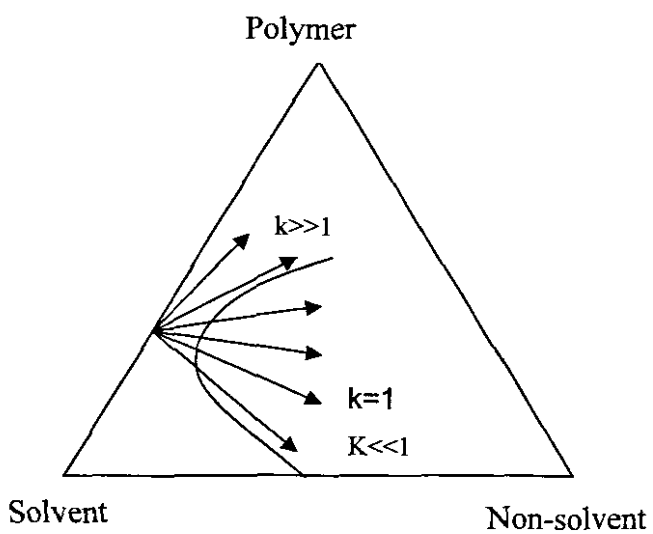

Figure 3.4.2 (c): Ternary diagram showing alternative composition paths of a forming membrane

In cases where k >> 1, the composition path remains entirely in the homogeneous region. This result in a steep (goes towards the polymer) composition line, that directly enters the

solidification region, leading to a dense polymer layer. For k <<1, the composition line has a less steep (goes towards the non-solvent) slope and crosses the binodal, into the region where phase separation will ultimately lead to a porous structure. If the k <<1, the composition line enters the binodal region at a much lower polymer concentration. In this way a more micro-porous structure is obtained and it is even possible to obtain a finger-like structure.

When the rate of solvent diffusing outwards from each layer is high compared to non-solvent diffusing in (k>>1), the resulting membrane is dense. On the other hand, when the rate of non-solvent diffusing in is greater than the rate of solvent diffusing out (k<<1), a micro-porous membrane is produced without a skin.

3.4.3 Proposed Model

Following Young and Chen (1991) approach described above for a flat sheet case, the rate of mass transfer will be determined based on their assumptions with the following additional assumptions:

If the capillary membrane can be cut length-wise and stretched out, it resembles a flat sheet case, which does not differ from a capillary in terms of diffusion process.

1. The diffusion process is one-dimensional, to the z direction.
2. The bulk flow of dope is neglected so that the mass transfer of component A, which is the solvent, into the non-solvent (B) is totally due to the molecular diffusion.
3. Non-solvent diffusing from bore fluid to dope is negligible.

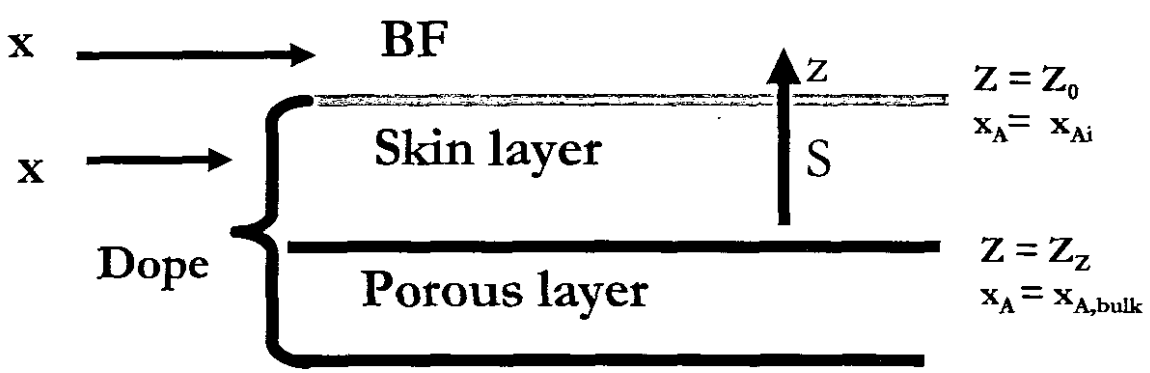

Figure 3.4.3: Experimental presentation of the membrane forming system

$$N_A = -D_{AB}\frac{dc_A}{dz} \quad \text{.....1}$$

Where N_A, is the molar flux of component A, C is the concentration, z is the thickness of the membrane and D_{AB} is diffusion coefficient of component A through B.

Solvent molecules at the interface diffuse into bore fluid very rapidly. A first thin film of skin layer is then formed and acts as a resistance to mass transfer.

Young and Chen (1999) stated that "Under special conditions the flux ratios on each layer are approximately equal, so that a homogeneous membrane is exhibited with each layer having the same composition path and structure. In that case, the N numbers of layers are reduced to one layer. Each layer has the same formation mechanism, that is, the lower layers are not influenced by the upper layers."

For a steady state system:

$$\frac{dN_A}{dz} = \frac{d^2c_A}{dz^2} = 0$$

Working with the mole fraction: x_A

Where $x_A = c_A/c$ and c is t $N_A = -cD_{AB}\frac{dx_A}{dz}$ 2

Within limits: $z = z_0 \quad x_A = x_{Ai}$

$z = z_Z \quad x_A = x_{A,bulk}$

$$N_A = -\frac{cD_{AB}}{z_z - z_0}x_{Ai} - x_{A,bulk} \quad \text{.....3}$$

3.4.4 Discussion of diffusion model theory

The skin thickness can be measured using a microscope. There is an uncertainty as to what diffusion co-efficient to use. It is known that at the bore fluid/dope interface, the solvent is diffusing directly into the non-solvent. Once a thin film of skin is formed, solvent diffuses through a dense skin formed then to the non-solvent. Anderson and Ullman (1973) and Castelli and Ottani (1981) cited by Altinkaya and Ozbas (2004) assumed finite film thickness, constant specified surface concentration and used self-diffusion co-efficient rather than mutual diffusion co-efficient. Tsige and Gary (2003) performed some simulation analysis of diffusion of solvent into a polymer. They reported that the diffusivity found from fitting Fick's second law, is found to be independent of time and equal to the self-diffusion

constant in the dilute solvent limit. Kools (1998) also performed simulations, where the following calculation procedures were followed:

i. An interfacial composition was arbitrarily chosen
ii. Diffusion profiles in the polymer dope were calculated using the D03PHF routine from the NAG-library to solve the set of differential equations
iii. The fluxes to and from the polymer dope were calculated
iv. Diffusion profiles in the casting bath were calculated using D03PHF routine from the NAG-library to solve the set of partial differential equations.
v. The fluxes to and from the casting bath were calculated and compared to those in step 3.
vi. The entire procedure was repeated with different interfacial compositions, until the fluxes from step 3 and 5 were equal.

Reuvers (1987) and Kools (1987) suggested that the friction co-efficients could be related to binary diffusion co-efficients through this equation:

$$R_{ij} = \frac{\bar{V}_j RT}{M_i D_{ij}}$$

With:

D_{ij} : binary diffusion between i and j

M : molecular weight of component i

R : universal gas constant

T : temperature

The binary co-efficient R_{ij} can be obtained by measuring the sedimentation co-efficient of the polymer in the solvent as function of the concentration. The diffusion co-efficients for NMP-PsF and NMP-water pairs were obtained from Kools, 1998 thesis.

$D_{NMP\text{-}WATER} = 6{,}01X10^{-10}\ m^2/s$

$D_{NMP\text{-}Psf} = 1{,}8x10^{(-8\text{-}4{,}386*\Phi PsF)}\ m^2/s$

$D_{NMP(self)} = 5{,}95x10^{-6}\ m^2/s$

Φ is the volume fraction

3.4.5 Local composition measurement

Phase separation gives rise to scattering of light, which can be followed by measuring light transmission through the polymer dope while precipitating (Kools, 1998). Light transmission experiments were performed by to obtain the onset and completeness times of phase

separation in the immersion-precipitation process. The principle of light transmission experiments is that the light transmittance of the casting dope decreases with the appearance of optical inhomogenities, which can either be induced by liquid–liquid de-mixing or solid–liquid de-mixing. Therefore, the time at which the light transmittance begins to decrease is identified as the outset of phase separation; whereas the time at which light transmittance drops to a stable constant value is considered as the completeness of phase separation.

To carry out the experiment, Young and Chen (1999) directed a light beam on the membrane dope. A detector continuously measured the transmitted light intensity and a computer was used to store and analyze the intensity profile. Beerlage et .al. and Kools (1998) cited the work of Reuvers (1987) who performed light transmission experiments to investigate the de-mixing behaviour of the system cellulose acetate-acetone-water. A large dish was filled with a mixture of solvent and non-solvent at the desired temperature. Below this casting bath a light sensor was placed, coupled to a recorder. A light source was used above the casting bath. The polymer dope was cast on a small glass plate using a knife with a casting thickness of 0.20 mm. A second glass plate was placed above the first one on top of four stubs to reduce the convective movement induced by the immersion in the casting bath. As soon as the glass plates are immersed in the bath, diffusion of non-solvent into and of solvent out of the film starts; the light transmission through the system is measured as a function of time. When de-mixing starts, i.e., when the film becomes turbid, the light transmittance decreases: $I_t < I_o$, with I_o the initial intensity. Delayed de-mixing occurs when the decrease in light transmission starts only after a certain period of time. If this process starts at the moment of immersion, instantaneous de-mixing occurs. The experimental set-up by Reuvers (1987) of light transmission measurements is illustrated in the figure below.

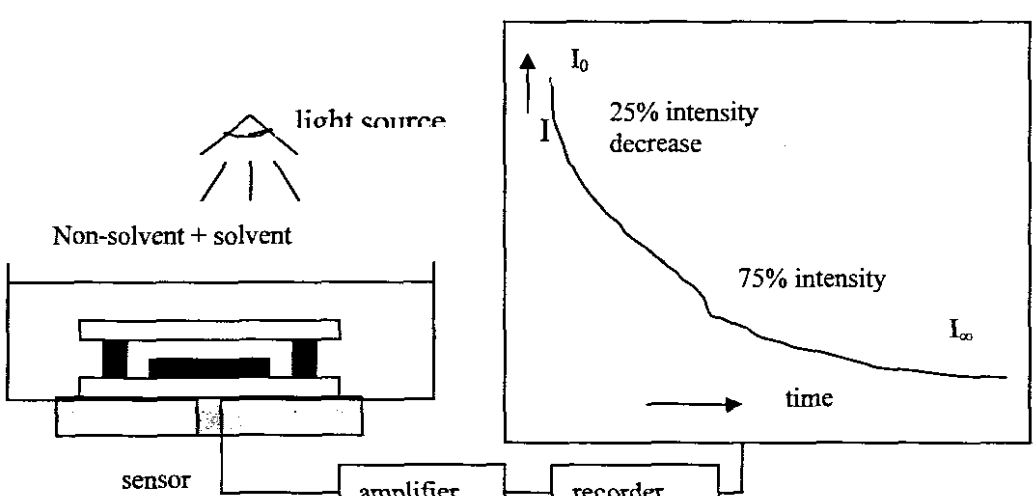

Figure 3.4.5: Experimental set-up of light transmission measurements

To determine the cloud point of a dope and the time taken for a membrane to form completely, this set-up could be used. The local concentration of the forming membrane could also be known.

3.4.6 Conclusions

To evaluate the model further experiments, such as local composition difference as a function of:

(a) thickening skin layer

(b) diffusion co-efficients are needed.

It is clear that the rate of mass transfer during membrane formation is related to the resultant membrane structure. That makes it possible to vary the structure from dense to porous asymmetric by either

(a) varying the chemical potential difference of solvent and non-solvent or

(b) varying the flow rates of bore fluid and dope.

This section served as a guide to what experiments to do. Hence the bore fluid and dope fluid flow rates were varied. The dope composition was also varied by not adding the polymer additive because it was learnt that the dope composition is related to the cloud point, which is a point in the ternary phase diagram. The chemical potential of solvent and non-solvent was experimented by using different bore fluid compositions (NMP and NaCl).

3.5 The effects of the distance between the spinneret and external spinning bath

Chung and Hu (1996) conducted a study on determining the effect of the distance between the spinneret and the external spinning bath by spinning double skinned membranes. The spinning dope and the bore fluid met at the tip of the spinneret, then passed through an air gap ranging from 0-14,4 cm before entering the external spinning bath. It was reported that an increase in air distance resulted in significant decrease in flux but an increase in rejection (Chung and Hu, 1996; Khayet, 2003; Aptel,1985). The inner diameter, outer diameter and thickness of the membrane decreased with an increase in distance between the spinneret and bath.

Two mechanisms were said to be taking place in the air distance during membrane formation (Chung and Hu, 1996):

i. Orientation of polymer molecules and phase separation

ii. Elongation stress because of gravity

Membranes spun with longest distance had one array of finger-like voids closed to the inner and outer surface. Membranes spun with no air gap had two arrays of finger-like voids closed to the inner and outer surface (Chung and Hu, 1996; Kim et. al., 1995). Kim et. al. (1995) gave the following explanation to be the cause of different membrane forming structures with the air gap distance. He stated that when the spinning height was zero, the phase separation occurred from both the inner and outer surfaces at the same time. That caused vigorous and convective type precipitation that occurred at both inner and outer surfaces. That is how a double finger-like void structure was created in the cross section of the ††wet spun membranes. With increasing air gap, phase separation started occurring from the inner surface of the hollow fibre and propagated toward the outside before the phase separation, by immersion, occurred from the outer surface. The resulting forming membrane also showed the more porous outer skin with increasing air gap distance.

Summary

- To avoid precipitation, which results in skin formation, on the outer surface of the nascent membrane, the external spinning bath has to be introduced near the spinneret.
- This external spinning bath has to be high in solvent content.
- There is a conflict of ideas concerning the effect of DER on the performance of the membrane. That is as a result of poor understanding of the behaviour (alignment, elongation and elasticity) of the polymer molecules when they extrude out of the spinneret.
- Addition of a polymer additive to the dope is known to increase the dope viscosity and enhance microvoid formation.
- The thickness, inner diameter and outer diameter were reported to decrease with increasing BFF.
- Increased air gap distance between the spinneret and external spinning bath may result in an external skin formation. The flux of the membranes decreases with increasing air gap whilst the rejection increases.

- The author does not know the distance at which the external skin is formed on increasing the air gap because this effect from the literature was investigated on double skinned membranes. The shortest distance used by the author then was 5 cm.
- Young and Chen and Smolders and Reuvers are the authors who gave a clear understanding to these factors.
- This author's experience under guidance of E.P. Jacobs at IPS concerning the use of external spinning bath made it easier to understand the literature.

---

††Wet spun membranes – means there was no air gap between the spinneret and the external spinning bath

CHAPTER 4

SELECTION OF EXPERIMENTAL VARIABLES

4.1 External spinning bath composition

External spinning bath composition was reported as one important parameter in the fabrication of externally unskinned membranes as discussed in details in section 3.1. This external spinning bath high in solvent content is introduced to avoid external skin formation or precipitation. The external spinning bath composition should have a solvent/non-solvent ratio near the dope's cloud point. The lower limit aqueous content of the external bath is the point at which the bath actually starts to re-dissolve the nascent membrane. No specific compositions were given as to what the high or low solvent contents are. However, externally unskinned membranes had previously been produced at IPS using external spinning bath composition of 94,5% solvent content. This was taken as a reference for this author's study, and then spinning bath compositions below and above this point were tested using 99, 96, 94 and 93% N, Methyl 2- pyrrolidone (NMP) content.

4.2 Dope extrusion rate and viscosity

DER

Due to lack of guidance from the literature as to specific minimum and maximum values of dope extrusion rates used, estimations on the experimental values of dope extrusion rates were made. The only guide was a personal suggestion given by Deon Koen at IPS, a person who has been in the field of membrane fabrication for a long time. The limitations of data, according to his suggestion were: -

- At too low dope extrusion rates, it will be difficult to produce a membrane. The reason being that, the very thin nascent membrane cannot stand the large volume of bore fluid flowing within. The pressure exerted by the bore fluid flowing within the dope can cause the nascent membrane to burst out.
- At too high dope extrusion rates, it is highly possible to obtain a membrane with an external skin layer. The reason being that, the nascent membrane could reach the

humidity chamber before it gets precipitated on the outer surface. Then vapour in the chamber will precipitate the jelly outer layer of the nascent membrane and a skin will be formed.

No specific values were given as to be the minimum and maximum dope extrusion rates. Therefore the dope extrusion rate experimental values were randomly chosen. The experiments were conducted at different dope extrusion rates namely: (2,5; 3,0; 4,0; 4,5 and 5,0 ml/min) while the bore fluid flow rate was held constant at 4,5 ml/min. The dope was spun at different external bath compositions stated in section 4.2. The conditions under which the experiments were conducted are shown in table 4.2 below.

Table 4.2: Conditions under which the dopes were spun

	(a)	**(b)**
Mixing date	16/09/02	22/09/02
Spinning date	23/09/02	25/09/02
Room temperature	25.5^{0}C	23.5^{0}C
Spinning dope temp.	room temperature	room temperature
External spinning bath temp.	20.5^{0}C	22^{0}C
Bore fluid temp.	room temperature	room temperature
Rinse bath temp.	19.5^{0}C	19^{0}C
Bore fluid composition	2%NMP + 98% water	2%NMP + 98%water
External spinning bath composition	96%NMP + 6% water	94%NMP + 4% water
Rinse bath composition	RO water	RO water

Viscosity

The viscosity of a polymer dope is said to have an effect on membrane structure (Torrestiana et. al., 2002; Han and Nam, 2002). Voids growth extent can be affected by dope viscosity. The polymer additives are known to increase the dope viscosity as discussed in section 3.2.2. Therefore, the standard dope formulation in table 6.1 was made without adding PEG 600 (the 600 refers the molecular weight of the polymer which is 600 Dalton). The quantity of PEG from the formula was substituted with the polymer (Psf)

4.3 Bore fluid flow-rate and composition

It was explained that the skin and microvoid formation depend mostly on the rate of solvent/non-solvent exchange between the bore fluid and the polymer dope. The literature review of the effects of BFF and composition are discussed in section 3.3. Then it was decided to study the effect of the volumetric flow rates of the bore fluid on membrane structure and performance. Five experiments were conducted at different bore fluid flow rates (1,5; 2,5; 3,5; 4,0 and 4,5 ml/min) while the dope extrusion rate was held constant at 4,0 ml/min. The experiments were spun under the same conditions represented in table 5.1 (see section 5.2)

The compositions of bore fluids were also changed. This was done in DER intervals between 3,0 ml/min and 4,0 ml/min. Two bore fluid compositions used were 2% NMP with water and 2% NaCl with water. Following is the table under which the experiments were conducted

Table 4.3: Conditions under which the dopes were spun

Mixing date	22/05/03
Spinning date	22/05/03
Room temperature	21.5^0C
Spinning dope temp.	room temperature
External spinning bath temp.	21^0C
Bore fluid temp.	room temperature
Rinse bath temp.	22^0C
Bore fluid composition	2%NMP + 98% distilled water; 2%NaCl +98% distilled water
External spinning bath composition	94%NMP + 4% water
Rinse bath composition	RO water

4.4 Spinneret position and size

As mentioned earlier in section 1.2.3, the externally unskinned membranes at IPS were produced by introducing the spinneret at the bottom of the spinning bath, and the membrane was drawn vertically from the spinneret by rollers. Alternatively, it was positioned very close (about 5cm) to the external spinning bath and the membrane was allowed to fall freely from the spinneret into the bath.

The last mentioned method was used in this study experiments because it gives the nascent membrane more time for diffusion of non-solvent from the bore fluid to the external surface, by running twice the bath length, before reaching the humidity chamber. Different spinneret sizes were used in determining the membrane dimensional effects.

4.5 Summary

The variables used in the experiments performed in this study are tabulated below.

Table 4.5: Summary table of experiments performed

Variables	Values
External spinning bath composition	99; 96; 94 and 93 % NMP
DER (initial experiments)	5,0; 4,5; 4,0; 3,0 and 2,5 ml/min
DER (final experiments)	3,90; 3,75; 3,60; 3,45; 3,30; 3,15 ml/min
DER (on using small spinneret)	3,0; 2,5; 2,0; 1,5; 1,3; and 1,1 ml/min
Dope viscosity	Dope formulation in table 6.1 with PEG 600 and without PEG 600
BFF	4,5; 4,0; 3,5; 2,5; 1,5 ml/min
Bore fluid composition	2%NMP + 98% distilled water; 2%NaCl + 98%distilled water
Spinneret size	Large spinneret (ID=0,063mm;OD=0,273mm). Small spinneret (ID=0,012mm;OD=0,056mm

CHAPTER 5

EXPERIMENTAL MATERIALS AND METHODS

5.1 Membrane materials

The experimental facilities and method used by Jacobs and Leukes (1996:151) were used for this study because they were successful and reliable. The following dope composition was used:

Table 5.1: Dope Formulation

Constituent	**Mass %**
N, Methyl 2- pyrrolidone (NMP)	35
Methyl Cellusolve (MC)	10
Poly Ethylen Glycol (PEG) 600	32
Polysulfone (Psf)	23

Table 5.2: Properties of polymer (Psf), solvent and non-solvent used at 298,15K

These are the properties of the polymer, solvent and non-solvent used in this study.

	Psf	**NMP**	**Water**
Molecular weight (g/mol)	30 000	99,133	18,015
Glass transition temperature (K)	462	143	137
Density (g/cm^3)	1,27	1,0251	0,9989
Boiling point (K)	-	477	373,15
Water absorption	0,2–0,8%	-	-
Liquid viscosity (Pa.s)	-	$1,66X10^{-3}$	$9,76X10^{-3}$
Supplier	BASF	Merck	RO water prepared at IPS

Chemical structure of NMP

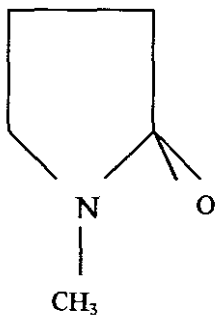

Figure 5.1.1 (a): Chemical structure of NMP

Chemical structure of Psf

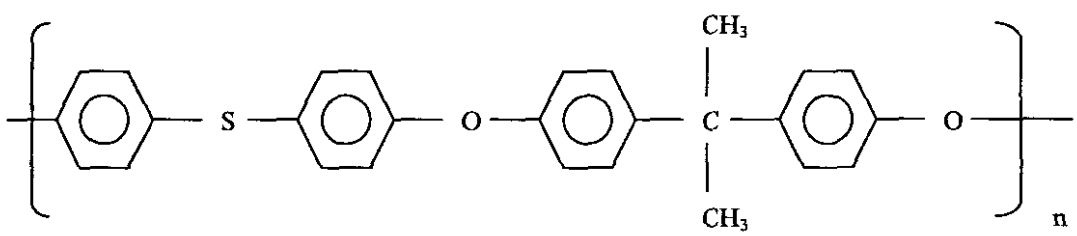

Figure 5.1.2 (b): Chemical structure of Polysulfone (Psf)

5.2 Materials and spinning dope preparation

Polysulfone (Psf), in the form of granules, was always oven dried for twelve hours at 45^0C before usage to extract any moisture absorbed. All polymer dopes were kept in closed bottles to avoid evaporation of solvent and to avoid water sorption. NMP is known to absorb water.

Grade 3010 Ultrason S Polysulfone, Psf from BASF was used. The N, Methyl 2- pyrrolidone (NMP) and Methyl cellosolve (MC), co-solvent, were vacuum distilled in an inert atmosphere and stored. A chemically pure grade of polyethylene glycol (PEG 600,i.e., molecular mass 600 Dalton) was used as low molecular mass surfactant. Dope was prepared in a 5-litre kettle equipped with high-speed overhead stirrer, and heated with oil. The shaft of the stirrer was passed through a Liebig condenser, which prevented loss of low boiling

solvent (397K), which is MC. The dope temperature was maintained below 60^0C. A minimum period of 48 hours was required to obtain a homogeneous dope solution. The dope was then decanted into 5-litre Schott bottles and vacuum degassed in a desiccator, directly before use.

A schematic presentation of equipment used in dope preparation is shown in figure 5.2 below

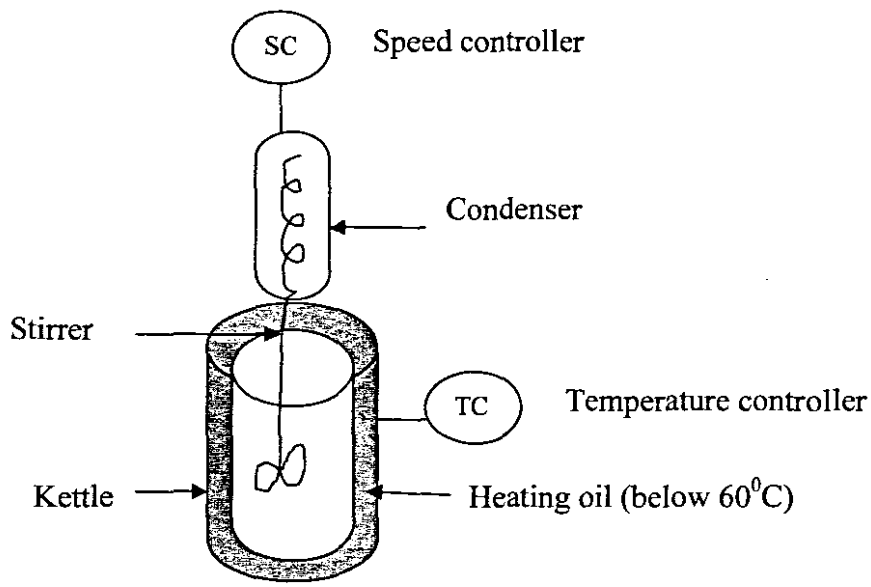

Figure 5.2: Schematic set-up of equipment used in casting dope preparation

5.3 Spinning process for externally unskinned capillary membranes

Externally unskinned membranes were formed by extruding a polymer dope through the annulus of a tube-within-tube spinneret. The dope was pumped from the reservoir by means of a stainless steel precision gear-metering pump. A pump speed controller regulated the pump speed. The outer diameters of the spinnerets were 0,273mm and 0,056mm whilst the inner diameters were 0,063mm and 0,012mm respectively.

To produce asymmetric capillary membranes with the skin on the inside, the precipitant, bore fluid was directed through the central bore. Thus, the precipitation progressed from the inside outwards.

The bore fluid used consisted of 2 % NMP (solvent) and 98 % water (non-solvent), pumped from the reservoir and passed through a filter. The flow rate of the bore fluid was monitored by a rotameter and controlled by a gear pump. The flow of bore fluid prevented the

membrane from collapsing before precipitation has taken place and also played a role in the precipitation process.

The spinneret was positioned 5 cm above the external spinning bath and the nascent membrane was allowed to fall freely from the spinneret into the external spinning bath. This height was selected so as to avoid nascent membrane precipitation from the external surface. The nascent membrane then went via a roller at the bottom of the external spinning bath whilst being drawn vertically upwards, then via the humidity chamber onto the take-up drum, guided by the rollers. The external spinning bath length was 116 cm. Therefore the forming membrane travelled twice that length before reaching the humidity chamber.

An air humidity chamber was positioned 10 cm above the external spinning bath to fix the membrane structure since the nascent membrane was still swollen, gel-like and soft when it was withdrawn from the external spinning bath. The membrane was guided through the guide-rollers to the non-solvent bath to rinse excess solvent filling the pores. The rinse bath was 9,92 meters long and the membrane ran three times the bath length within the bath and was then collected by the take up drum.

The external spinning bath contained N, Methyl 2- pyrrolidone (NMP), a solvent that has the hazardous effects listed in appendix B. Protective gloves, a gas mask, safety spectacles and protective clothing were worn when spinning the membranes. The spinning bath had to be covered at all times to prevent NMP vapour emission into air. With the membrane having to be spun directly in the bath, this was difficult to achieve. Extraction fans were used then to avoid accumulation of NMP vapour. Below is the schematic presentation of this study spinning line.

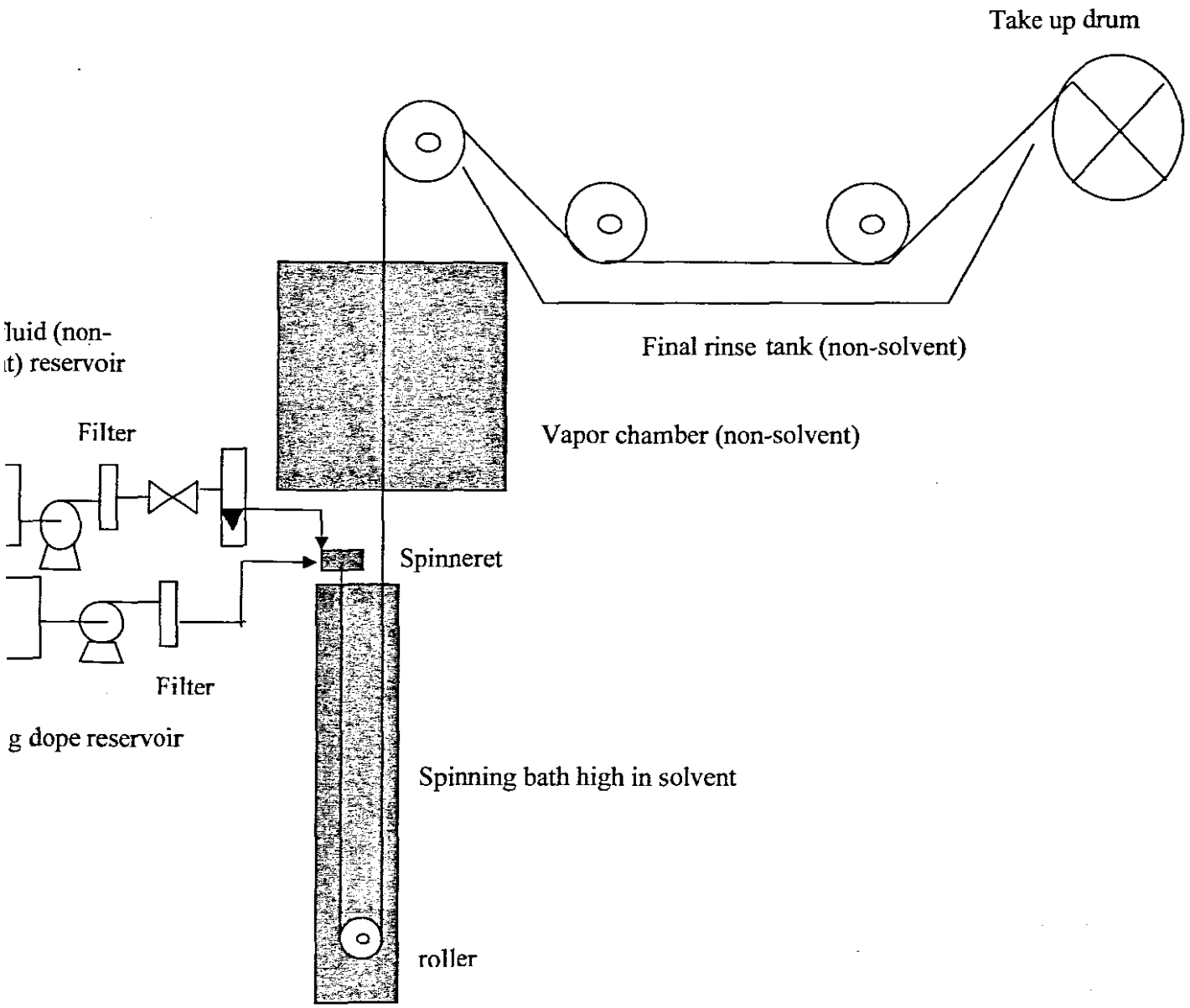

Figure 5.3: Schematic presentation of experimental spinning line

5.4 Measurement of membrane characteristics and performance

5.4.1 Module fabrication

The capillaries produced were tested for flux and rejection by building membrane modules in the following manner. Ten membrane capillaries, 35 cm long, were assembled into bundles. Each end of the bundle was sealed with a five minutes rapid solidifying quickset epoxy resin (Araldite ®). The bundle was potted into steel tubes at both ends. The tube side of the capillaries was kept open to fluid flow. The prepared module was fitted into a stainless steel pressure cell for water permeation measurement at 100 and 200 kPa.

5.4.2 Membranes performance tests

Feed, which consisted of 0,5 % PEG 35 000 (MW) solute in solution with water, was pumped from the feed tank by means of a Hydrocelle pump and entered the bore side of the capillary bundle. This molecular weight of solute was chosen because it is within the range of molecules that Ultra-filtration membranes can separate. The temperature in the feed tank was kept constant by means of a coil at 20^0C. The feed passed through a filter, to the membrane module. The flow rate was kept constant at 1 l/min using a flow controller and the readings were taken using a rotameter. The pressure was kept constant at 100 and 200 kPa and readings were taken using a pressure gauge. Permeate was collected at the membrane cell using a volumetric flask and the retentate was returned to the feed tank. The figure below represents the set up of the membrane performance test as presented by the Encyclopaedia Polymer (1989).

Red dye was added to the feed tank to easily detect if the test cells are leaking and /or membranes rejection is poor. Pure water was then allowed to run through test cells for 30 minutes before taking pure water flux readings. Then the feed containing PEG was tested afterwards for UF flux.

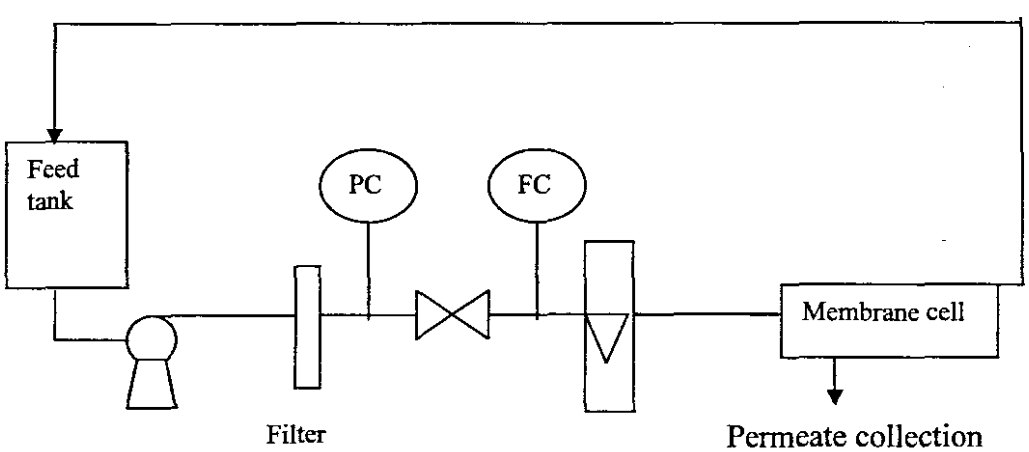

PC – is the pressure controller
FC – is the flow controller

Figure 5.4.2 (a): Schematic presentation of the membrane performance test (Open loop system for Ultra-filtration)

The open loop system where retentate is returned to the feed tank was used in our experiments because the cross flow velocity and trans-membrane pressure are controlled with

one centrifugal pump and a backpressure valve. The alternative method is a closed loop system shown in the figure:

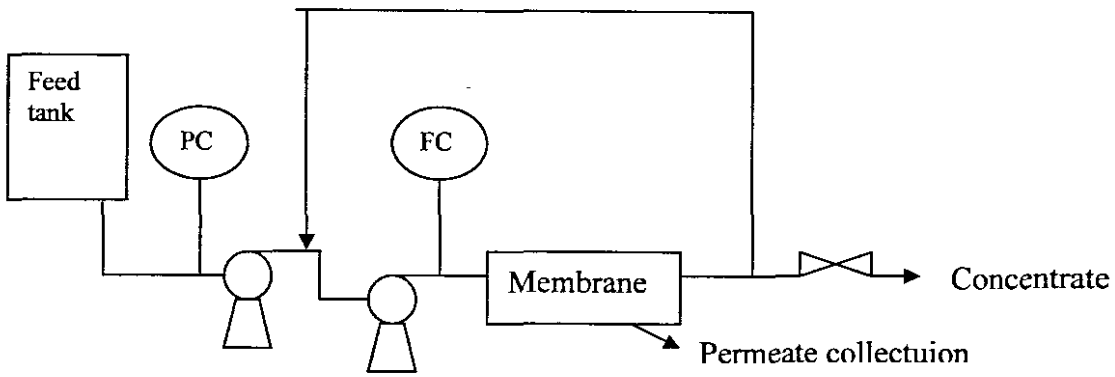

Figure 5.4.2 (b): Closed loop system for Ultra-filtration

Empty beakers were cleaned, dried and weighed using a weighing balance that is accurate to four decimals (0.0001g). Two 50 ml samples of both feed and permeate were collected, evaporated and dried in an oven at 45^0C and weighed when cool. The times taken to fill in the 50ml of permeate was recorded and the membrane flux was calculated using the formula:

$$F = \frac{A.V}{t}$$

Where A, is the effective membrane area; V, is the volume of the collected sample and t the time taken to fill 50 ml volume.

The effective area was calculated using the formula $A = 2\pi rln$

where r, is the radius of the membrane; l, is the length of the cell and n, the number of capillaries making up the cell module.

Rejection was determined using the formula: $R = 1 - \frac{C_P}{C_f}$

Where C_p and C_f are permeate and feed concentrations respectively.

The concentrations were determined by subtracting the value of the dried empty beaker from that of the dried beaker containing feed and permeate, which gives the amount of PEG in a 50ml samples of feed and permeate.

Table 5.4: Example of masses of dried samples collected (feed, permeate and retained)

Dried feed sample mass	Dried permeate sample mass	Mass solids retained
0,1190	0,0035	0,0055
0,1193	0,0041	0,1152
0,0998	0,0348	0,0650
0,0931	0,0566	0,0365

5.4.3 Diameter determination

Sample membranes were fractured at liquid nitrogen temperatures in order to obtain smooth surfaces. This was done by dipping the sample membrane into liquid nitrogen. The sample membrane freezes or solidifies then it is easily fractured without damaging the membrane structure. Three samples were taken in each experimental membrane, a travelling microscope was used to determine their diameters and an average was taken.

5.4.4 SE M photos

Membranes were fractured in liquid nitrogen (70K) and then gold sputtered. The gold sputtering does not change the structure of a membrane but gives better scattering when the photos are taken. This was important to do because membrane samples are polymeric so they are poor conductors of electricity. For an SEM to work well, the samples have to be conductive. Specimen membranes were observed with a Leo Model at 1430 variable pressure. The voltage used was 7 kV and the working distance = 6 mm. If the distance is too short, the light rays may damage the membrane by melting it.

5.4.5 Solvent removing methods and their effects

One factor, which was thought to be having an effect on membrane dimensions and hence on the performance, was the presence of solvent within the voids. It was decided to determine this effect by removing solvent from the voids of the membranes. The usual procedure for solvent removal in polysulfone membranes at the IPS is to soak them in 50% aqueous glycerol solution for 24 hours and then hang them to dry for a week in a high humidity atmosphere. However, this leaves some glycerol in the membrane pores. These are referred

to as 'wet' membranes. The pure water flux of these membranes was found to be lower than expected. Therefore alternative means of solvent removal were investigated.

An alternative solvent removal procedure was proposed by Van de Walt (1999) in which membranes were soaked in methanol for 24 hours, dried in a methanol atmosphere for three days, and then hung in the laboratory atmosphere for another day. As methanol has a lower surface tension and is much more volatile than glycerol, all of it evaporates from the membrane pores and/or voids and leaves them filled only with air, without damaging the pore structure. These are referred to as "dry membranes". However the test methods for all membranes were the same, whether treated with glycerol or alcohol.

CHAPTER 6

EXPERIMENTAL RESULTS AND DISCUSSIONS ON FABRICATION VARIABLES AND THEIR EFFECTS ON MEMBRANE STRUCTURE AND PERFORMANCE

6.1 Effect of external spinning bath composition

6.1.1 Results

The external spinning bath was found to have the effect reflected by the SEM photos on membrane structures. The resultant structures are discussed in the discussion section below. Below are cross sections of membranes spun at different external spinning bath compositions.

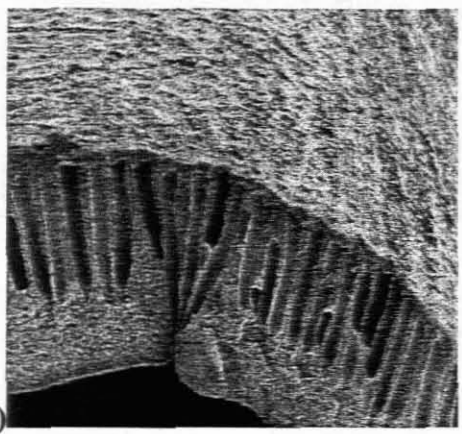

(a) 93 % NMP (e)

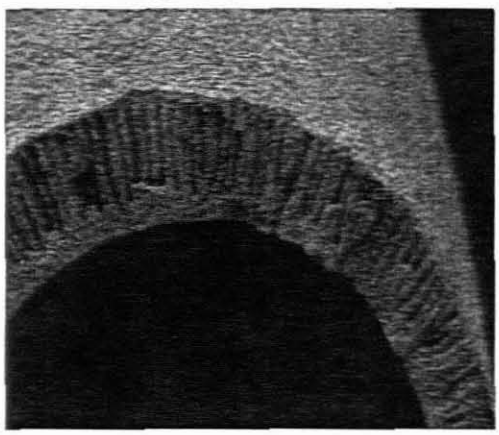

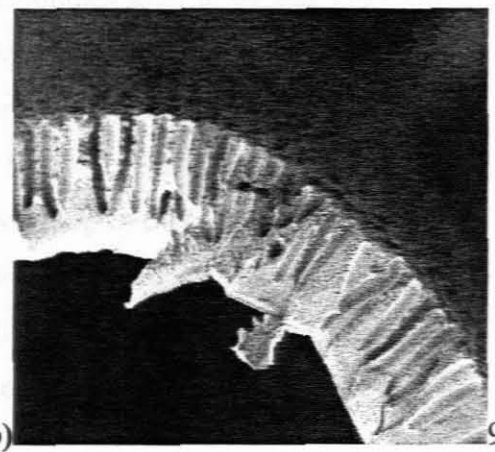

(b) 94%NMP (f)

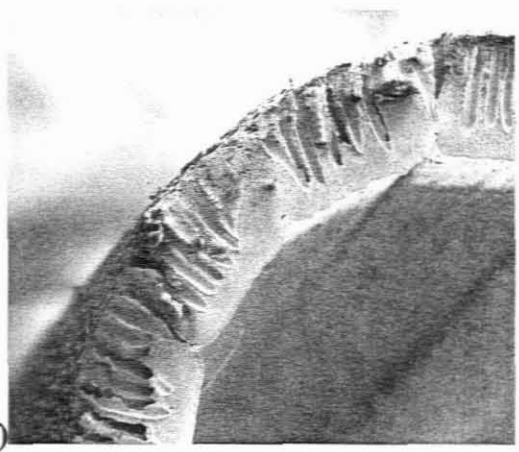

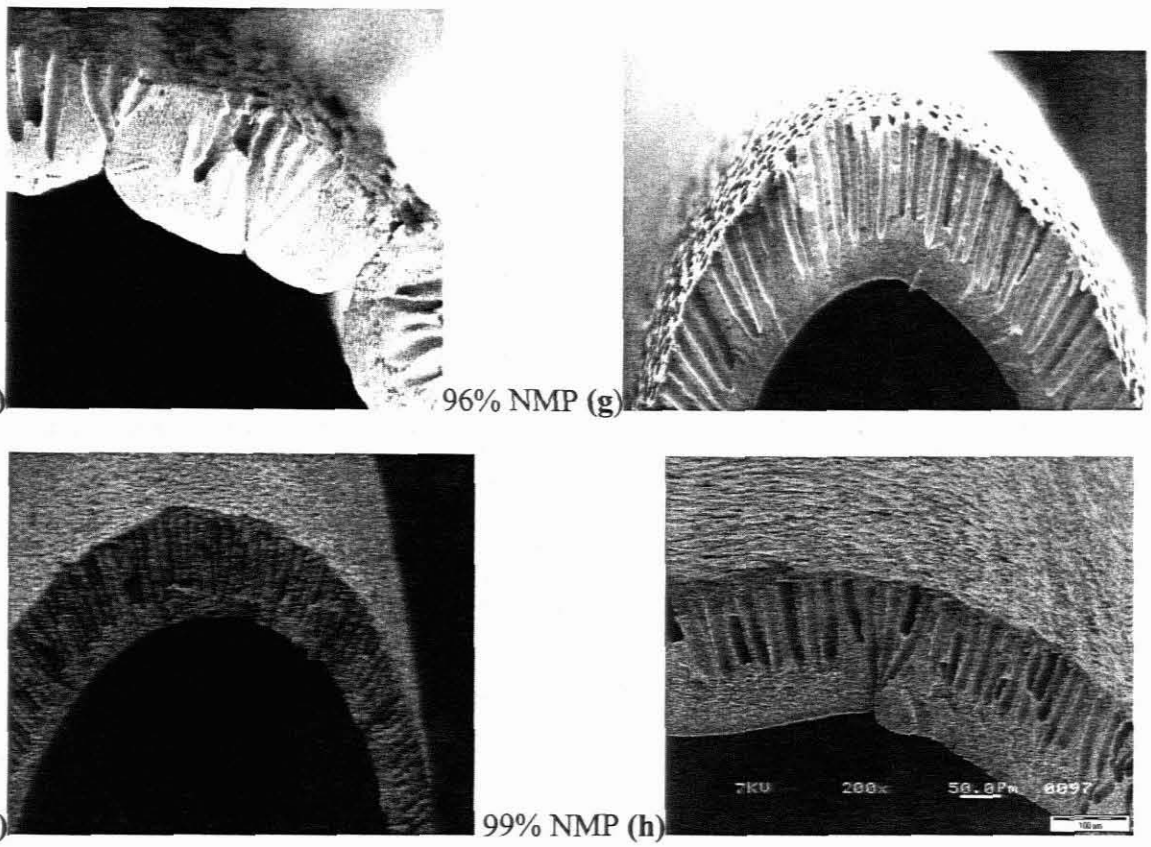

Figure 6.1.1: Spun with, DER = 2,5 ml/min (along the left); DER = 3,0 ml/min (along the right) and spinning bath compositions are shown at the centre.

6.1.2 Discussion of experimental effects of external spinning bath composition on membrane resultant structures

Membranes spun at 99 and 93% NMP, external spinning bath compositions, had an external skin layer. Even at low DER of 2,5 and 3,0 ml/min, no externally unskinned membranes were formed. At 99% NMP content, the reason could be that precipitation did not take place on the outer surface. Instead the polymer slowly dissolved in the external spinning bath. According to Smolders et. al,(1992) this happens at too high bath solvent concentrations. In that case, when the nascent membrane reached the humidity chamber, the outer surface was still a jelly-like dope. It was then precipitated by the vapour in the humidity chamber and an external skin layer was formed.

At 93% NMP content, the 7% water content must have been high enough to precipitate the external surface of the nascent membrane. Externally unskinned membranes were produced at 94 and 96% NMP external bath compositions. These external bath contents must be the ones near the dope's cloud point. That means the point or rate at which the dope gets precipitated depends on its composition. According to Jacobs and Leukes (1996), the

preferred external bath composition is the one with solvent/non-solvent content near the dope's cloud point.

6.2 Effect of dope extrusion rate and viscosity

The first experiments performed on determining the dope extrusion rate were conducted using 2,5; 3,0; 4,0; 4,5 and 4,5 ml/min DER. From these experiments it was noticed that an externally unskinned membrane was formed at 3,0 ml/min DER but not at 4,0 ml/min DER. It was then decided to take small intervals between these two extremes to determine where exactly does the external skin layer begin to form. Therefore six experiments were conducted at dope extrusion rates of 3,15; 3,3; 3,45; 3,6; 3,75 and 3,9 ml/min. while the bore fluid flow rate was held constant at 4,5 ml/min. The results for the last experiments are shown in table C1 in the appendix because they were thin and fragile although they had no external skin layer. Therefore, they are not suitable for the study objective of producing a thick-skinned membrane.

The following are the experimental results showing dimensions and performance of the produced membranes, spun at different external spinning bath compositions, on varying DER. The results presented in the tables and graphs in this section are for the membranes spun at 94 and 96% NMP content and the others (93 and 99% NMP) are presented in appendix C. These were found to be the bath compositions where externally unskinned membranes can be produced.

All membranes spun at 2,5ml/min DER burst at 100kPa when pure water flux was tested. New sets of test cells were built to check if they were leaking or bursting and all the membranes did burst. This can be seen from the table below. The structure of these membranes were thin distorted inner skin with few finger-like voids and externally unskinned. It is evident that these membranes were very weak and fragile to maintain a pressure of 100kPa. Then the membranes spun at 3,0ml/min DER could stand the pressure of 100 kPa but not the 200kPa because they also burst at 200kPa.

6.2.1 Results

Table 6.2.1(a): Experimental results on varying DER, BFF held constant at 4,5 ml/min and external spinning bath composition = 96% NMP

Exp No.	Pure Water Flux (L/m^2h)		Ultra-filtration flux (L/m^2h)		Retention (%)		I.D. (mm)	O.D. (mm)	Thickness (mm)	Burst pressure (kPa)	Conditions	Memb. Structure	Effective area (m^2)
	100	200	100	200	100	200					BFF,DER,BATH		
E07	membrane cells burst						0.13	0.185	0.053		4,5;2,5;96%NMP	Thick inner skin, few finger-like voids, polymer rich inbetween. Distorted inner surface. Externally unskinned.	
E06	228		145	membrane cells burst			0.11	0.182	0.071		4,5;3,0;96%NMP	Thick inner skin, voids becoming many, starting just below the skin and extend to the outside. Externally unskinned.	0.0122
E05	166	332	39	66	51	22	0.11	0.206	0.101	1300	4,5;4,0;96%NMP	Thick inner skin, voids becoming short, some start far from the inner skin while some do not reach the outer skin	0.0117
E08	123	296	32	40	44	35	0.11	0.2	0.093	1700	4,5;4,5;96%NMP	Thick inner skin, voids narrow and extend to the outer skin. Small pores @ the end of voids. Thick outer skin	0.0119
E09	202	404	38	58	40	26	0.12	0.225	0.103	1700	4,5;5,0;96%NMP	Inside skin reduced, too many needle like voids, starting just below the inner and extend to the outer skin. Thick outer skin.	0.0108

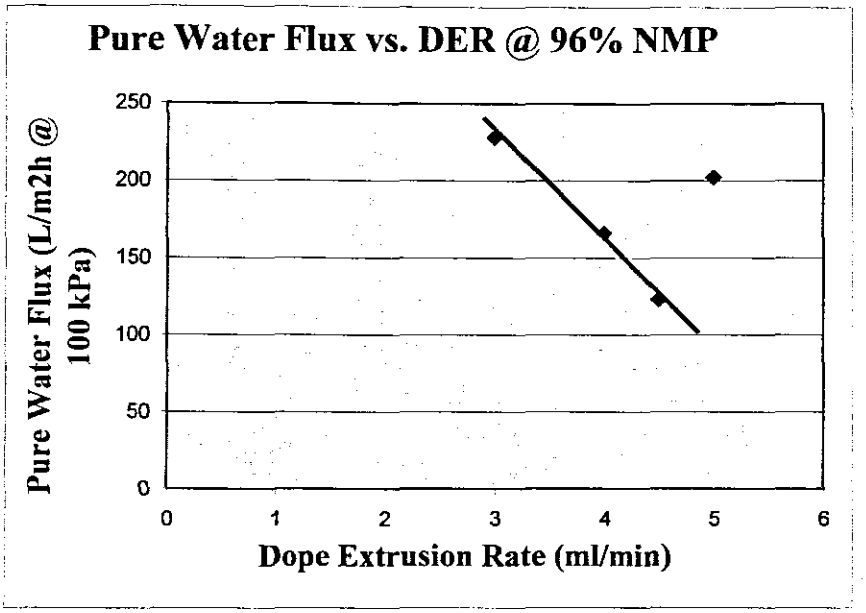

Figure 6.2.1(a): Graphical presentation of Flux vs. Dope Extrusion Rate at 96% NMP

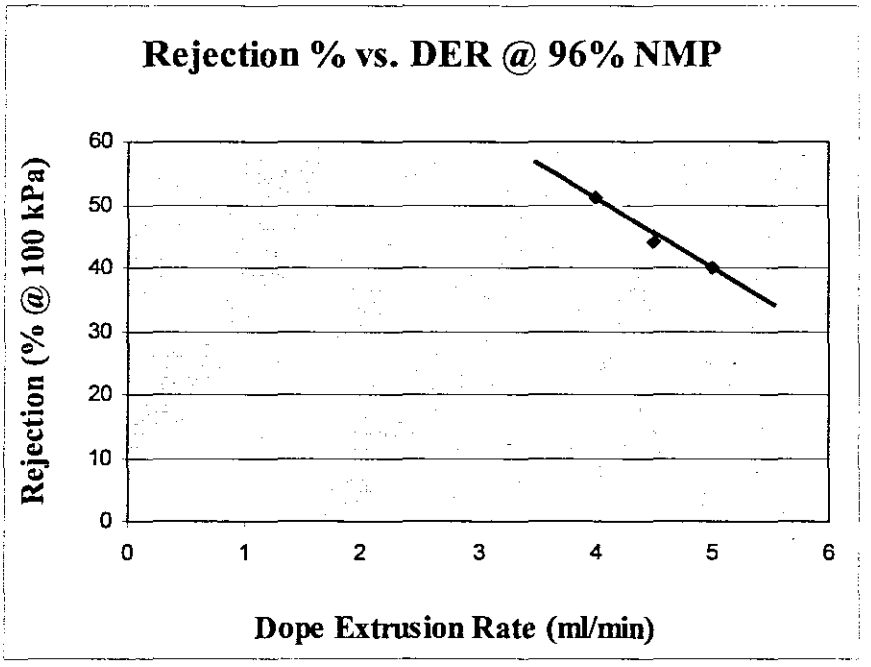

Figure 6.2.1(b): Graphical presentation of Rejection vs. Dope Extrusion Rate at 96% NMP

Table 6.2.1 (b): Experimental results on varying DER, BFF held constant at 4,5 ml/min and external bath composition = 94% NMP

Exp No.	Pure Water Flux (L/m^2h)		Ultra-filtration flux (L/m^2h)		Retention (%)		I.D. (mm)	O.D. (mm)	Thickness (mm)	Burst pressure (kPa)	Conditions	Memb. Structure	Effective area (m^2)
	100	200	100	200	100	200					BFF,DER,BATH		
E15	membrane cells burst						0.13	0.19	0.053		4,5;2,5;94%NMP	Thick inner skin, few finger-like void, polymer rich inbetween. Distorted on the inner surface. Externally unskinned.	
E16	100		42	membrane cells burst			0.15	0.22	0.067		4,5;3,0;96%NMP	Thick inner skin, voids starting below the skin and extend outwards. Externally unskinned.	0.0147
E14	211	384	41	63	67	32	0.11	0.21	0.094	900	4,5;4,0;96%NMP	Thick inner skin, narrow needle like voids. Pores on the underlying outer thin skin.	0.0126
E17	137	232	38	59	40	40	0.12	0.22	0.098	1700	4,5;4,5;96%NMP	Thick inner skin, needle like voids extending to the outer skin. Small pores at the end of voids. Thick outer skin	0.0096
E18	107	199	30	43	66	47	0.13	0.23	0.092	1700	4,5;5,0;96%NMP	Inside skin reduced, needle like voids starting just below the inner skin extending to the outer thin skin.	0.0103

The pure water flux (PWF) is expected to be linearly related to pressure since there is no fouling. In this study experiments, the results did not show such relationship. The following explanation could explain why the results are not as expected.

The feed passed through the pressure controller, and then the flow controller. The flow was held constant at 1 ml/min at both 100 and 200 kPa. The open loop system where retentate is returned to the feed tank was used in this study experiments because the cross flow velocity and trans-membrane pressure are controlled with one centrifugal pump and a backpressure valve. There might have been back pressure created by the backpressure valve. Therefore, the pressure reflected by the pressure gauge could have been an incorrect reflection.

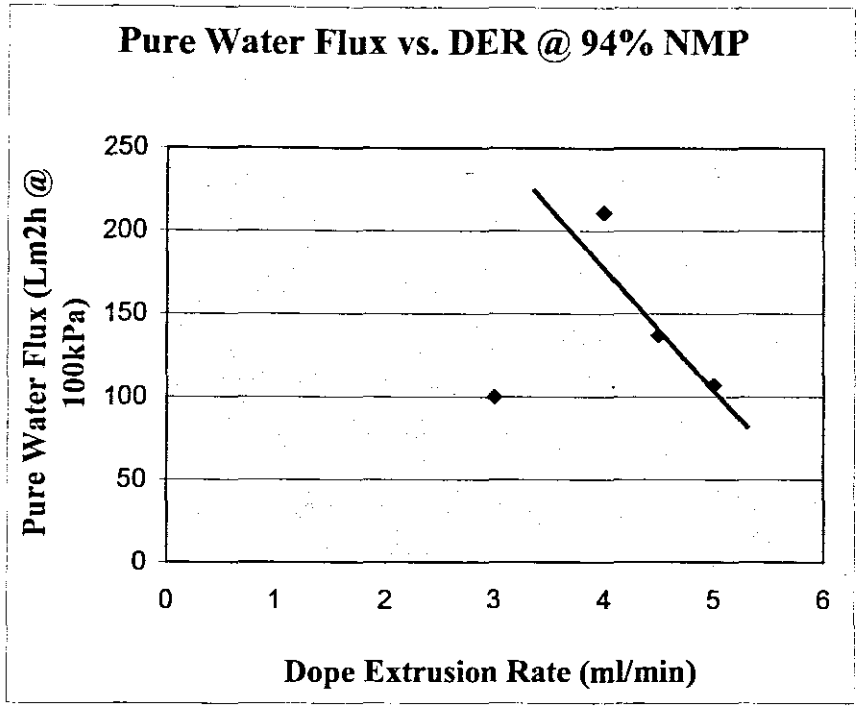

Figure 6.2.1(c): Graphical presentation of Flux vs. Dope Extrusion Rate at 94% NMP

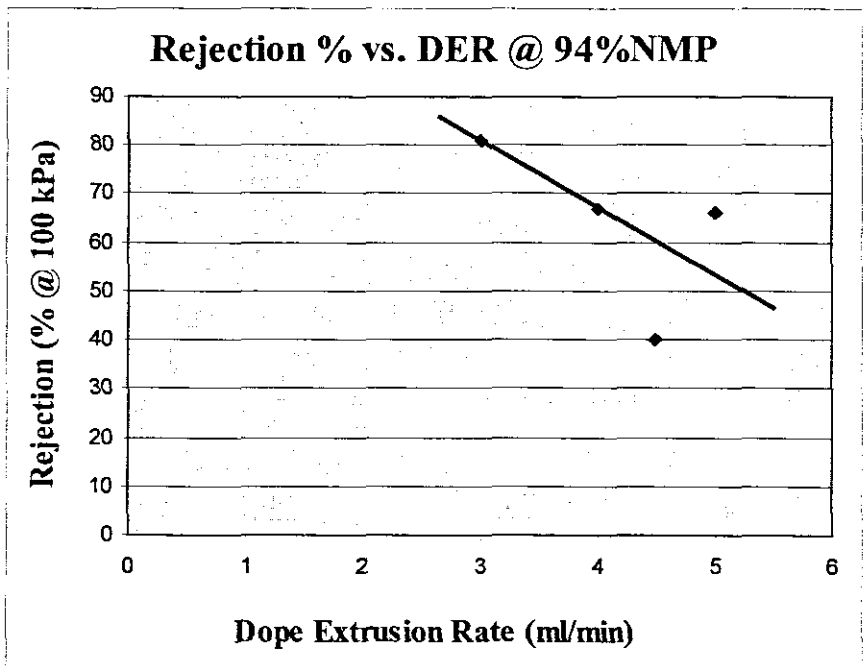

Figure 6.2.1(d): Graphical representation of Rejection vs. Dope Extrusion Rate at 94% NMP

6.2.2 Discussion of experimental effects of DER on membrane structure and performance

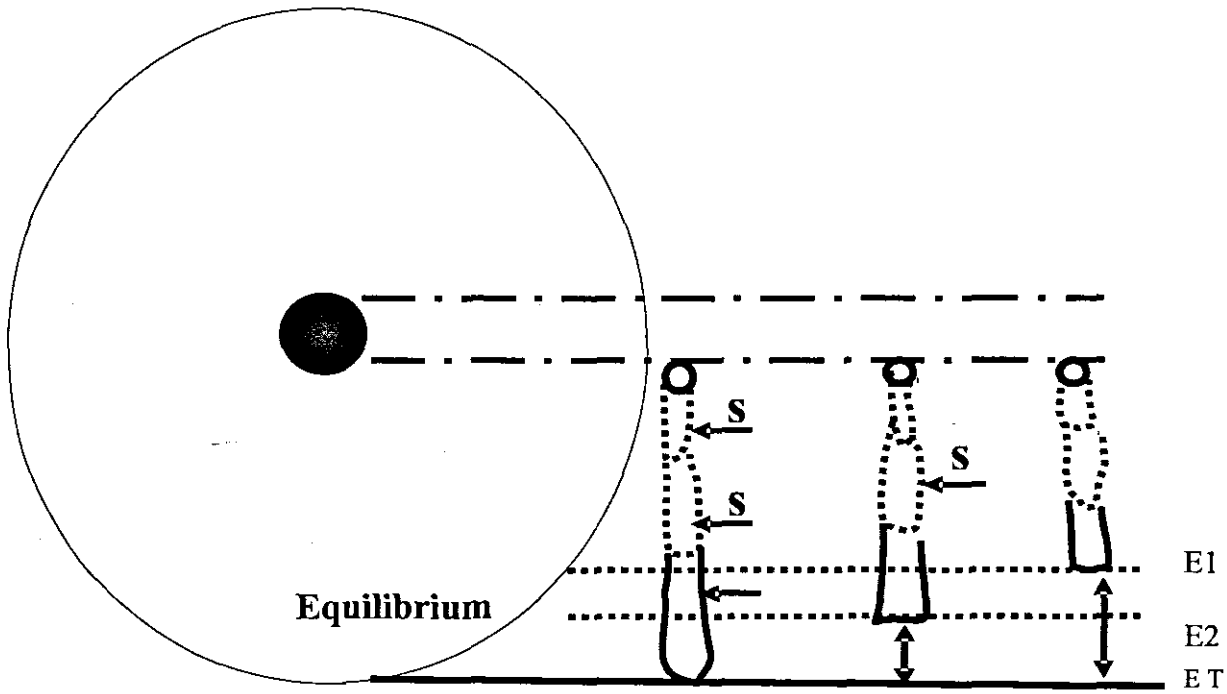

Figure 6.2.2 (a): Schematic presentation of possible diffusion process during void formation

Externally unskinned membranes were formed at low dope extrusion rates (2,5 and 3,0 ml/min). From figure 7.2, points E1 and E2 can be considered as the equilibrium points, meaning that, no more diffusion took place beyond those points. At the same time, point ET is where complete diffusion of solvent/non-solvent mixture took place up to the full width of the nascent membrane. It can be deduced that at 2,5 and 3,0 ml/min DER, the non-solvent in Bore Fluid reached point t before it got saturated with solvent from the polymer dope. At high DER, that is, greater than 3,0 ml/min, an external skin layer was formed. Increasing DER means that the volume of solvent in dope diffusing into the bore fluid is increased. Therefore, the volume of non-solvent has to be also increased.

Since the bore fluid was kept constant, the volume of non-solvent was not enough to take up the excess solvent. Then the bore fluid or non-solvent got saturated with solvent at points E1 and E2. At that point, the diffusion process stopped before the solvent/non-solvent mixture reached the outer surface of the nascent membrane. The outer surface of the nascent membrane was still jelly-like polymer dope when it reached the humidity chamber. The

humidity chamber precipitated the jelly-like polymer dope and that is why an external skin layer was formed.

The membrane performance results showed a decrease in flux with increasing DER. That can be caused by the external skin layer getting thicker with increasing DER. Rejection also seemed to decrease with increase in DER and that is a rear situation. According to Qin, the rejection would be expected to increase with dope extrusion rate. Polymer concentration in the spinning dope also plays a role in the performance and structure of the resulting membrane (Qin, 2001). The elasticity of the polymer and its disorientation when in solution has to play a role in the structure hence the performance of the membrane. The reason for the difference we could think of is that different polymers might not behave the same under shear.

Membranes formed at 2,5 ml/min DER showed signs of distortion on the inner surface. That could be the result of shear stress caused by the bore fluid at high flow rate of 4,5 ml/min whilst the dope is extruding at a very low rate. The dope was too much less viscous such that it could not be spun. It did not flow as a continuous fluid out of the spinneret and it seemed impossible to solidify in the coagulant bath. No membranes could be produced out of that dope. A 25 ml of the spinning bath content was collected in a beaker and a small amount (10 ml) of polymer dope was added into the beaker and left overnight. The polymer dope did not even show a sign of clouding; it remained a dope. For this reason, this study would agree with the statement by Jacobs (1977) that more viscous dopes are near the cloud point.

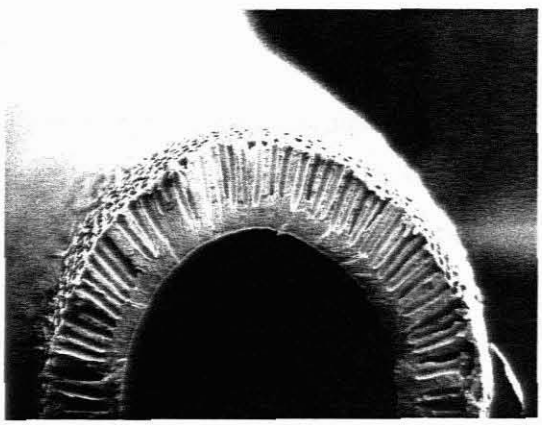

(b) 96% NMP content spinning bath

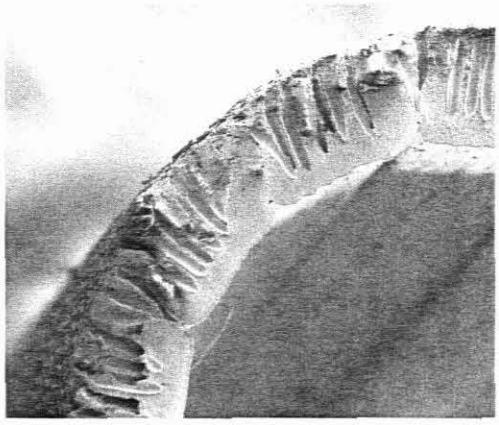

(c) 94% NMP content spinning bath

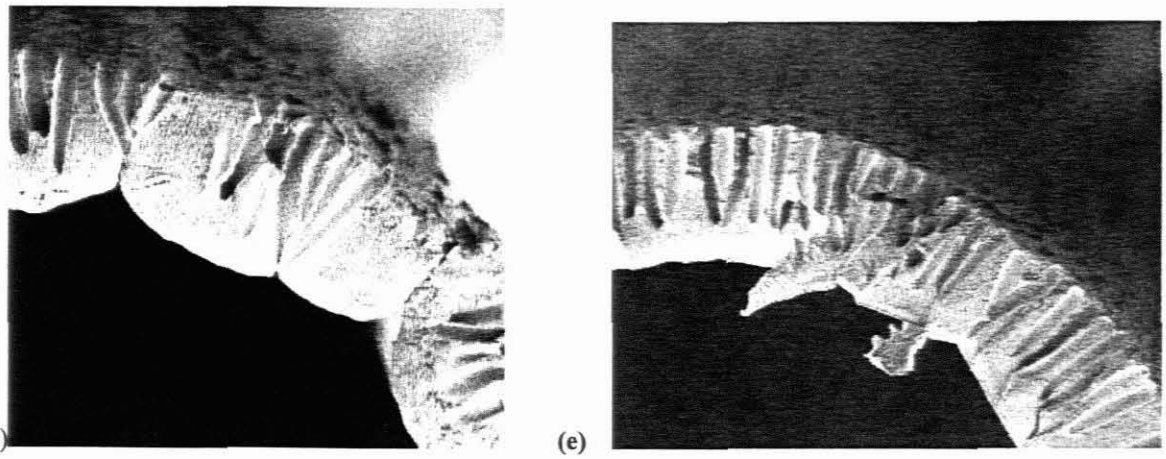

Figure 6.2.2: SEM photos of externally unskinned membranes formed at low DER, (a) and (b) spun at 3,0 ml/min and (c) and (d) at 2,5 ml/min.

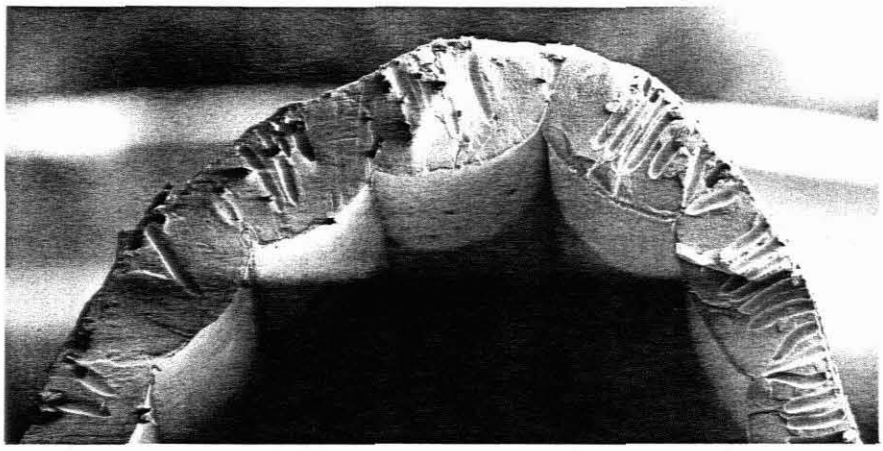

Figure 6.2.2 (f): SEM photo of a distorted inner surface capillary membrane fabricated at 4,5 ml/min BFF and 2,5 ml/min DER

6.3 Effect of bore fluid flow rate and composition

Five experiments were conducted at different bore fluid flow rates (1,5; 2,5; 3,5; 4,0 and 4,5 ml/min) while the DER was held constant at 4,0 ml/min. The experimental results showing dimensions and performance of the produced membranes, spun at 94 and 96% NMP bath content on varying DER are presented in tables and graphs below.

6.3.1 Results

Table 6.3.1(a): Experimental results on varying BFF, DER held constant at 4,0 ml/min and external spinning bath composition = 96% NMP

Exp. No.	Pure water flux (L/m^2h)		Ultra-filtration flux (L/m^2h)		Retention(%)		I.D (mm)	O.D.(mm)	Thickness (mm)	Burst pressure (kPa)	Conditions	Memb. Structure	Effective area (m^2)
	100	200	100	200	100	200					BFF;DER;BATH		
E 01	108	190	34	57	25	24	0.102	0.2	0.098	2000	1,5;4,0;96%NMP	Thick skin inside, voids wide not close to each other, Thin outward skin.	0.0114
E 02	201	344	39	58	41	18	0.11	0.193	0.083	>1000	2,5;4,0;96%NMP	Thick inner skin, voids wide, elongated to the outer skin. Thick polymer rich inbetween voids.	0.0123
E 03	159	259	49	72	62	20	0.11	0.208	0.098	1500	3,5;4,0;96%NMP	Thick inner skin, voids extending to an outer skin	0.0123
E 04	165	274	48	64	42		0.122	0.2	0.078	1300	4,0;4,0;96%NMP	Thick inner skin, voids wide and not much elongated,some start from inner skin whilst others don't reach the outer skin	0.0136
E 05	166	271	39	66	51	22	0.105	0.206	0.101	1300	4,5;4,0;96%NMP	Thick inner skin,voids becoming short, some start far from the inner skin while some don't reach the outer skin.	0.0117

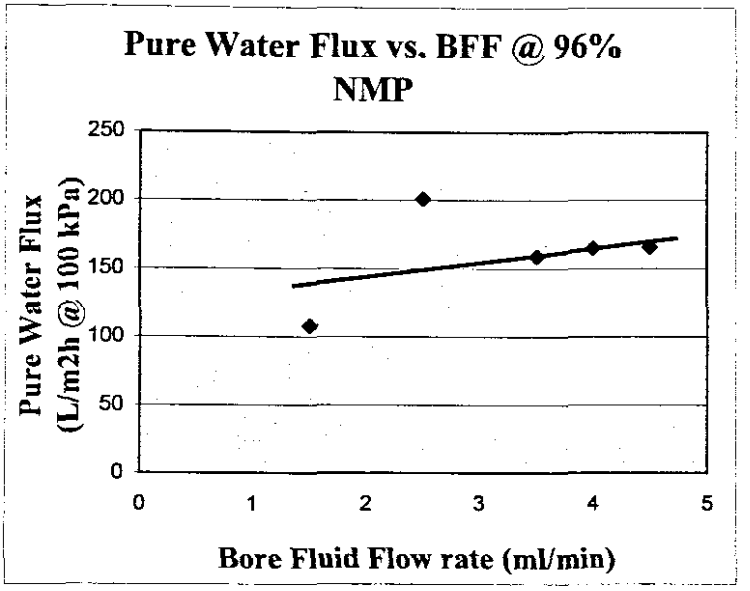

Figure 6.3.1(a): Graphical presentation of Flux vs. Bore Fluid Flow rate at 96% NMP

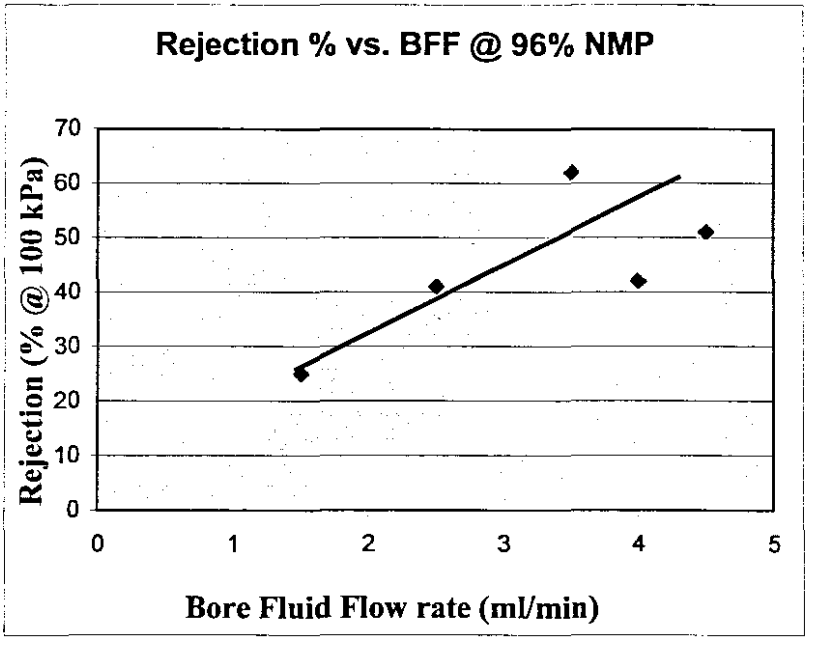

Figure 6.3.1 (b): Graphical representation of Rejection vs. Bore Fluid Flow rate at 96% NMP

Table 6.3.1 (b): Varying BFF, DER held constant at 4,0 ml/min and external spinning bath composition = 94% NMP

Exp. No.	Pure water flux (L/m^2h)		Ultra-filtration flux (L/m^2h)		Retention (%)		I.D (mm)	O.D.(mm)	Thickness (mm)	Burst pressure (kPa)	Conditions	Memb. Structure	Effective area (m^2)
	100	200	100	200	100	200					BFF;DER;BATH		
E 10	72	125	21	28	84	73	0.113	0.202	0.089	1800	1,5;4,0;94%NMP	Inside skin thin, too many needle like voids extending to the outer skin.	0.0126
E 11	99	193	32	44	67	46	0.11	0.198	0.088	1700	2,5;4,0;94%NMP	Thin inner skin, too many needle like voids. Small pores at the end of voids. Thinner outer skin.	0.0123
E 12	136	236	45	62	66	49	0.115	0.2	0.085	1600	3,5;4,0;94%NMP	Inside skin reduced, too many needle like voids, starting just below the inner skin and extend to the outer skin.Outer skin reduced	0.0128
E 13	112	216	49	64	73	68	0.116	0.25	0.134		4,0;4,0;94%NMP	Inner skin getting thin, voids narrow and extend to the outside skin. Thin outer skin	0.0129
E 14	211	384	41	63	67	32	0.113	0.207	0.094	900	4,5;4,0;94%NMP	Thin inner skin, narrow needle like voids. Pores on the underlying outer thin skin.	0.0126

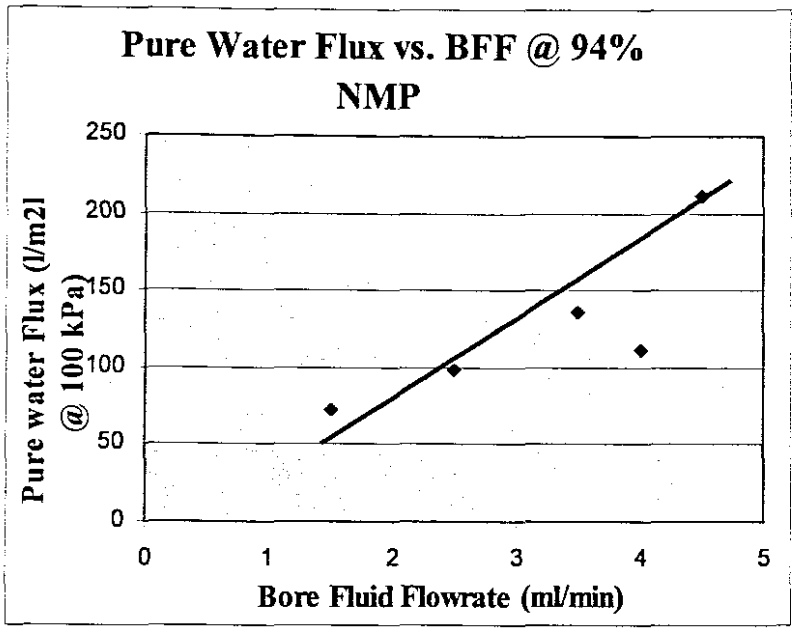

Figure 6.3.1 (c): Graphical representation of Flux vs. bore fluid flow rate at 94% NMP

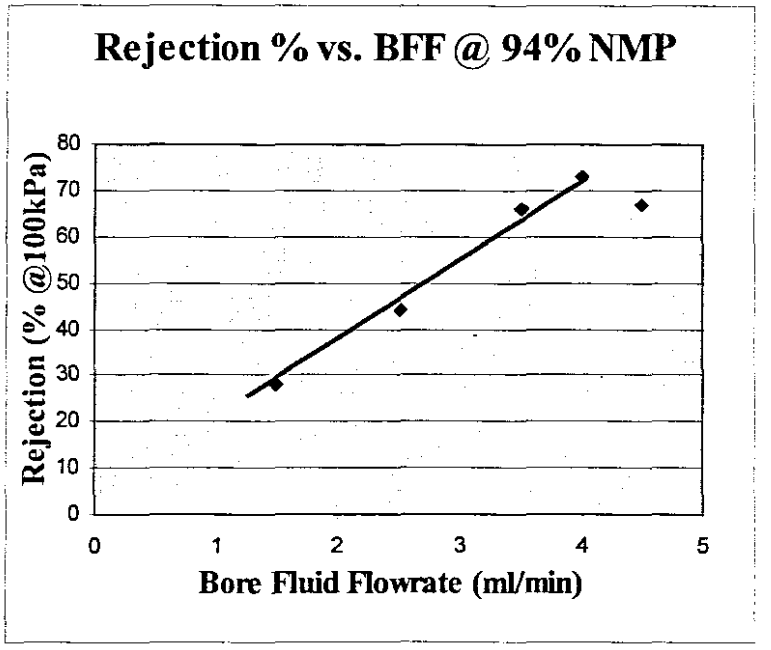

Figure 6.3.1 (d): Graphical representation of Rejection vs. Bore Fluid Flow rate at 94% NMP

6.3.2 Discussion of experimental results on bore fluid flow rate effects on membrane structure and performance

The SEM photos showed that the microvoid length and number increased with an increase in bore fluid flow rate. The inner skin layer was reduced with an increase in bore fluid flow rate. Idris (2002) stated that the cause for the decrease in wall thickness, which is the inner skin, as BFF increases, is that the polymer dope velocity on the inner surface also increases. According to the skin formation theory, if the solvent diffusion rate from the polymer dope to the bore fluid is faster, a thin skin will be formed with a finger-like structure (Termonia, 1983; Porter, 1990). When the BFF is high, the diffusion rate is also expected to be faster (Idris, 2002). This is because the volume of non-solvent is larger to allow for more solvent diffusion within the pore. A large volume of solvent can get mixed with non-solvent before it gets saturated. That allows for further diffusion of solvent/non-solvent mixture within the pore through the nascent membrane thickness.

When the external spinning bath composition was 94%NMP aqueous content, membranes formed had thin external skins. The flux increased with BFF increase, as per Feng (2001), because the resistance was the inner thin skin layer, which also got thinner with BFF increase. That explains the increase in retention with increase in BFF. The external skin layer was not as dense as the inner one because it was not as a result of precipitation by the solvent. This skin layer was formed because the nascent membrane was not precipitated to the external surface before reaching the humidity chamber.

When the external spinning bath composition was 96% NMP aqueous content, membranes formed had a thick inner skin layer. There was an increase in rejection also with BFF increase (this can be seen in figures 6.3.1 b and d). The reason for an increase in rejection could be the inner thick skin layer. Rejection also increased with increase in BFF. In this case, as the BFF increases, the exchange rate between the solvent/non-solvent in contact increases resulting in a dense skin being formed. As the exchange rate between solvent and non-solvent in contact increases, the inner skin formed becomes dense and thin. Therefore, as the skin becomes denser, its resistance to fluid penetration becomes more. That could be the explanatory reason for the increase in rejection with increase in BFF.

No externally unskinned membranes were formed. The constant dope extrusion rate must have been high to allow for complete precipitation of the nascent membrane by the bore fluid before reaching the humidity chamber.

6.4 Effect of spinneret size

A small spinneret with an inside diameter (ID) of 0,012 mm and an outside diameter (OD) of 0,056 mm was used instead of the 0,063mm ID and 0,273mm OD. Deon Koen suggested low dope extrusion rates when using small spinneret, though no exact figures were stated. The values used were randomly chosen. The maximum DER, the spinneret could allow was 3,0 ml/min. At 3,0 and 3,2 ml/min DERs, the production line became too slack and entangled. Increasing the rollers and take up speeds did not help. The bore fluid flow rate was held constant at 3,5 ml/min. Six experiments were conducted at different dope extrusion rates of 1,1; 1,3; 1,5; 2,0; 2,5 and3,0 ml/min.

6.4.1 Result

Table 6.4.1: Varying DER using small spinneret, BFF held constant at 3,5 ml/min and external bath composition = 94% NMP

Exp. No.	Pure water flux (L/m^2h)		Ultra-filtration flux		I.D (mm)	O.D.(mm)	Thickness (mm)	Conditions	Memb. Structure	Effective area (m^2)
	100	200	100	200				BFF;DER;BATH		
E 19	416		802		0.065	0.083	0.018	3,5;1,1;94%NMP	Thick dense inner skin.Very,very few, wide, short finger like voids extending to the outer surface.Externally unskinned membranes.	0,0101
E 20	378	367	638	635	0.058	0.094	0.036	3,5;1,3;94%NMP	Thick dense inner skin. Few, wide, short finger like voids extending to an outer surface. Externally unskinned membranes.	0,0096
E 21	307		561		0.065	0.1	0.0345	3,5;1,5;94%NMP	Thick dense inner skin. Many uniform finger like short wide voids extending to the outer surface.Externally unskinned membranes.	0,0108
E 22	286	239	342	353	0.06	0.096	0.036	3,5;2,0;94%NMP	Thick dense inner skin. Many uniform elongated finger like voids extending to the outer surface. Externally unskinned membranes.	0,01
E 23	270	244	545	538	0.069	0.105	0.0365	3,5;2,5; 94%NMP	Thick dense inner skin. Many uniform elongated, narrow finger like voids extending to the outer surface. Externally unskinned membranes.	0,0114
E 24	244	286	485	478	0.062	0.105	0.043	3,5;3,0;94%NMP	Thick dense inner skin. Many uniform elongated, narrow finger like voids extending to the outer surface. Externally unskinned membranes.	0,0104

In the table above, the PWF @200kPa is lower than that obtained @100kPa. It can not be explained why the PWF decreased as the pressure was increased but conclusions drawn from the membranes spun using a small spinneret, are based on SEM photos. The only conclusion drawn was that they could not be considered for the research objective that of production of a thick walled membrane because they were very thin and fragile for the attachment of fungi. The question of flux being low is unexplainable.

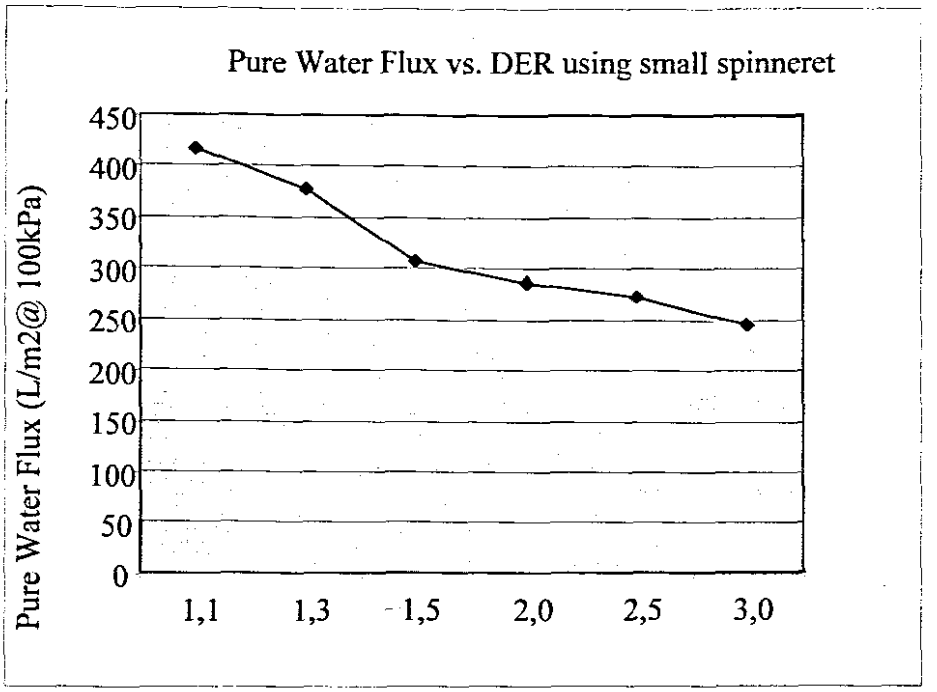

Figure 6.4.1: Graphical presentation of Flux vs. Dope Extrusion Rate using a small spinneret

6.4.2 Discussion of experimental results on spinneret size effects on membrane structure and performance

All the membranes produced using a small spinneret were externally unskinned. Very high fluxes, > 200 L/m^{2}h, were obtained but the retentions were very low. After some time of running pure water with the dye through the membranes, permeate came out with the dye. With UF tests, no clear permeate was obtained. For that reason, no samples were taken for retention tests. At 200 kPa pressures, permeate was also not clear.

The pores on the outer surface of the membranes became wide and many with increase in dope extrusion rate. The void length and number also increased with increase in dope extrusion rate. This was also noticed when a larger spinneret was used. The reason for the shorter voids when the dope extrusion rate was low is from the skin and pore formation theory. After the thin dense skin was formed, only a small amount of non-solvent at a very few sites could penetrate into the underlying layer and that was a short length to the membrane exterior. If only a few pores and microvoids were formed, a few pores on the outer surface will be formed. This is clear in figures 7.4.2 (g, h and i)

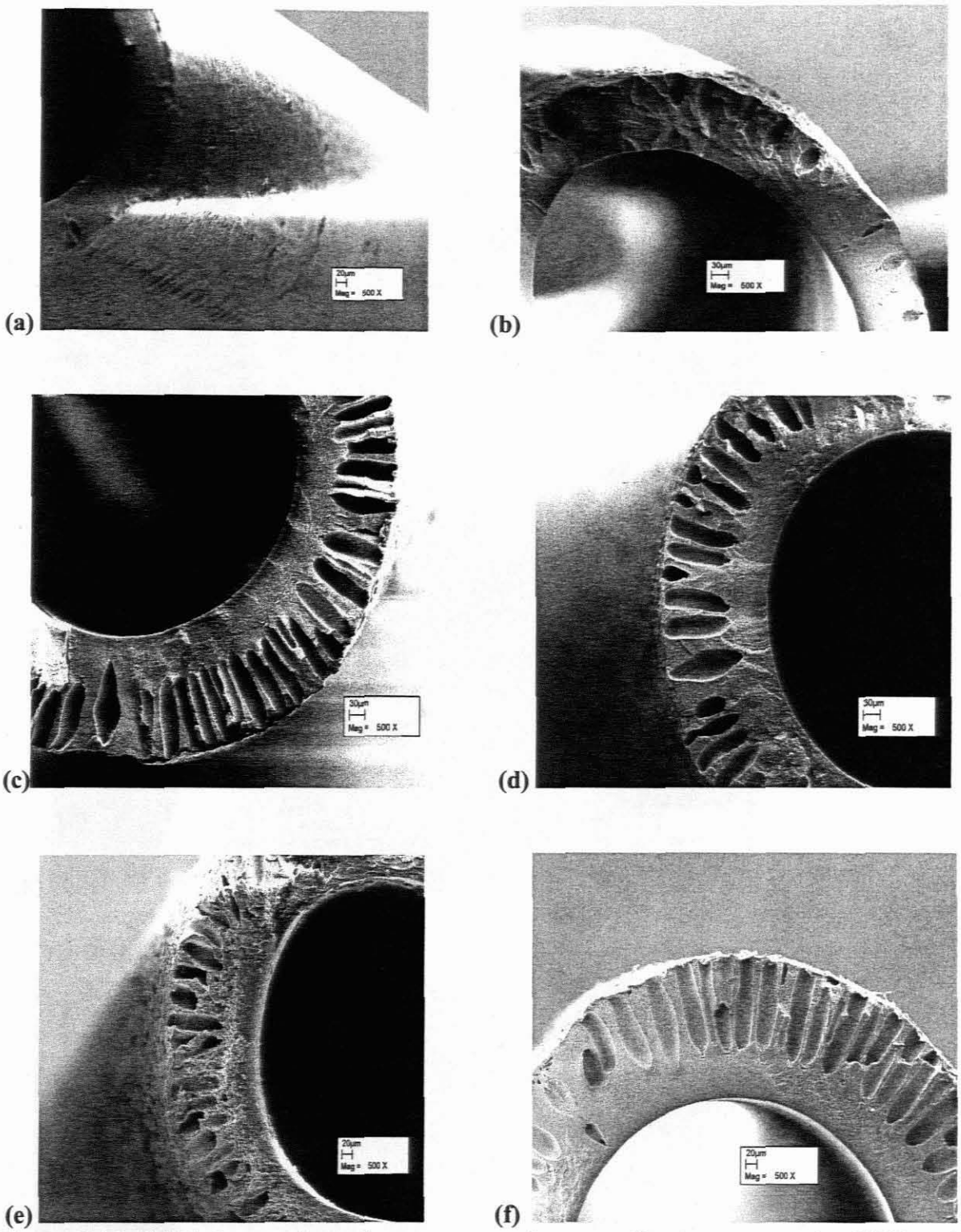

Figure 6.4.2: SEM photos of membranes spun using a small spinneret varying DER and external spinning bath composition of 94% NMP [(a) spun at 1,1; (b) at 1,3; (c) at 1,5; (d) at 2,0; (e) at 2,5; and (f) at 3,0 ml/min]

(g) 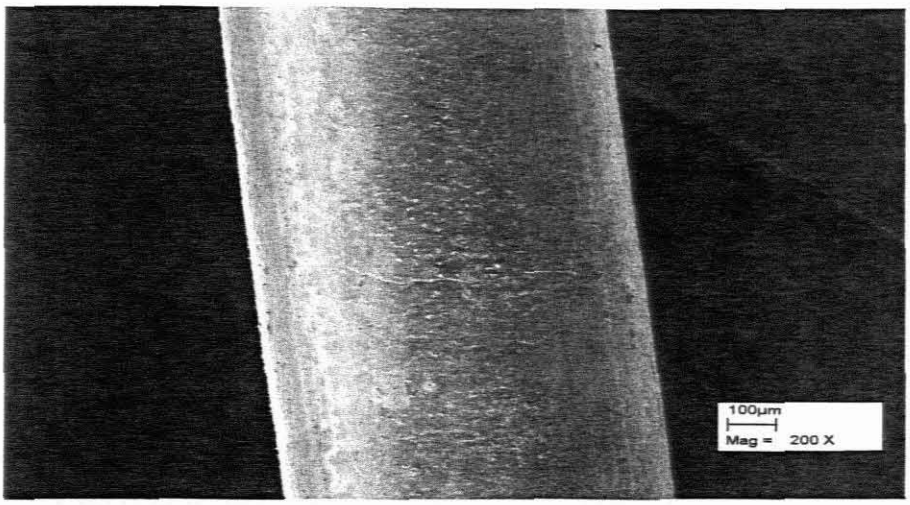

DER = 1,1 ml/min

(h) 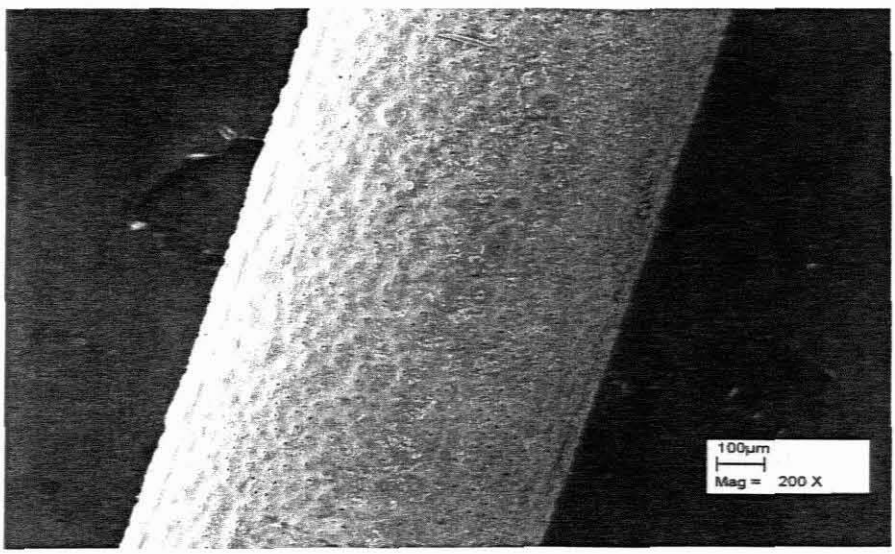

DER = 1,3 ml/min

(i) 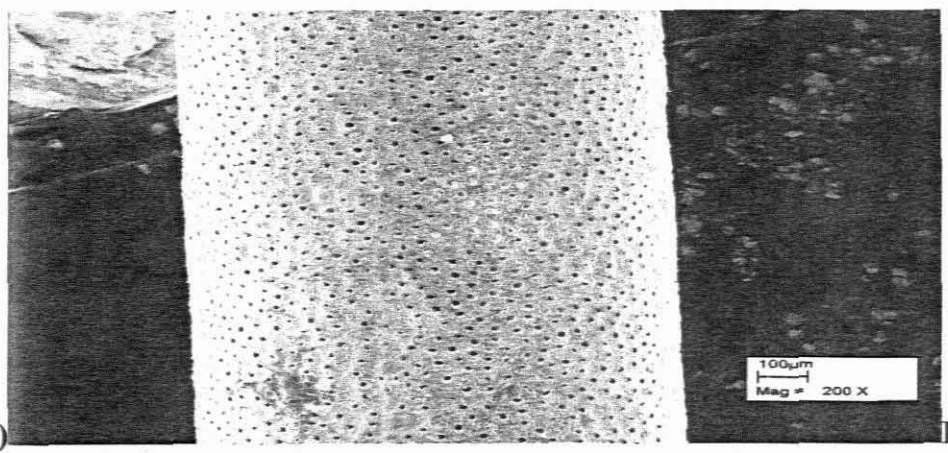

DER =1,5ml/min

Figure 6.4.2 (g, h and i): SEM photos of external surfaces of membranes spun using a small spinneret at different Dope Extrusion Rates

6.5 Effects of solvent removal from the membrane pores and/or voids

Removing solvent from the membrane pores using the alcohol method seemed to be having a good effect on the dimensions and performance of the membranes. The thickness of the membranes was reduced when the solvent was removed with alcohol (see section 5.4.5 for solvent removal methods). Flux and rejection of the membranes after solvent was removed were higher than when the membranes had solvent within the pores.

Results showing the performance of the same experimental membranes when solvent is being removed are shown in tables C4 a, b and c in the appendix.

CHAPTER 7

CONCLUSIONS AND RECOMMENDATIONS

7.1 CONCLUSIONS

1. The DER where an externally unskinned membrane could be formed with a thick wall was found to be 3,0 ml/min.
2. The BFF of 4,5 ml/min was found to be satisfactory for production of externally unskinned membrane with the DER of 3,0 ml/min.
3. External spinning bath composition ranging between 94 to 96 % NMP was found suitable for production of externally unskinned membranes.
4. A small spinneret use was found unsuitable for the production of thick-walled membranes.

7.1.1 External spinning bath composition

a) This study confirms the findings of Smolders et. al,(1992) that when the solvent content in the external spinning bath is too high, it starts to re-dissolves the polymer in the dope, and then an external skin is formed.
b) High non-solvent content in the external spinning bath precipitates the dope and a skin is formed on the outer surface.
c) That means precipitation process starts externally at the spinning bath/dope interface inwards at the same time at the bore fluid/dope interface.
d) That implies there is a range of spinning bath composition where an externally unskinned membrane could be produced.

7.1.2 DER and viscosity

a) Increasing DER results in an external skin being formed and getting thicker.
b) Going below the suitable DER results in production of a thin-walled membrane.
c) The membrane performances and thickness were compared with previously produced externally unskinned membranes using the same dope formulation.
d) The thickest membrane produced previously at IPS was 5mm. The thickest membrane produced in our experiments at 3,0 ml/min DER was 7,1mm. Which means a membrane thicker by 2,1 mm was produced with improved performance.

e) Low viscous dopes are difficult or unable to precipitate.
f) This indicates that there is a range of DER for obtaining externally unskinned membranes.

7.1.3 BFF and composition

a) Too high bore fluid flowing within a slow flowing dope leads to a production of a membrane with a distorted inner surface.
b) Too low BFF result to a formation of an external thick skin.
c) This shows that the rate of solvent/non-solvent exchange rate decreases with BFF decrease.

7.1.4 Small spinneret use

a) For production of a thick-walled membrane, a small spinneret is not recommended.
b) The thickest membrane produced with a small spinneret at 3,0 ml/min DER was thinner than the one produced with a larger spinneret at the same DER.
c) The membranes produced using small spinnerets were brittle so they are not suitable for the research objective.
d) Although they gave very high fluxes, the membranes could hardly stand the pressures about 200 kPa.

7.2 RECOMMENDATIONS

The results were considered satisfactory in view of the experience of Deon Koen (the experienced person in membrane fabrication) because they do give an indication of the effects of experimental variables. The experiments could not be repeated due to limitations of time, access to experimental facilities and costs of repetition of experiments. The following recommendations were then made:

1. Behaviour of different types of polymers under shear (when extruding out of the spinneret) should be investigated. That is, the molecular alignment, tensile strength and elongation of different polymers might be different and that could be the reason for Qin, Idris and Feng's results for membrane performances to be different.

2. A spinning technique where the nascent membrane would not have to go via a roller in the external spinning bath yet allowing it to spend more time in the bath should be developed. The nascent membrane experiences some shear stress on coming into contact with the roller.
3. A standard ratio (1:1,5 in this author's study) of DER to BFF where a satisfactory membrane will be produced should be investigated.
4. Addition of polymer additives to enhance the dope viscosity is recommended.

Table 7.1.1: Showing the relationship between DER and BFF in order to produce externally unskinned membranes

DER (ml/min)	BFF (ml/min)
2,5	✔
3,0	✔
4,0	✘
4,5	✘
5,0	✘

✔ - shows that externally unskinned membranes were formed
✘ - shows that an external skin layer was formed

Table 7.1.2: Showing the relationship between DER and External bath composition in order to produce externally unskinned membranes

2,5	✘	✔□	✔□	✘
3,0	✘	✔□	✔□	✘
4,0	✘	✘	✘	✘
4,5	✘	✘	✘	✘
5,0	✘	✘	✘	✘
	99	96	94	93

REFERENCES

Altinkaya, S.A. and Ozbas, B. (2004) Modeling of asymmetric membrane formation by dry-casting method. *J. Membrane Sci.* 230: 71-89

Aptel, P., Abidine, N., Ivaldi, F. and Lafaille J.P. (1985) Polysulfone Hollow Fibers – Effect of spinning conditions on Ultrafiltration Properties. *J. Membrane Sci.* 22: 199-215

Barth, C., Goncalves, M.C., Pires, A.T.N., Roeder, J. and Wolf, B.A. (2000) Asymmetric polysulfone and polyethersulfone membranes: effects of thermodynamic conditions during formation on their performance. *J. Membrane Sci.* 169: 287-299

Broadhead, K.W. and Tresco, P.A. (1998) Effect of fabrication conditions on the structure and function of membranes formed from poly(acrynitrile-vinylchloride*). J. Membrane Sci.* 147: 235-245

Cabasso, I., Klein, E., James K.S. (1977) Polysulfone hollow fibers II. Morphology. *J. Appl. Pol. Sci.* 21: 165 – 180

Capanelli, G., Vigo, F. and Munari, S. (1983) Ultrafiltration membranes-Characterization method. *J. Membrane Sci.* 15: 289-313

Chung, T.S. and Hu, X. (1997) Effect of air gap distance on the Morphology and Thermal Properties of Poly Ether Sulfone (PES) Hollow Fibers. *J. App. Pol. Sci* .66: 1067-1077

Chung, T.S., Teoh, S.K., Hu, X. (1997) Formation of ultrathin high performance polyethersulfone hollow-fiber membranes. *J.Membrane Sci.* 133: 161-175

Electronic reference (2004) Fundamentals: Mass transfer, [ONLINE].
Available: http://www.spl.ethz.ch/fundamentals-masstransfer-filmodel.php

Elshof, J.E. (2001) Porous membranes [ONLINE].

Available: http://ims.ct.utwente.nl/algemeen/technology.html

Encyclopaedia Polymers. (1989) Ultrafiltration. 17, 72 - 106

Feng,C.Y., Khulbe, K.C., Chowdhury, G., Matsuura, T., Sapkal, V.C. (2001) Structural and performance study of micro-porous polyetherimide hollow fiber membranes made by solvent spinning method. *J. Membrane Sci.*189: 193-203

Field, R.W., Wu., D., Howell, J.A. and Gupta, B.B. (1995) Critical flux concept for microfiltration fouling. *J. Membrane Sci.* 100: 259-272

Graham, P.D., Brodbeck, K.J. and McHugh, A.J. (1999) Phase inversion dynamics of PGLA solutions related to drug delivery. *J. Controlled release* 58: 233-245

Han, M.J. and Nam, S.T. (2002) Thermodynamic and Rheological variation in polysulfone solution by PVP and its effect in the preparation of phase inversion membrane. *J. Membrane Sci.* 202: 55-61

Idris, A., Noordin, M.Y., Ismail, A.F., Shilton, S.J. (2002) Study of shear rate influence on the performance of cellulose acetate reverse osmosis hollow fiber membranes. *J. Membrane Sci.*202: 205-215

Jacobs, E.P. and Leukes, W. (1996) Formation of an externally unskinned psf capillary membranes. *J. Membrane Sci.* 121: 149-157

Jacobs, E.P. and Sanderson R.D. (1997) Capillary membrane production development. *WRC report* No 632/1/97

Karode, S.K. and Kumar, A. (2001) Formation of polymeric membranes by immersion precipitation : an algorithm for mass transfer calculations. *J. Membrane Sci.* 187: 287-296

Kesting, R.E. (1990) The four Tiers of Structure in Intergrally Skinned Phase Inversion Membranes and Their Relevance to the Various Separation Regimes. *J. Appl. Pol. Sci.* 41: 2739 – 2752

Khayet, M. (2003) The effect of air gap length on internal and external morphology of hollow fiber membranes. *Chemical Engineering Science.* 58: 3091 - 3104

Kim, J.H., Park, Y.I. Jegal, J. and Lee, K.H. (1995) Effect of Spinning Conditions on the Structure Formation and Dimension of Hollow-Fiber Membranes and Their Relationship with the Permeability in Dry-Wet Spinning Technology. *J. Appl. Pol. Sci* 57: 1637-1644

Khulbe, K.C., Gagne, S., Tabe Mohammadi, A., Matsuura, T. and Larmarche, A.-M. (1995) Investigation of polymer morphology of integral-asymmetric membranes by ESR and Raman spectroscopy and its comparison with homogeneous films. *J. Membrane Sci.* 98: 201-208

Kools, W.F.C. (1998) Membrane formation by phase inversion in multi-component polymer systems. Mechanism and morphologies. *Ph.D. dissertation,* University of Twente, Enschede

Lin, D.T., Cheng, L.P., Kang, Y.J., Chen, L.W. and Young, T.H. (1998) Effect of precipitation conditions on the membrane morphology and permeation characteristics. *J. Membrane Sci.* 40: 185-194

McKelvey, S. A. and Koros, W.J. (1996) Phase separation vitrification, and the manifestation of macrovoids in polymeric asymmetric membranes. *J. Membrane Sci.* 112: 29 – 39

McKelvey, S. A., Clausi, D.T. and Koros, W.J. A guide to establishing fiber macroscopic properties for membrane applications. *J. Membrane Sci.* 124: 223-232

Munari S., Bottino A. and Moretti, P. (1989) Permoporometric study on ultrafiltration membranes. *J. Membrane Sci.* 41: 69-86

Munari S., Bottino S, Camera Roda G. and Capannelli G. (1990) Preparation of ultra-filtration membranes. State of the Art, *Desalination.*77: 85-100

Ochoa, N.A., Pradanos, P., Palacio, L., Pagliero, C., Marchese, J. and Hern`andez, A. (2001) Pore size distributions based on AFM imaging and retention of multidisperse polymer solutes, Characterization of polyethersulfone UF membranes with dopes containing different PVP. *J. Membrane Sci.* 187: 227- 237

Paul, D.R. (1968) Diffusion during the coagulation step of wet spinning. *J. App. Pol. Sci.*12: 383-402

Pekny, M.R., Zartman, J., Krantz, W.B., Greenberg, A.R., Todd, P. (2003) Flow-visualization during macrovoid pore formation in dry-cast cellulose acetate membranes. *J. Membrane Sci.* 211: 71-90

Pekny, M.R., Greenberg, A.R., Khare, V., Zartman, J., Krantz, W.B. and Todd, P. (2002) Macrovoid pore formation in dry-cast cellulose acetate membranes: buoyancy studies. *J. Membrane Sci.* 205: 11-21

Pesek, S.C. and Koros, W.J. (1993) Aqueous quenched asymmetric polysulfone hollow fibers prepared by dry/wet phase separation. *J. Membrane Sci.* 88: 1 – 19

Porter, Mark C. (1990) Synthetic membranes and their preparation. *Handbook of industrial membrane technology*

Qin J.J. and Chung T.S. (1999) Effect of dope flow rate on the morphology, separation performance, thermal and mechanical properties of ultra-filtration hollow fiber membranes. *J. Membrane Sci.*157: 35-51

Qin, J.J., Wang, R. and Chung, T.S. (2000) Investigation of shear stress effect within a spinneret on flux, separation and thermodynamical properties of hollow fiber ultra-filtration membranes. *J. Membrane Sci.* 175: 97-213

Qin, J.J., Gu, J. and Chung, T.S. (2001) Effect of wet and dry-jet wet spinning on the shear induced orientation during the formation of ultrafiltration hollow fiber membranes. *J. Membrane Sci.* 182: 57-75

Reuvers, A.J., Altena, F.W. and Smolders, C.A. (1986) De-mixing and gelation behavior of ternary cellulose acetate solutions. *J. Pol. Sci.: Part B: Pol. Phy.* 24: 93-804

Reuvers, A.J., Van de Berg, J.A.W. and Smolders, C.A. (1987) Formation of membranes by immersion precipitation. Part 1. A model to describe mass transfer during immersion precipitation. *J. Membrane Sci.*37: 45-65

Solomons, N.S. (2001) Membrane bio-reactor production of lignin and manganese peroxidase. *M-Tech dissertation.* Cape Technikon: Cape Town.

Stropnik, C., Musil, V. and Brumen, M. (2000) Polymeric membrane formation by wet-phase separation; turbidity and shrinkage phenomena as evidence for the elementary processes. *Polymer* 41: 9227 – 9237

Termonia, Y. (1995) Molecular modeling of phase-inversion membranes: Effect of additives in the coagulant. *J. Membrane Sci.* 104: 173-180

Torrestiana-Sanchez, B., Ortiz-Basurto, R.I. and Brito-De La Fuente, E. (1999) Effect of non-solvents on properties of spinning solutions and polyethersulfone hollow fibre ultra-filtration membrane. *J. Membrane Sci.* 152: 19-28

Tsai, H.A., Li, L.D., Lee, K.R., Wang, Y.C., Li, C.L., Huang, J. and Lai, J.Y. (2000) Effect of surfactant addition on the morphology and pervaporation performance of asymmetric polysulfone membranes. *J. Membrane Sci.* 176: 97-103

Tsige, M. and Grest, G.S. (2003) Molecular Dynamics Simulation of Solvent-Polymer Interdiffusion. I. Fickian diffusion. *Sandia National Laboratories*, Albquerque

Van de Witte, P. (1996) Phase separation processes in polymer solutions in relation to membrane formation. *J. Membrane Sci.*117, 1-31

Van der Vegt (1998) Molecular dynamics simulations of sorption and diffusion in rubbery polymers, Chapter 1. *Ph.D. dissertation,* University of Twente, Enschede

Van der Walt, A. (1999) Design and characterization of a transverse flow membrane module for gas transfer operations. *PhD. dissertation.* University of Stellenbosch: Cape Town.

Vera, I. (1989) Polysulfone membrane formation. *Biotechnology.* White sands Missile Range, New Mexico [ONLINE].
Available: http://mgravity.itsc.uah.edu/microgravity/micrex/exps/vercn1b.html

Wang, D., Li, K. and Teo, W.K. (1995) Relationship between mass ratio of nonsolvent-additive to solvent in membrane casting solution and its coagulation value. *J. Membrane Sci.*98: 233-240

Wang, D.M., Wu, T.T., Lin, F.C. and Lai, J.Y. (2000) A novel method for controlling the surface morphology of polymeric membranes. *J. Membrane Sci.* 169, 39-51

Wang, R., Chung, T.S. (2001) Determination of pore sizes and surface porosity and the effect of shear stress within a spinneret on asymmetric hollow fiber membranes. *J. membrane Sci.*188: 29-37

Welty, J.R., Wicks, C.E., Wilson, R.E., Rorrer, G. (2001) Steady-State Molecular Diffusion. *Fundamentals of Momentum, Heat and Mass Transfer.*, 4TH Edition, John Wiley and Sons, Ch. 26. USA

Wienk, I.M., Olde Scholtenhuis, F.H.A., van den Boomgard, Th. And Smolders, C.A. (1995) Spinning of hollow fiber ultrafiltration membranes from a polymer blend. *J. Membrane Sci.* 106: 233-243

Wijmans, J.G., Baaij, J.P.B. and Smolders C.A. (1983) The mechanism of formation of micro-porous or skinned membranes produced by immersion precipitation. *J. Membrane Sci.*14: 263-274

Yeong-Jin Han, M. and Nam, Suk-Tae (2002) Thermodynamic and rheological variation in polysulfone solution by PVP and its effect in the preparation of phase inversion membrane. *J. Membrane Sci.* 202: 55-61

Yilmaz, L. and McHugh, A.J. (1986) Modeling of asymmetric membranes. Formation 1 critique of evaporation models and development of diffusion equation formalism for the quench period. *J. Membrane Sci.*28: 287-310

Young, T.H. and Chen, L.W. (1991) A diffusion-controlled model for wet casting membrane formation. *J. Membrane Sci.*59: 169- 181

Young, T.H., Chen, L.W. (1993) Roles of bimolecular interaction and relative diffusion rate in membrane structure control. *J. Membrane Sci.* 83: 153-166

Young, T.H., Chen, L.W. (1995) Pore formation mechanism of membrane from phase inversion process. *Desalination.* 103: 233-24

Young, T.H., Cheng, L.P., Lin, D.J., Fane, L. and Chuang, W.Y. (1999) Mechanisms of PVDF membrane in soft (1-octanol) and harsh (water) non-solvents. *Polymer*. 40: 5315-5323

Zhou, B. (2003) Simulation of Formation of Polymeric Membrane by Immersion Precipitation. *PhD. dissertation.* Massachusetts Intitute of Technology, Canbridge, USA

APPENDICES

APPENDIX A

Optimization of equipment

Dope pump

The pump used to force the dope out of the spinneret was an SI Duty type with power of 0,18 kW, current of 1,21 Amps, 220 Volts, 50 Hz and running at 1400 revolutions per minute. A speed controller was connected to this pump. The rate at which the dope was pumped was monitored and adjusted. To determine the accuracy of the pump, extruding dope samples were collected using a measuring cylinder and the time taken to fill that volume was recorded. Four sets of readings for time and volume filled at each speed were recorded and the average was taken. The records for pump reading, volume filled and time taken to fill that certain volume are shown in table A.

Table A1 (a): Readings taken on determining the relationship between the Dope Pump Reading and volume collected manually

pump reading	volume filled/min (ml)	time taken (sec.)	SD	Var.
1.5	1.86	88	0.25456	0.0648
2	2.5	106	0.35355	0.125
2.5	2.98	78	0.33941	0.1152
4.5	5	75	0.35355	0.125

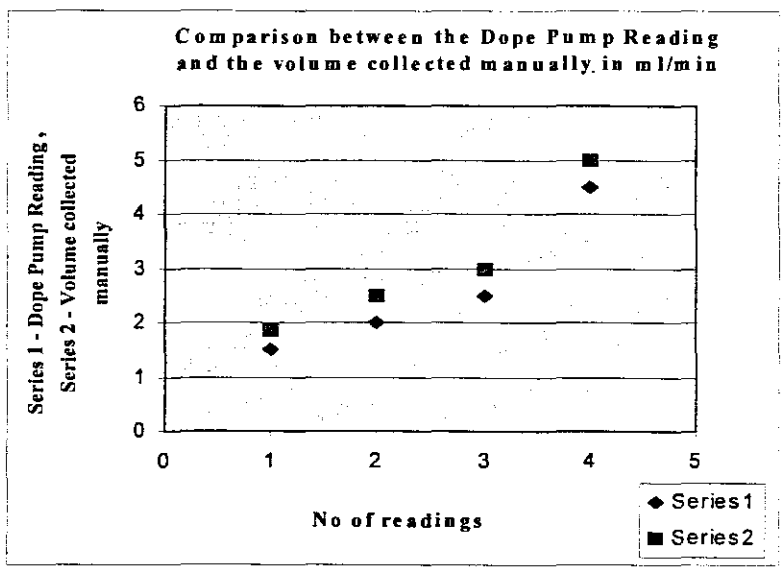

(a)

Figure A1 (a): Graph showing a relationship between a dope pump reading and a manual collected volume

Bore fluid pump and Rotameter

The accuracy of varispeed pump for bore fluid and rotameter was determined. This was done by collecting a volume of bore fluid, using a measuring cylinder, at certain pump speeds and the time taken to fill that volume was recorded.

Table A1 (b): Readings taken on determining the relationship between the bore fluid pump reading and volume collected manually

pump reading	volume filled/min(ml)	time taken (sec.)	SD	Var.
1.5	0.8	79	0.49497	0.245
2	2.5	102	0.35355	0.125
2.5	2.8	78	0.21213	0.045
4.5	5.5	94	0.70711	0.5

(b)

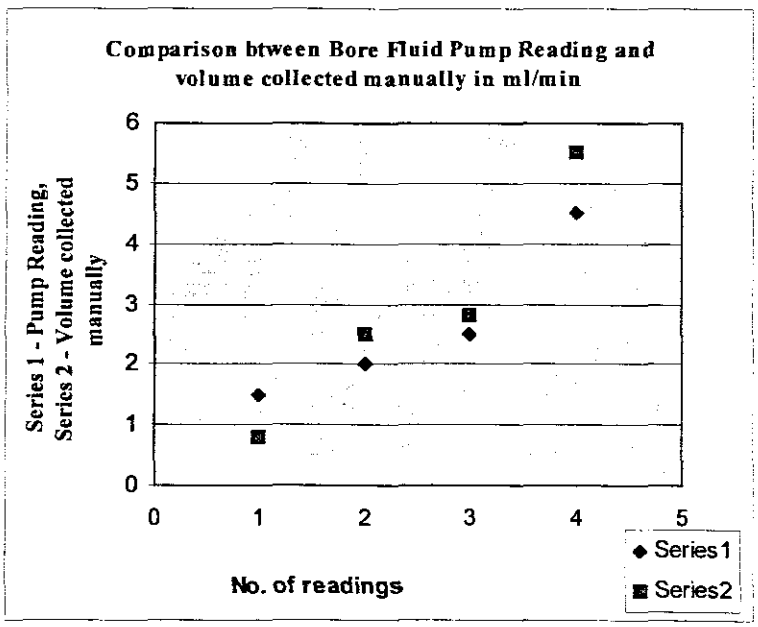

(b)

Figure A1 (b): Graph showing a relationship between a bore fluid pump reading and manual volume collection

To determine the accuracy of rotameter, the pump was set to its maximum speed, which is 60 Hz, and the rotameter readings were considered. A measuring cylinder was used to collect the volume of bore fluid reflected by the rotameter and the time to fill that volume was recorded.

Table A1 (c): Readings taken on determining the relationship between the rotameter reading and volume collected manually

Rota meter reading (ml/min)	volume would have been filled in 1 min.	volume filled/min (ml)	time taken (sec.)	SD	Var.
1.5	1.76	1.5	51	0.1838	0.03
2	2.22	2	54	0.1556	0.02
2.5	2.88	2.5	52	0.2687	0.07
4.5	5.19	4.5	52	0.4879	0.24

(c)

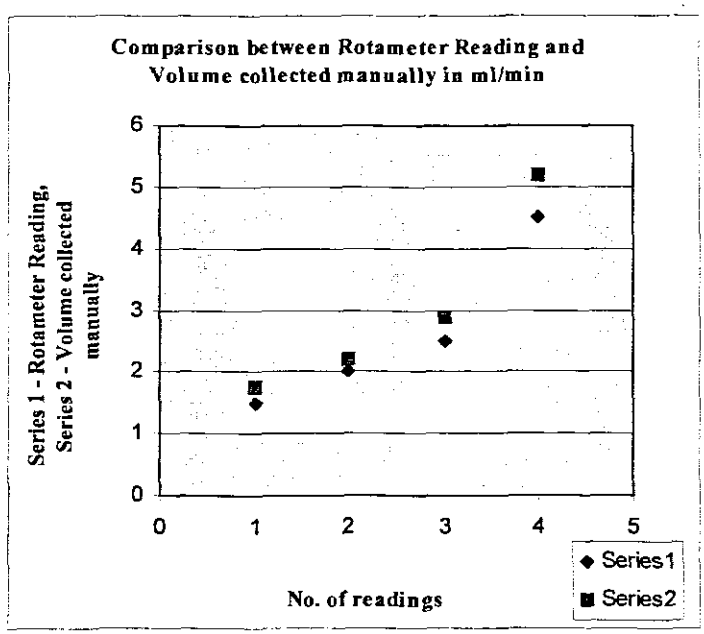

(c)

Figure A1 (c): Graph showing a relationship between a rotameter reading and the volume collected manually

The fore fluid flow rates were set using rotameter as it showed more accuracy than the pump readings. The standard deviation and variance for the rotameter readings is less to those of the pump. Which means the values deviate and the factor at which they vary is less.

Relating pumps and take-up

The relationship between the dope pump speed and the production rate was investigated. Production rate at each pump speed was recorded. The records are shown in tables A.

Table A1 (d and e): Readings taken on determining the relationship between the DER and membranes production rate

pump reading	No.of rev.	Time taken (min)	No of rev/min
3	11	7.48	1.47059
4	9	5.28	1.70455
4.5	6	3.41	1.75953
5	6	3.41	1.75953

(d)

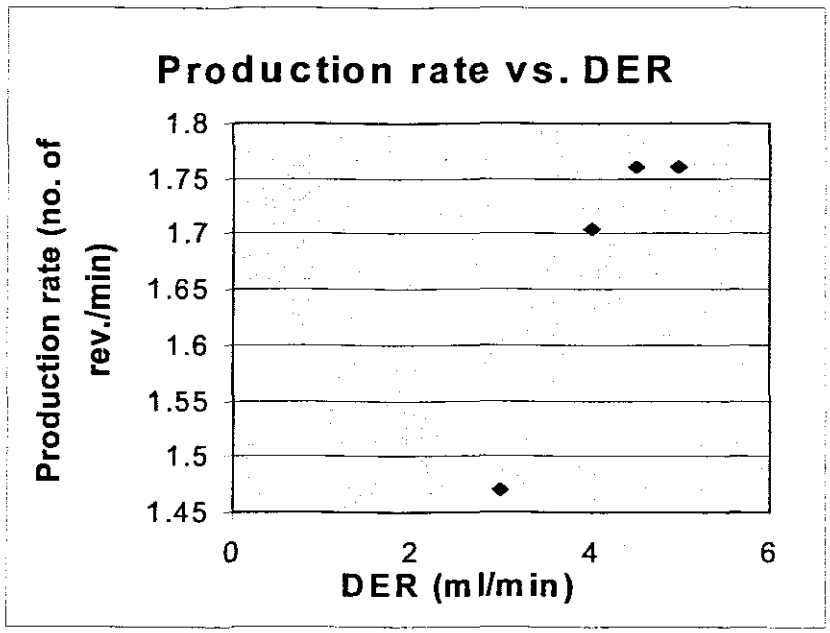

(d)

pump reading	No.of rev.	Time taken (min)	No of rev/min
3.15	5	2.37	2.1097
3.3	5	2.36	2.11864
3.45	5	2.34	2.13675
3.6	5	2.3	2.17391
3.75	5	2.29	2.18341
3.9	5	2.29	2.18341

(e)

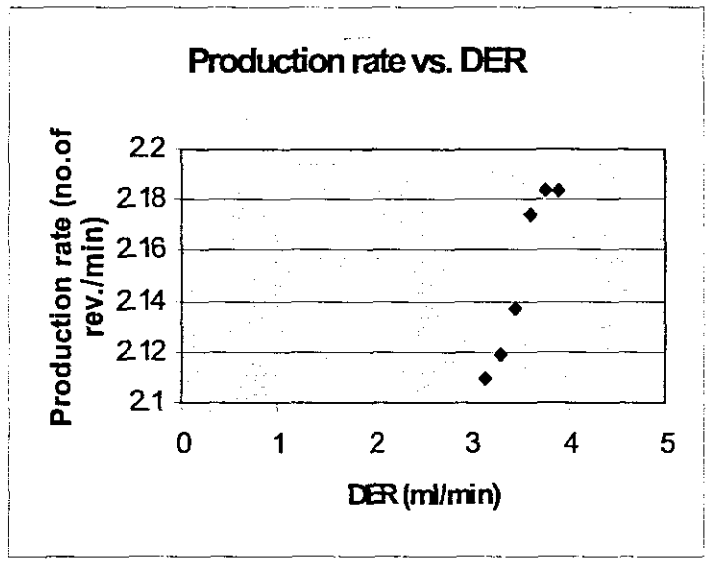

(e)

Figure A1 (d and e): Graphs showing a relationship between DER and membranes production rate

The results show that the rate at which the membranes are produced increases with an increase in dope extrusion rate. There seems to be a critical point, though, where the take up speed cannot be increased any more. In the study experiments, the line was too slack at high DER (3,0 and 3,2 ml/min) when the small spinneret size was used such that increasing the rollers and take up speed did not help. The spinning line only became entangled.

A2: The water content determination in NMP

The external spinning bath composition was maintained at different NMP + water aqueous contents. The percentages of these two (NMP and water) in a 25-litre bath were determined using the following method. A 50 ml NMP was mixed with 100 ml benzene put in a round bottom flask and heated by a heating mantle to their boiling points. A condenser was placed

above the flask and the condensate came down the calibrated collector. Benzene has a boiling point of 80^0C, water of 100^0C and NMP of 189^0C. This shows that benzene and water have low boiling points than NMP. These two boil long before NMP does. Water and NMP are miscible but not benzene and water. Water and benzene come to the collector first and the amount of water can be easily detected because of their immiscibility. Since water is dense than benzene, it settles down below the benzene level in the collector. By the time NMP boils, all the water content present, has been extracted and can be read thru the calibrated collector. The amount of water in a 50 ml NMP volume becomes known and a percentage of water present in NMP can be worked out.

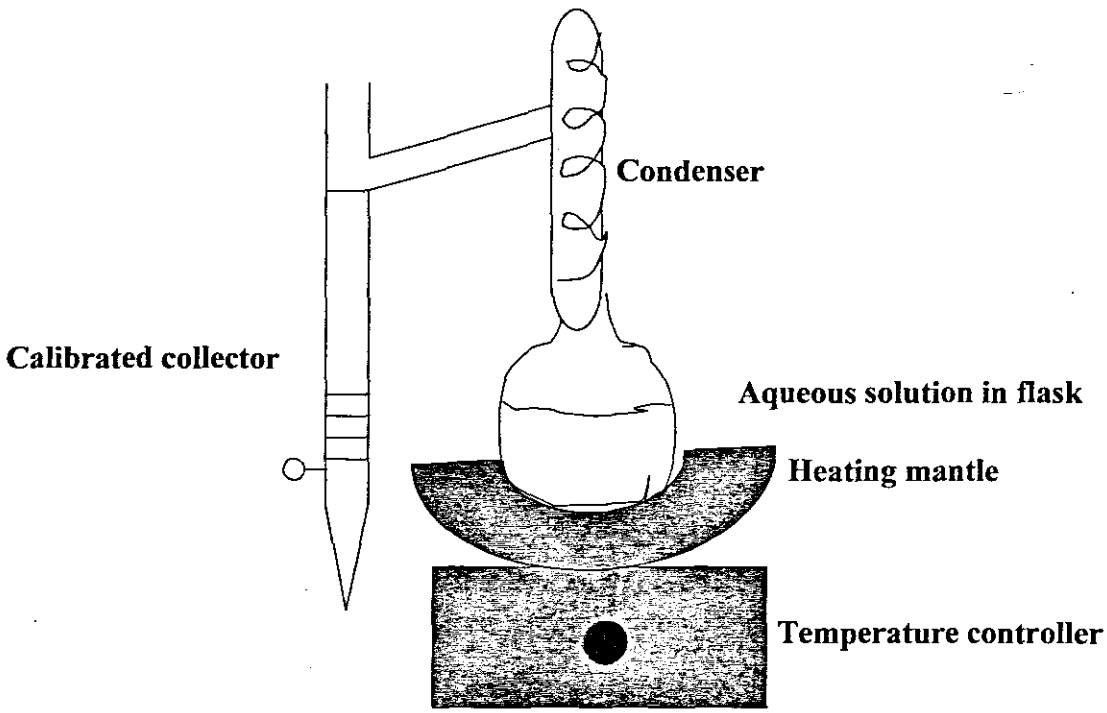

Figure A2: The set-up for water content determination in NMP

APPENDIX B

NMP and Psf Hazards

NMP

Physical and chemical properties

N- Methyl – 2- pyrrolidone is a water miscible organic solvent. It is a hygroscopic, colourless liquid with a mild amine or garlic odour. NMP is a polar and basic compound with high stability but unstable on exposure to moisture. It has a boiling point of 189 ^{0}C, flash point of 88^{0}C and vapour pressure of 20^{0}C. It is soluble in ethanol, ether, acetone, and chloroform. It is used in the manufacturing industries including cosmetics, drugs, insecticides, herbicides and fungicides.

NMP may enter the environment as emission to the atmosphere, as the substance is volatile, it is also mobile in soil. On burning, it releases toxic and corrosive gases or vapours like nitrous vapours, sulphur oxides. It reacts with many compounds e.g. oxidizers. It has an increased risk of fire or explosion. Heat sources, combustible materials, oxidizing agents, reducing agents, acids, and metals are the materials to be avoided. Routes of exposure include ingestion, inhalation, eyes and skin.

Effects/ symptoms on exposure

After inhalation there will be signs of slight irritation, headache, dizziness and feeling nausea. After ingestion the victim may vomit, have abdominal pains, diarrhoea, gastrointestinal complaints and symptoms similar to those listed under inhalation. If the substance is absorbed through the skin, there will be tingling or irritation of skin, itching and symptoms similar to those listed under inhalation. On continuous skin contact, there will develop skin rash or inflammation and blisters. After eye contact, there will be irritation of the eye tissue, visual disturbance and the redness of the eye tissue. On continuous or repeated exposure, there will be gastrointestinal complaints, feeling of weakness, enlargement or affection of liver and the breath will have characteristic odour.

Personal protection

For eye protection, one has to wear a face shield.

For hands protection, gloves have to be worn.

For skin protection, protective clothing must be worn.

For respiratory protection, gas mask with filter type A must be used.

Eye contact:

- Rinse eyes immediately with plenty of water for 15 minutes.
- Do not apply neutralizing agents
- Consult a doctor or medical service if irritation persists

Skin contact:

- Wash immediately with lots of water and soap for 15 minutes
- Remove clothing before washing
- Consult a doctor/medical service if irritation persists

After inhalation:

- Remove the victim into fresh air
- Unconscious: maintain adequate airway and respiration
- Consult a doctor/medical service if breathing problems develop

After ingestion:

- Never give water to an unconscious person
- Give nothing (little) to drink
- Consult a doctor/medical service if you feel unwell

Suitable extinguishing media:

- Water spray
- Alcohol foam
- BC powder

Clean-up:

- Take up liquid spill into a non combustible material e.g.: sand
- Scoop absorbed substance into closing containers
- Clean contaminated surfaces with an excess of water

Storage:

- Keep container tightly closed
- Store in a dry area
- Meet the legal requirements
- Keep away from: heat sources, combustible materials, oxidizing agents, reducing agents, acids, metals

Psf

Physical and chemical properties

Udel® Polysulfone is a light amber, amorphous thermoplastic, available as rods of 0.125" to 5.000" in diameter, sheets of 0.020" to 4.500" thickness, films of 0.005" to .010" thickness and tubes of 0.250" X 0.187", 0.750" X 0.625". Polysulfone has a very high dimensional stability with no carcinogenic effects known. The change in linear dimensions after exposure to boiling water or air at 149^0C is generally 1/10 of one percent or less.

Polysulfone is tough, rigid and maintains its properties over a wide temperature range from – 100°C to above 149°C with a softening point of 190^0C. It offers high chemical resistance to acidic and salt solutions, and good resistance to detergents, hot water, and steam. Polysulfone is not resistant to polar organic solvents such as ketones, chlorinated hydrocarbons and aromatic hydrocarbons. It is negligibly (below 0,1) soluble in water and essentially odorless. Toxicity is expected to be low based on insolubility of the polymer in water. It is soluble in NMP, DMAc and DMF.

Effects/ symptoms on exposure

Ingestion is not a possible route of exposure. Molten Polysulfone causes thermal burns on the skin and causes mechanical irritation of the eyes. It is irrespirable; therefore, inhalation is also not a possible route of exposure and has no chronic effects known.

Personal protection

For eye protection, safety glasses are recommended to prevent particulate matter from entering eyes while grinding or machining.

For skin protection, protective gloves are required when handling hot polymer. Also, long sleeve cotton shirt and long pants if handling molten polymer.

No Respiratory protection needed under normal processing, if ventilation is adequate. Grinding and machining of parts should be reviewed to assure that particulate levels are kept at recommended levels.

Skin contact:

If molten polymer contacts skin, cool rapidly with cold water. Do not attempt to peel polymer from skin. Obtain medical attention to thermal burn. Wash skin with soap and plenty of water.

After inhalation:

If exposed to fumes from overheating, move to fresh air. Consult a physician if symptoms persist.

Eye contact:

Flush eyes with water. Consult a physician if symptoms persist.

Suitable extinguishing media:

Water spray or any class A extinguishing agent.

Clean-up:

Clean up by vacuuming or sweeping to prevent falls.

Storage:

Store in a dry area.

Keep containers closed to prevent contamination.

APPENDIX C

Experimental results

C1 External bath composition

Introduction

These first two experiments conducted on determining the effect of external bath composition were 99 and 93% NMP content. These two extremes were chosen based on the previous experiments conducted at IPS, where externally unskinned membranes were produced at an external bath composition of 94,5% NMP aqueous content.

Table C3 (a): Conditions under which the experiments were conducted Table C3 (b)

Mixing date	16/07/02	16/07/02
Casting date	18/07/02	17/07/02
Room temperature	18^0C	16.5^0C
Casting solution temp.	room temperature	room temperature
External coagulant temp.	17.5^0C	16.5^0C
Lumen coagulant temp.	room temperature	room temperature
Rinse coagulant temp.	16^0C	15^0C
Lumen coagulant composition +98%distilled water	2%NMP + 98% distilled water	2%NMP
External coagulant 1 composition water	99%NMP + 4% water	93%NMP + 7%
External coagulant 2 composition	RO water	RO water
Rinse coagulant composition	RO water	RO water

SEM photos (shown in section 7.1) were taken and it was found that in both cases a skin layers were formed on the outer surfaces. As stated in the discussions under the effect of external spinning bath, at 99% NMP, the polymer must have re-dissolved in the bath and precipitated on reaching the humidity chamber. At 93% NMP, the water content must have been high enough to precipitate the nascent membrane from the external surface.

C2 DER Effects

Introduction

The first experiments to determine the effect of DER were conducted at 2,5; 3,0; 4,0; 4,5; and 5,0 ml/min. The SEM photos of those experimental membranes showed that an externally unskinned membrane was produced at 3,0 ml/min. but an external skin layer was formed when the DER was 4,0 ml/min. Small intervals in-between two extremes were taken. The conditions under which the experiments were conducted are shown in tables 7.1 (a and b). The results from those experiments are shown in the table below.

Results

Table C1: Experimental results on varying the DER, BFF held constant at 4,5 ml/min and external bath comp = 94 % NMP

Exp. No.	Pure water flux (L/m^2h)		Ultra-filtration flux (L/m^2h)		Retention (%)		I.D (cm)	O.D.(cm)	Thickness (cm)	Burst pressure (kPa)	Conditions	Effective area (m^2)
	100	200	100	200	100	200					BFF;DER;BATH	
E 25	193	315	30	49	5	11	1,14	1,9	0,76	1500	4,5; 3,15; 94% NMP	0,01223
E 26	169	282	33	57	15	28	1,1	1,9	0,8		4,5; 3,3; 94% NMP	0,01223
E 27	186	303	30	44	39	21	1,14	1,9	0,76	1500	4,5; 3,45; 94% NMP	0,01199
E 28	208	357	31	46	37	20	1,1	1,91	0,81	>1600	4,5; 3,6; 94% NMP	0,01223
E 29	113	177	36	51	41	24	1,1	1,9	0,8	1800	4,5; 3,75; 94% NMP	0,01223
E 30	118	192	38	53	7	28	1,12	1,83	0,71	2000	4,5; 3,9, 94% NMP	0,01249
E 31	120	210	33	53	42	25	1 075	1 865	0,79	1500	4,5; 3,9, 94% NMP	0,01199
E 32	155	299	35	52			1,14	1,89	0,75	1500	4,5; 3,75; 94% NMP	0,01289
E 33	141	209	39	54	11	23	1,1	1,81	0,71	1600	4,5; 3,6; 94% NMP	0,01223
E 34	196	348	25	72	50	26	1 115	1,74	0,625	1600	4,5; 3,45; 94% NMP	0,01243
E 35	212	446	45	70	50	23	1,1	1,7	0,6	1600	4,5; 3,3; 94% NMP	0,01223
E 36	276	493	49	72	51	32	1,01	1,81	0,8	>1600	4,5; 3,15; 94% NMP	0,01223

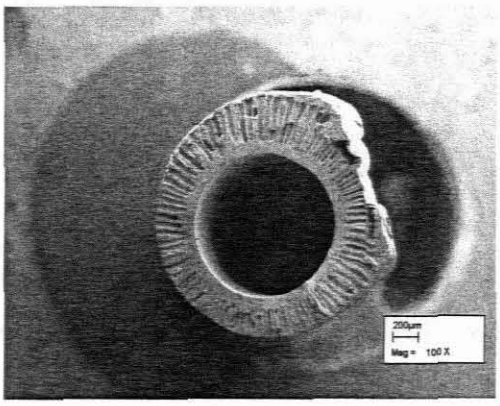

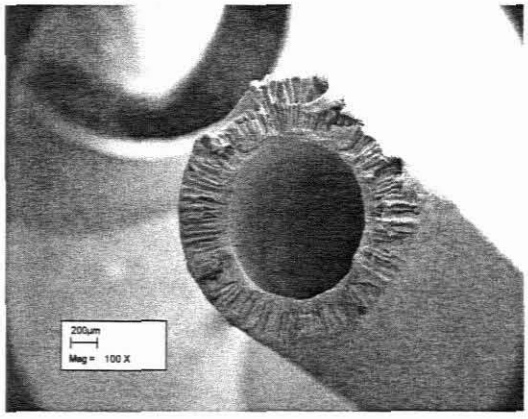

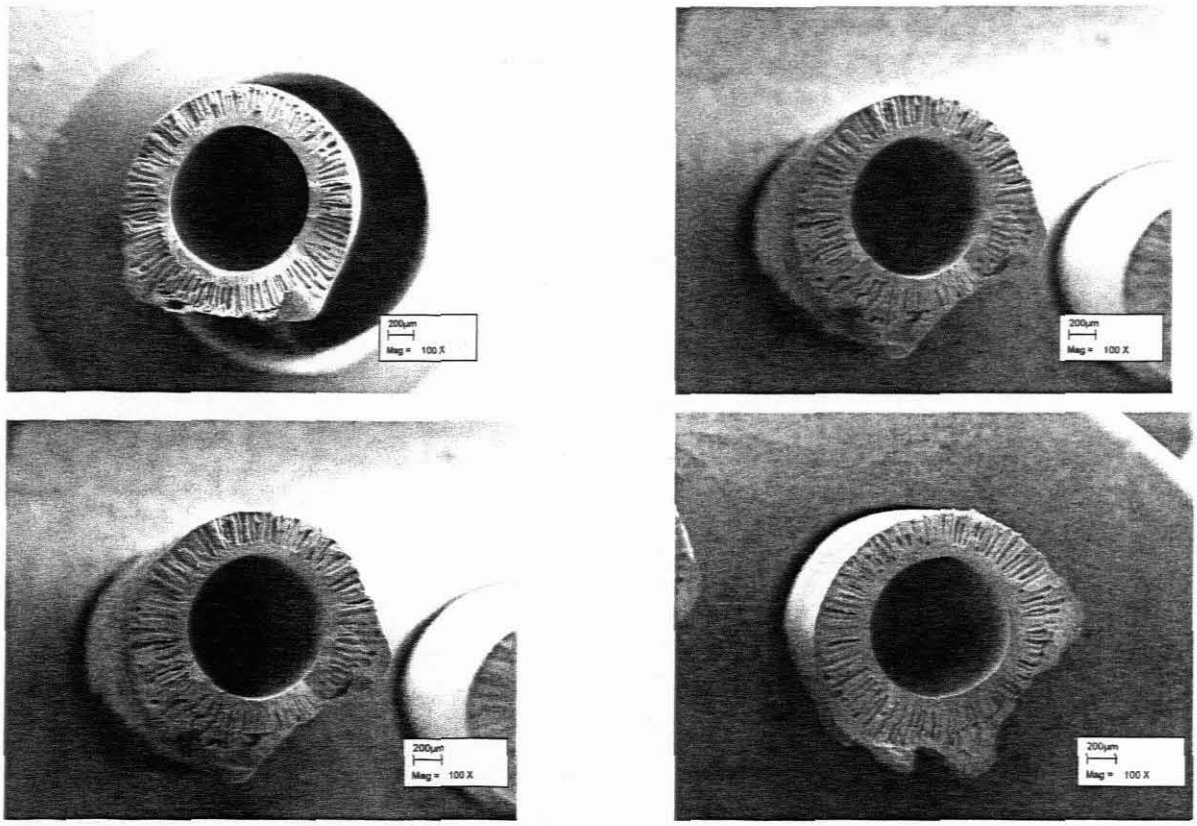

Figure C1: Cross sections of membranes spun between 3,0 and 4,0 ml/min. DER

All the membranes produced between these dope extrusion rates had a very thin external skin layer. This could mean that 3,0 ml/min is the maximum DER that can be used with 4,5 ml/min BFF to produce externally unskinned membrane. 4,5ml/min was the maximum BFF that the rotameter could give.

C2 BFF composition effects

Introduction

At Dope Extrusion Rates between 3,0 and 4,0 ml/min, two bore fluid compositions were used. . These were 2% NMP with water and 2% NaCl with water. The results for these experiments are shown in table CI above. From experiments 25 to 30; 2 % NMP+ water was used and from 31 to 36; 2% NaCl + water was used as a bore fluid.

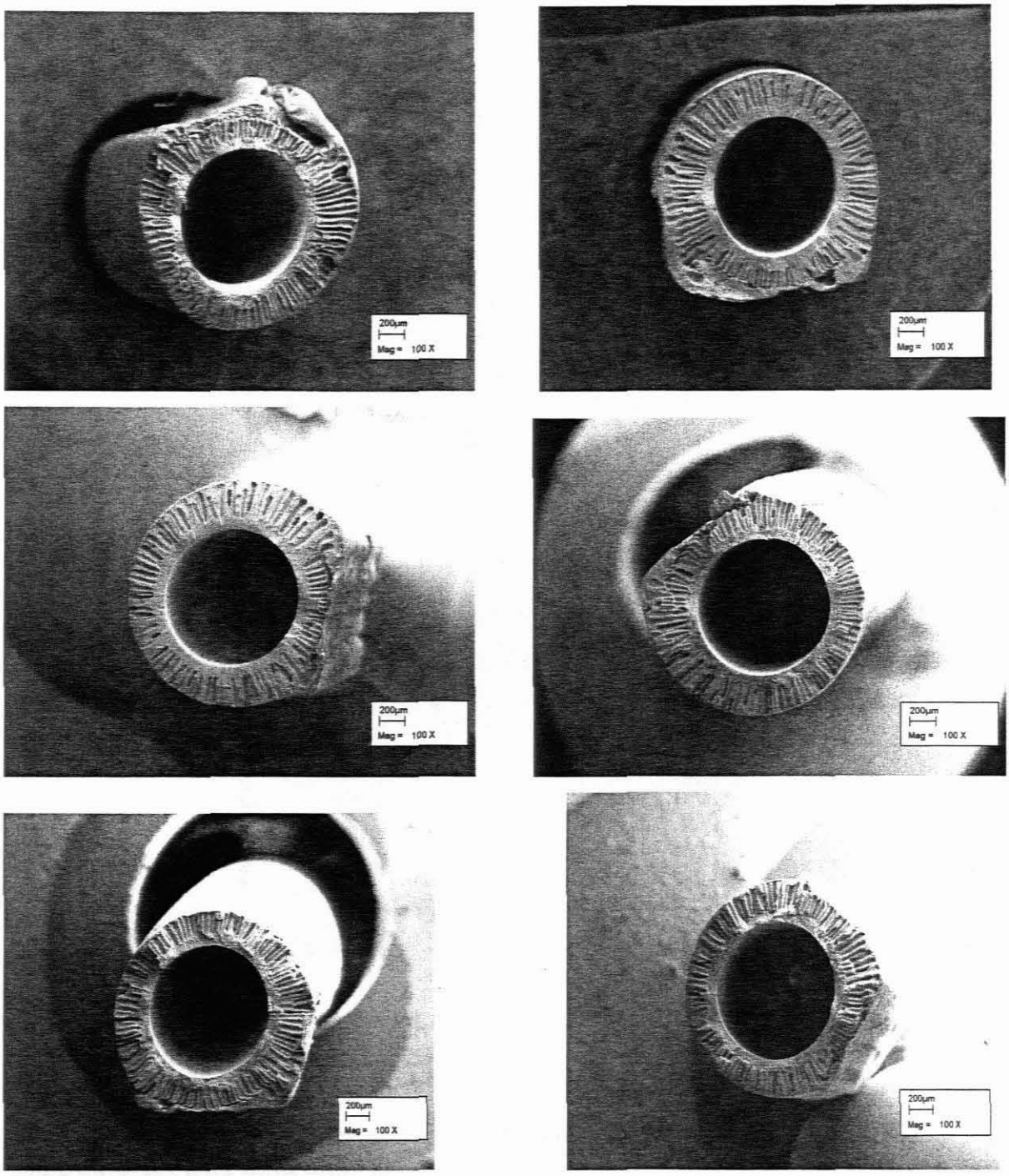

Figure C2.1: Cross section of membranes spun between 3,0 and 4,0 ml/min. DER using 2 % NaCl bore fluid composition

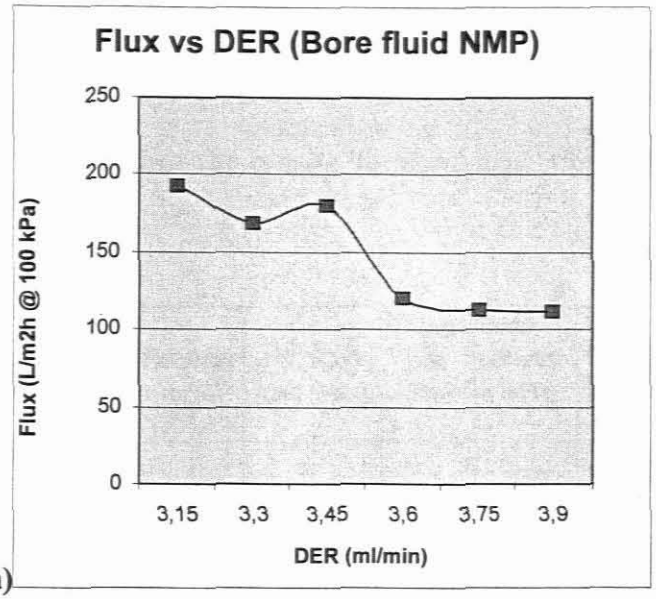

(a)

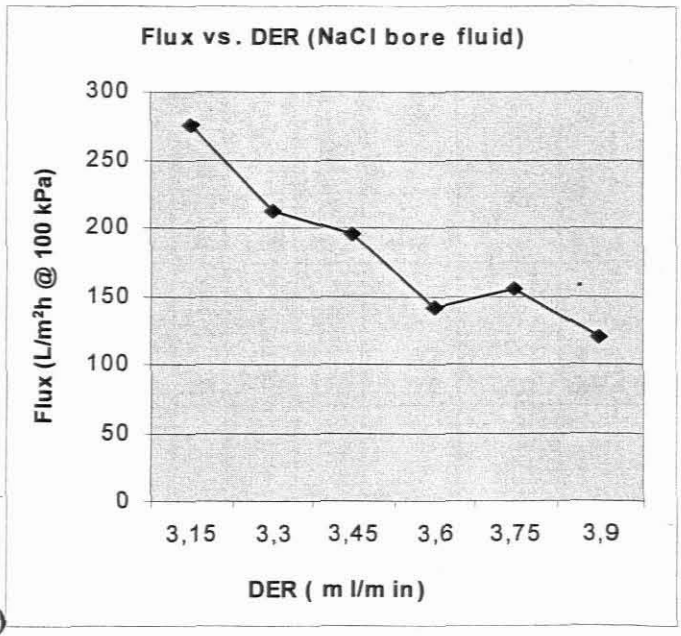

(b)

Figure C 2.2 (a and b): Experimental results showing flux versus Dope Extrusion Rate using different bore fluid compositions

The flux of membranes in both cases, that is when salt and NMP was added to the bore fluid, decreased with an increase in DER. In the case where salt was added, the flux was higher to that of membranes spun with NMP added to the bore fluid. Adding salt to the bore fluid rather than NMP gave good results as indicated by the graphs.

C4 Drying effect

The results obtained from drying the membranes with Ethanol are shown in the tables below

Tables C4 (a, b and c): Show the results obtained after the membranes were dried with alcohol

(a)

Exp. No.	Pure water flux (L/m^2h)		Ultra-filtration flux (L/m^2h)		Retention(%)		I.D (cm)	O.D.(cm)	Thickness (cm)	Burst pressure (kPa)	Conditions	Memb. Structure	Effective area (m^2)
	100	200	100	200	100	200					BFF;DER;BATH		
E 01	145	232	32	39	80	54	1	1,85	0.85	>1700	1,5;4,0;96%NMP	Thick skin inside, voids wide not close to each other, Thin outward skin.	0.0114
E 02	168	351	37	51	54	34	1.05	1.72	0.67		2,5;4,0;96%NMP	Thick inner skin, voids wide, elongated to the outer skin. Thick polymer rich inbetween voids.	0.0123
E 03	275	322	43	61	49	26	1.07	1.83	0.755	1200	3,5;4,0;96%NMP	Thick inner skin, voids extending to an outer skin	0.0123
E 04	175	281	43	84	43	18	1	2	1	1700	4,0;4,0;96%NMP	Thick inner skin, voids wide and not much elongated,some start from inner skin whilst others don't reach the outer skin	0.0136
E 05	173	275	36	51	45	27	1	1.97	0.97	1600	4,5;4,0;96%NMP	Thick inner skin,voids becoming short, some start far from the inner skin while some don't reach the outer skin.	0.0117

(b)

Exp. No.	Pure water flux (L/m^2h)		Ultra-filtration flux(L/m^2h)		Retention (%)		I.D (cm)	O.D.(cm)	Thickness (cm)	Burst pressure (kPa)	Conditions	Memb. Structure	Effective area (m^2)
	100	200	100	200	100	200					BFF;DER;BATH		
E07				leaked			1.32	1.85	0.53		4,5;2,5;96%NMP	Thick inner skin, few finger like voids, polymer rich inbetween thich. Distorted on the inner surface.Externally unskinned	
E06											4,5;3,0;96%NMP	Thick inner skin, voids becoming many, starting just below the skin and extend to the outside. Externally unskinned.	0.0122
E05	166	271	39	66	51	22	1	1.97	0.97		4,5;4,0;96%NMP	Thick inner skin,voids becoming short, some start far from the inner skin while some do not reach the outer skin.	0.0117
E08	268	442	67	89	49	36	1	1.96	0.96	1700	4,5;4,5;96%NMP	Thick inner skin, voids narrow and extend to the outer skin. Small pores @the end of voids.Thick outer skin.	0.0119
E09	268	277	41	60	50	30	1.2	2.13	0.93	1800	4,5;5,0;96%NMP	Inner skin reduced, too many needle like voids, sarting just below the inner skin and extend to the outer skin.Thick outer skin	0.0108

(c)

Exp. No.	Pure water flux (L/m^2h)		Ultra-filtration flux (L/m^2h)		Retention (%)		I.D (cm)	O.D.(cm)	Thickness (cm)	Burst pressure (kPa)	Conditions	Memb. Structure	Effective area (m^2)
	100	200	100	200	100	200					BFF;DER;BATH		
E 10	86	152	28	38	73	68	1.1	2	0.9	1700	1,5;4,0;94%NMP	Inner skin thin, too many needle like voids extending to the outer skin.	0.0126
E 11	94	199	27	43	61	43	1	1.94	0.94	1700	2,5;4,0;94%NMP	Thin inner skin, too many needle like voids. Small pores at the end of voids. Thinner outer skin.	0.0123
E 12	129	266	36	42	63	45	1.07	1.89	0.815	1300	3,5;4,0;94%NMP	Inner skin reduced, too many needle like voids, starting just below the inner skin and extend to the outer skin.Outer skin reduced	0.0128
E 13	90	178	25	36	57	37	1.13	1.89	0.76	1750	4,0;4,0;94%NMP	Inner skin getting thin, voids narrow and extend to the outside skin. Thin outer skin	0.0129
E 14	170	328	32	47	51	33	1.1	2	0.9	2000	4,5;4,0;94%NMP	Thin inner skin, narrow needle like voids. Pores on the underlying outer thin skin.	0.0126

The structure of the membranes was not checked after drying with alcohol, so the membrane structures given here are the ones obtained initially. The inside diameter, outer diameter and thickness of the dried membranes decreased.

APPENDIX D

Capillary membrane applications

D1 Introduction

There are an increasing number of areas where membrane bio-reactors are serious alternatives to conventional chemical reactors. Many UF capillary membranes are available on the market. The research on developing a new membrane was conducted by Luekes, W and Jacobs, E ; in association with other WRC-funded projects so that it would complement the development of membrane-process technology. The programme areas concerned were in the fields of biotechnology (membrane bioreactors and new membranes for use in membrane bioreactors) and in the production of potable water from highly coloured water in the Southern Cape (Jacobs and Leukes, 1996)

D2 Water treatment applications

Many waste materials are recognized to contain potentially useful components, further processing should be cost effective. Membranes can be used for treatment of domestic sewage. Both potable-water supply and industrial applications of membranes are increasing concomitantly with the technical improvements and cost reductions of membranes, modules and systems. Solomon (2001) pointed out that according to Howell (1993), the performance of membrane systems is determined by transport processes. These influence the three independent stages, which involve:

- Convective and diffusive flows on the feed side of the membrane
- Permeation of material through the membrane
- Transfer of material into the permeate stream

Micro filtration (MF) membranes are typically used to reject suspended solids. Ultra filtration (UF) membranes containing much smaller pores, are able to reject macromolecular solutes in the molecular weight range of about 10^{-3} to 10^{-6} .In the case of nano filtration (NF) the pores are small that they are able to reject micro-solutes in the range of 200 to 1000 Dalton (Da). Low-molecular –mass cut-off ultra filtration membranes provide not only the means to reduce microbial counts in water, but readily remove components that contribute color and turbidity to such water. It is a filtration that can be applied to wastewater

remediation and pre-treatment of sea-water and other water, for desalination by reverse osmosis.

D3 Biotechnological applications

It has been demonstrated that membranes have notable potential in biotechnological applications and much research is being conducted internationally in this area. For the biotechnological application, the envisaged membrane had to provide a unique substructure matrix within which a filamentous fungus could be immobilized for bio-catalysis.

In order to cultivate the fungus in a membrane bioreactor, it was reasoned that the membrane support matrix had to provide some protection for the fungus. It was argued that a suitable membrane for this application should be one that was internally skinned; with a substructure containing closely packed narrow-bore macro voids that extend all the way from just below the skin layer to the membrane periphery. The fungus is to be grown within the confines of these macro voids. Further to inoculate microvoids with spores, the microvoids had to be accessible from the outside. This would be possible only if the membrane had no skin layer on the outside. Immobilized enzymes may be incorporated into continuous process streams and can be continuously recycled when used with batch systems. In addition immobilized forms are often more stable than free enzymes.

D4 Biomedical applications

The use of phase-inversion membranes to encapsulate living cells prior to transplantation into an immunological incompatible host is being developed as a treatment for a variety of diseases (Broadhead and Tresco, 1998). Recent studies indicate that sustained secretion of bioactive molecules from such devices allows them to treat conditions such as Parkinson's disease, amyotrophic lateral sclerosis, Alzeheimer's disease, insulin dependant diabetes and chronic pain.

The perm-selective encapsulating barrier allows essential nutrients, waste products and bioactive cell secretions to pass, while preventing the inward movement of large host immune system components. The encapsulating membrane is used to physically isolate the transplanted cells from host tissue, to provide a level of safety by preventing the transplanted cells from forming a tumour and can be used to facilitate implant retrieval. Phase-inversion membranes used for cell encapsulation have been formed from thermoplastics and elastomers

such as polysulfone, polyurethane, polyvinyl alcohol, polyamide and polyacrylonitrile-co-vinylchloride(PAN-PVC)

APPENDIX E

Membrane modules and flow channels

E1: Membrane modules

Membranes are available in several different configurations, e.g. tubular, hollow fibre, flat sheet and spiral wound. These configurations can be made into various membrane modules depending on the suitability of the configuration to that specific module.

Spiral wound module

A flat sheet is wound around a central tube. The membranes are glued along three sides to form "leaves" attached to a permeate channel (tube) along the unsealed edge of the leaf. The internal of the leaf contains a permeate spacer designed to support the membrane without collapsing under pressure. The permeate spacer is porous and conducts the permeate to the permeate tube. Several leaves are connected to the tube. A feed channel spacer (a net-like sheet) is placed between leaves to define channel height and provide mass transfer benefits. The leaves are wound around the permeate tube and given an outer casting.

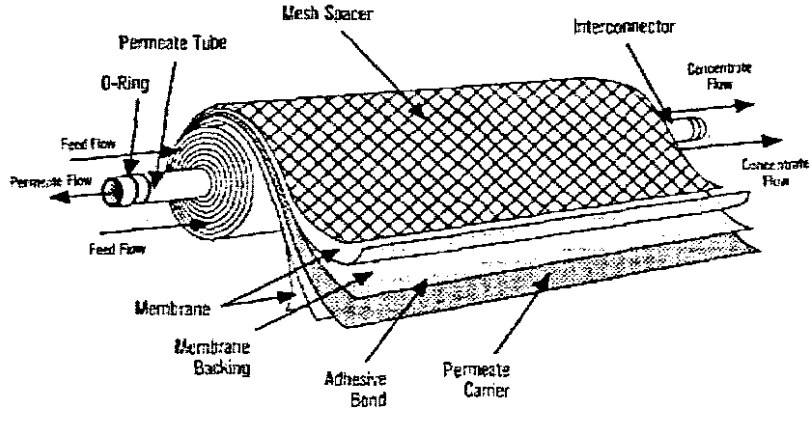

Figure E 1.1: Spiral wound module
(Source): www.membranes.nist.gov/Bioremediation/fig.pages/f3.html

❖ Hollow fibre modules

These modules use membranes that are self-supporting, i.e. walls are string enough to avoid collapse or bursting. The outer diameter may be < 0,3 to 0,8 mm. Hollow fibre modules contain thousands of fibres arranged in a bundle and potted in epoxy to seal the element. This type of module is used for RO, UF and MF.

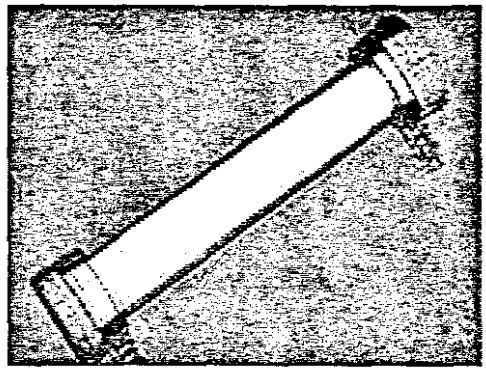

Figure E 1.2: Hollow fibre module
(Source): www.membranes.nist.gov/Bioremediation/fig.pages/f3.html

❖ **Flat sheet/Flat plate**

Flat sheet membranes are sitting on a plate that provides a porous support for permeate outlet. The flow channels are usually thin, 1 to 3 mm and sometimes fitted with a mesh-like channel spacer. The membranes are stacked in flow channels connected in series or parallel.

Plate-and-Frame

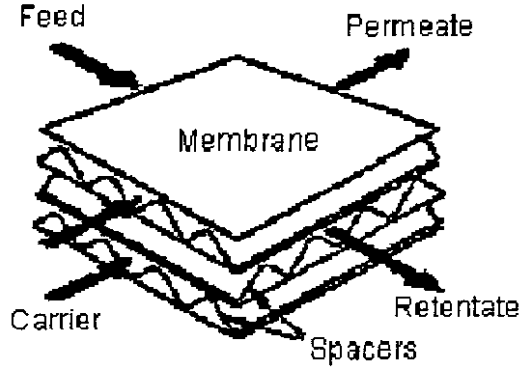

Figure E 1.3: Plate and frame module
(Source): www.membranes.nist.gov/Bioremediation/fig.pages/f3.html

❖ **Tubular module**

This module is similar to the shell and tube heat exchanger with tubes connected in series or parallel. Sometimes the membrane tubes are inserted into perforated metal support tubes, sometimes the tubes are self supporting.

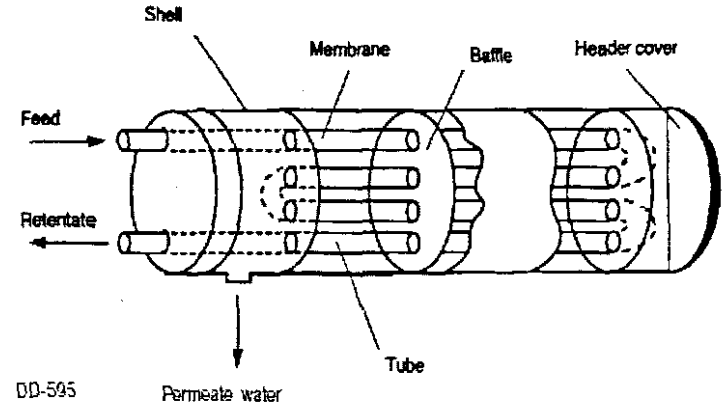

Figure E 1.4: Tubular module

E2: Different flow channels in modules with capillary membranes

Membranes have been packaged in modules of various designs. For micro-filtration and ultra-filtration applications, capillary membranes are often used since they are self supporting. They can be easily produced in different dimensions and morphologies. Furthermore, a high membrane-surface to module-volume ratio can be obtained. Three possibilities for the feed flow can be:-

2.1 The feed flow is through the bore of the capillaries; a capillary bore fed module design. The advantages of this shell-and-tube heat exchanger design are the well-controlled hydrodynamics of the feed and the good possibilities of cleaning.

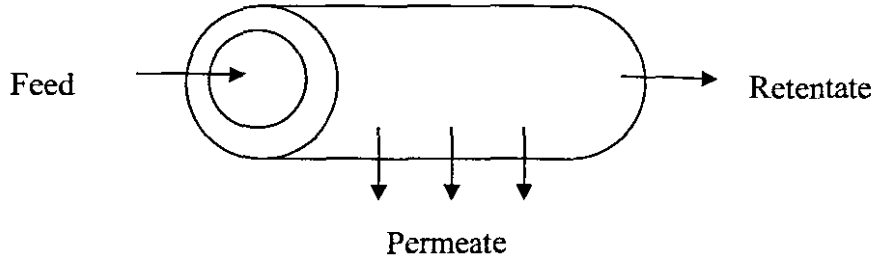

2. 2 The feed flows outside the capillary membranes, a shell-side fed module design. The shell-side fed module design can be designed and constructed in many different ways. Two essential different types can be distinguished:

(i) Longitudinal flow: The flow of the feed is parallel to the capillary membranes.

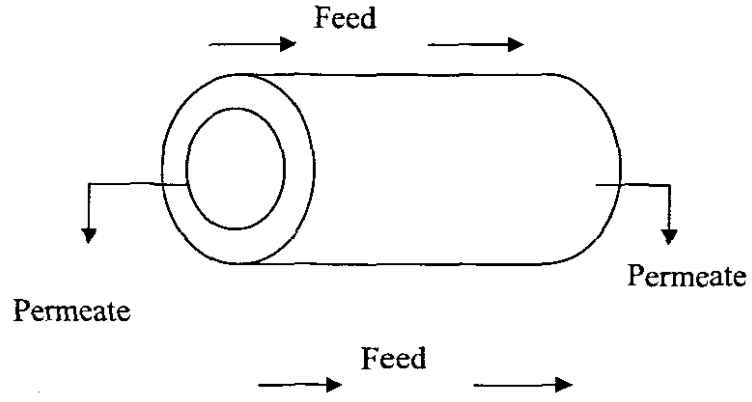

(ii)Transverse flow: The flow of the feed is perpendicular to the capillary membrane axis.

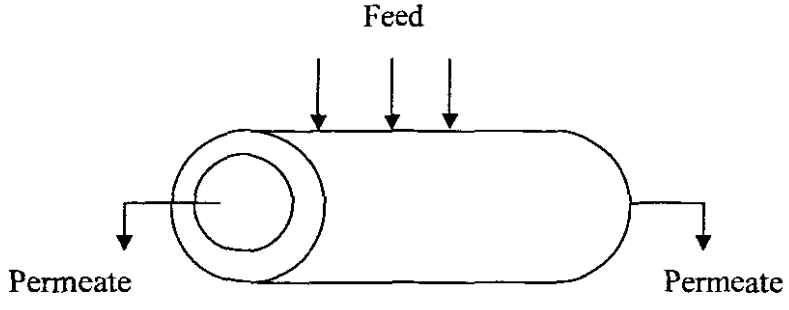

The disadvantages of this type of module is that the flow conditions are not always well-controlled since e.g. channelling easily occurs and it easily plugs or is difficult to clean (Roesink,1989). It is not appropriate to ascribe these disadvantages to all kinds of shell-side fed module though since many different designs can be distinguished.

Figure E 2 (a, b and c): Schematic presentation of flow arrangements in a membrane module

APPENDIX F
Flat sheet membrane fabrication

- Industrial preparation of flat sheet membranes is that they are generally manufactured on a casting machine. A polymer dope is cast by a casting knife on a polyester or polyethylene support paper, which is continuously supplied from a roll.
- The cast polymer film is fed to the precipitation bath, where the actual membrane is formed.
- After a certain residence time in a rinse bath, where residue solvent is removed, the membrane is collected as a flat sheet on the take up roll.
- The membranes that are obtained can be made up to 2m wide continuous sheet.

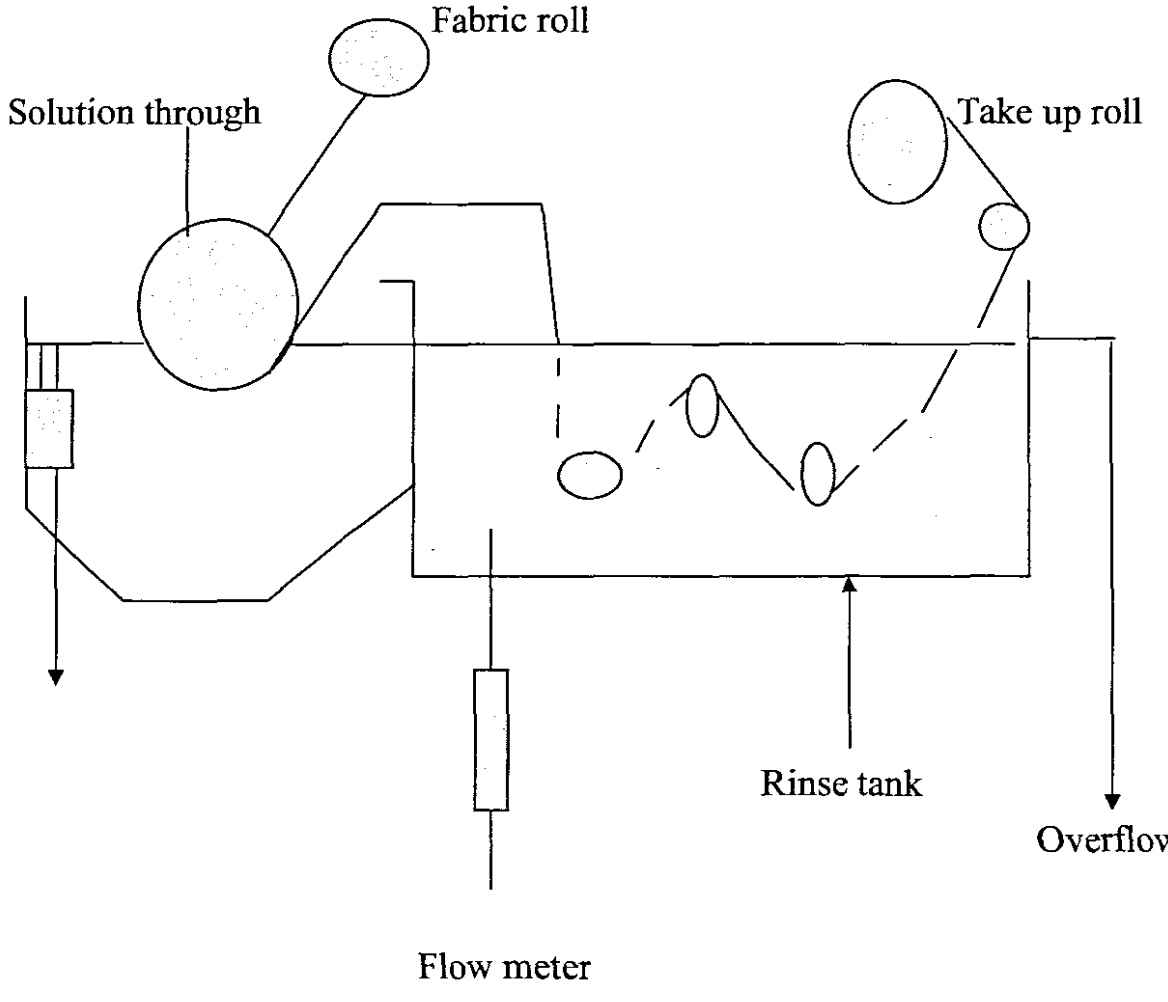

Figure F: Schematic presentation of flat sheet membrane fabrication

The first flat sheet cellulose acetate membranes developed by Loeb and Sourirajan using phase separation process in 1960s were asymmetric membranes (Young and Chen, 1993). Flat sheet membranes can be made to be symmetric or asymmetric.

F 1.1 Symmetric membranes

Symmetric membranes are also referred to as dense homogeneous membranes. The active layer of these membranes is dense. They do not separate on the basis of ordinary sieving mechanism. The separation mechanism for dense membranes is called solution-diffusion process. The separation is that the filter traps the particles within the structure. In small scale, a solution is made and spread as a 20-200μm thick film. A phase inversion technique is used. That causes the homogeneous solution to separate into a solid polymer and a liquid solvent. This precipitated polymer forms a porous structure containing a network of more or less uniform pores. By varying the polymer concentration, precipitation medium and precipitation temperature, these membranes can be made with a very large variety of pore sizes. These membranes show a high tendency of adsorption because of their extremely large internal surface.

F 1.2 Asymmetric Micro porous membranes

This type of membrane consists of a very thin layer approximately 0.1 - 1μm selective skin layer on a highly porous approximately 100 – 200 μm thick substructure. The very thin skin represents the actual membrane. The membrane separation characteristics are determined by the nature of the polymer and the pore size, while the mass transport rate is determined by the membrane thickness. The porous sub- layer serves only as a little support for the thin and fragile skin and has an insignificant effect on separation characteristics or the mass transfer rate of the membrane. In small scale, the process of preparation is explained under immersion phase separation method.

APPENDIX G

Factors affecting practical UF membrane performance

G1: Introduction

Ultra-filtration (UF) is a pressure driven filtration separation occurring on a molecular scale. A process fluid containing dissolved and/or suspended material contacts one side of a membrane. A pressure gradient is applied across the membrane. The liquid, including small dissolved molecules, is forced through the pores. Sieving retains large dissolved molecules, colloids and suspended solids. The process fluid retained by the membrane is called concentrate or retentate. Those portions passing through the membranes are called filtrate, ultra filtrate or permeate. The rate at which material permeates the membrane per unit area is called flux. The objective of ultra-filtration may be to recover or concentrate materials in the retentate or to produce a purified permeate.

The performance of an asymmetric polymeric membrane must be specifically related to the morphology of the dense layer, where separation properties against solutes (the so-called cut-off) arise (Capanelli et. al., 1983). The separation performance of a membrane is dependent not only on the dimensions of the solute molecules, but also on their shape, flexibility and interactions with the membrane surface. Ultra-filtration membranes separate particles that range from 0,01 to 0,1 microns in size.

G2: Membrane-Retentate interactions in UF

If the solute size is greater than the UF pore dimensions, mechanical sieving retains the solute. Retained species are transported to the membrane surface at the rate $J_i = JC_{Bi,}$ where J is the permeate flux and C_{Bi} is the bulk concentration of the retained species. Retained materials accumulate at the membrane surface, forming a fouling layer, which thickens with time as shown in figure 4.3. That clogs the membrane pores and is called fouling. Fouling is caused by either adsorption of material or consolidation. When the permeability of this layer is low, it can reduce the membrane flux (Field, 1995; Munari et al., 1989). The deposit is a mixture of material that may have been suspended in the original process fluid plus precipitates and slimes formed when retained solutes have exceeded their solubility.

G3: Retained species affect the UF membrane performance (rejection and flux)

1. Retained components may adsorb onto the membrane surface, reducing the apparent pore size and flux. Adsorption is one type of fouling.
2. The fouling layer then becomes the operating membrane and the underlying ultra-filtration membrane acts as a support.
3. Solute-solute interactions increase rejection and lower flux. Small particles may similarly adsorb onto larger particles.

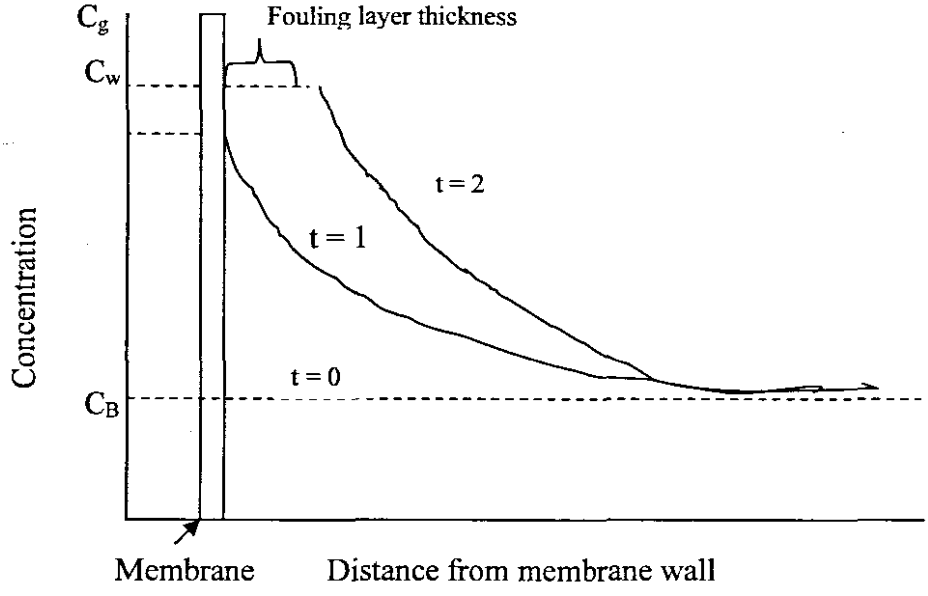

Where C_w = concentration at membrane wall; C_B = bulk concentration; C_g = gel concentration (Ref. Encyclopaedia Polymer (1989))

Figure 4: Schematic presentation of thickening concentration polarization with time

G4: Membrane cleaning methods

Selecting appropriate membrane material that does not adsorb species in the process stream controls fouling. Fouling films are removed from the membrane surface by chemical methods. A cleaning regimen must detach the fouling layer and be compatible with the materials used to construct the membrane modules and equipment. Forcing the process fluid at right angle with the membrane can control the gel polarization thickness. Mechanical cleaning physically dislodges foulants. Scouring agents such as rubber crumb may be added to the feed for continuous operation. Sponge balls scour the inside of tubes. Hollow fibres and membranes attached to rigid support can be back-pressured.

Nomenclature

D_{ij}	binary diffusion between i and j
D	diffusion co-efficient
m	fixed position for the dope in the moving boundary between the spinning bath and dope
X	position of the boundary between the dope and the spinning bath measured in position co- ordinate
t	time (s)
k	flux ratio of solvent to non-solvent (constant)
n_2	flux of solvent
n_1	flux of non-solvent
$N_{i,1,2}$	hypothetic layers of the nascent membrane parallel to the surface of the casting dope
ρ	dope density
r	density ratio of pure solvent to non-solvent
N_A	rate of solvent or non-solvent diffusion
C	concentration
z	membrane thickness
Z	diffusion direction
S	solvent
NS	non-solvent
F	flux of the membranes (L/m^2h)
A	effective area of a module (m^2)
v	volume of the collected samples (ml)
r	radius of the membrane (cm)
l	length of the tested module (cm)
n	number of capillaries making up the module
R	rejection of the membrane
C_p	permeate concentration
C_f	feed concentration
$\Delta\mu$	chemical potential difference over the dope/bath interface
ϕ_i	volume fraction of component i in the casting bath
$u_{i,}$	volume fraction of component i in the external spinning bath
v_i	molar volume of component i
g_i	interaction parameter between component i and j
x	Cartesian spatial position co-ordinate perpendicular to the membrane surface
c_i	concentration of component i (kg/m^3)
V	collected volume in a specific time (ml)
M	molecular weight
R	Rejection (%)
T	temperature